



CAR AIR-CONDITIONING TEST RIG PERFORMANCE ANALYSIS

MUHAMMAD MUZAWAR ARIFFIN BIN MOHD NAZIM
B092110462

**BACHELOR OF MECHANICAL ENGINEERING
TECHNOLOGY (MAINTENANCE TECHNOLOGY) WITH
HONOURS**

2025



Faculty of Mechanical Technology and Engineering

CAR AIR-CONDITIONING TEST RIG PERFORMANCE ANALYSIS

MUHAMMAD MUZAWAR ARIFFIN BIN MOHD NAZIM

**Bachelor of Mechanical Engineering Technology (Maintenance Technology) with
Honours**

2025

CAR AIR-CONDITIONING TEST RIG PERFORMANCE ANALYSIS

MUHAMMAD MUZAWAR ARIFFIN BIN MOHD NAZIM



Faculty of Mechanical Technology and Engineering

UNIVERSITI TEKNIKAL MALAYSIA MELAKA (UTeM)

2025

DECLARATION

I declare that this Choose an item. entitled “CAR AIR-CONDITIONING TEST RIG PERFORMANCE ANALYSIS” is the result of my own research except as cited in the references. Choose an item. has not been accepted for any degree and is not concurrently submitted in candidature of any other degree.

Signature

:

Name

:

Muhammad Muzawar Ariffin bin Mohd Nazim

Date

:

31th December 2025

APPROVAL

I hereby declare that I have checked this thesis and, in my opinion, this thesis is adequate in terms of scope and quality for the award of the Bachelor of Mechanical Engineering Technology (Maintenance Technology) with Honors.

Signature :
Supervisor Name : *Ts Dr. Nor Azazi Bin Ngatiman*
Date : 31^h December 2025

اونيورسيتي تېكنيكل مليسيا ملاك
UNIVERSITI TEKNIKAL MALAYSIA MELAKA

DEDICATION

For my family, who always supported me even when I doubted myself. Your persistent belief and continual support have served as my beacon during this experience. This thesis belongs to both of us equally. To my mentor, whose assistance and knowledge have been extremely valuable. You have pushed me, motivated me, and enlightened me beyond what words can convey. I will always be thankful for your patience and commitment. To my friends, who have supported me and kept me grounded and sane during the craziness of deadlines and research. Your sense of humor, generosity, and friendship have not only made this journey bearable, but also enjoyable. I appreciate everyone. This thesis is devoted to you.

اونيورسيتي تېكنيكل مليسيا ملاك
UNIVERSITI TEKNIKAL MALAYSIA MELAKA

ABSTRACT

It has been well evidenced that test rigs enhance learning activities in the classroom, facilitate students' understanding of difficult concepts, as well as enhance the level of practical skills. In the context of engineering education, it serves as a useful tool for establishing the link between theory or different fields of studies, and their application. However, the literature lacks articles related to various kinds of compressors that can be used in car's HVAC systems. The purpose in this work is to create a test rig for the car air-conditioning compressors with the use of Honda Jazz Hybrid 2016 system and to determine the performance characteristics of different types of the compressor in various conditions. The 2nd aim is to measure and compare critical performance variables such as temperature, pressure, refrigerant flow rate and system efficiency, which can provide helpful information with respect to enhancing automotive air conditioning systems. It also entails the latest sensors like, thermocouples for monitoring temperatures, temperature and pressure sensors, and accelerometers to capture the performance of the compressors at a given time. MATLAB is used for data analysis so that detailed examination of acquired data is possible with or without techniques like accelerometer for vibration frequencies. At the initial development of the Car Air Conditioning Compressor Test Rig, some of the activities to be done are as follows: In addition, this study posits to help reduce the gap in teaching by providing learners with an efficient physical learning aid that can help them study and learn from real HVAC parts. The test arrangement is utilized for both study and instructional purposes, offering students the chance to conduct experiments and be exposed to new knowledge concerning sophisticated HVAC technologies at the same time.

UNIVERSITI TEKNIKAL MALAYSIA MELAKA

ABSTRAK

Test Rig telah telah dibuktikan mampu meningkatkan gaya pembelajaran dalam lingkungan pendidikan dengan menawarkan pengalaman teknikal, membantu pelajar memahami idea yang kompleks dengan lebih baik, serta membina kemahiran praktikal. Ia menjadi alat berguna untuk menghubungkan pemahaman teori dengan praktikal dalam kursus-kursus kejuruteraan. Namun, masih terdapat kekurangan penyelidikan mengenai jenis-jenis kompresor dalam sistem Pengudaraan, Penyejuk, dan Penghawa Dingin Automotif (HVAC). Dalam kajian ini, tujuan pertama adalah untuk membangun rangkaian ujian kompresor sistem pengudaraan automotif Honda Jazz Hybrid 22016 untuk mengkaji efisiensi kompresor yang berbeza dalam situasi yang berbeza. Tujuan kedua adalah untuk menilai dan membandingkan faktor-faktor kinerja yang penting seperti suhu, tekanan, aliran cecair refrigeran, dan efisiensi sistem, memberikan maklumat berguna untuk memperbaiki sistem HVAC automotif. Rangkaian ujian ini juga termasuk senjata terkini seperti termokupel, senjata suhu dan tekanan, serta akelerometer untuk mengumpulkan data real-time mengenai cara kompresor berfungsi. MATLAB digunakan untuk interpreting data, membolehkan analisis yang mendalam data yang dikumpul, seperti pengukuran frekuensi getaran menggunakan akelerometer. Semasa tahap awal Pembangunan test rig Kompresor Sistem Pengudaraan Automotif (CACTR), beberapa langkah dalam pembangunan projek telah diselesaikan, manakala yang lain masih dalam proses. Selain itu, kajian ini juga bertujuan untuk mengurangkan kekangan pendidikan dengan menawarkan pelajar Teknikal untuk melihat dan lebih mendalami dengan bahagian-bahagian HVAC, sehingga mampu menambah baik proses pembelajaran mereka. Rangkaian ujian ini digunakan untuk penyelidikan dan memberikan pelajar peluang untuk melakukan ujian dan belajar mengenai teknologi HVAC melalui pengalaman praktikal.

ACKNOWLEDGEMENTS

In the Name of Allah, the Most Gracious, the Most Merciful

First and foremost, I would like to thank and praise Allah the Almighty, my Creator, my Sustainer, for everything I received since the beginning of my life. I would like to extend my appreciation to My supervisor Ts. Dr. Nor Azazi Bin Ngatiman and Universiti Teknikal Malaysia Melaka (UTeM) for providing the research platform.

My utmost appreciation goes to to the members of my thesis committee, Dr. Sharif, Dr. Muhammad Nur, and Ammar, for their constructive feedback and invaluable contributions to this work. His constant patience for guiding and providing priceless insights will forever be remembered.

Finally, from the bottom of my heart I express gratitude to my beloved family, for their encouragements and who have been the pillar of strength in all my endeavors. My eternal gratitude also to all my friends, for their patience and understanding and for their endless support, love and prayers. Finally, thank you to all the individual(s) who had provided me with the assistance, support, and inspiration to embark on my study.

TABLE OF CONTENTS

	PAGE
DECLARATION	ii
APPROVAL	iii
DEDICATION	iv
ABSTRACT	v
ABSTRAK	vi
ACKNOWLEDGEMENTS	vii
TABLE OF CONTENTS	viii
LIST OF TABLES	xi
LIST OF FIGURES	xii
LIST OF SYMBOLS AND ABBREVIATIONS	xiv
LIST OF APPENDICES	xvi
INTRODUCTION	1
1.1 Background	1
1.2 Problem Statement	2
1.3 Research Objective	2
1.4 Scope of Research	3
LITERATURE REVIEW	4
2.1 Introduction	4
2.2 Development of automotive air conditioning test rig using a centrifugal compressor	5
2.3 Automotive air conditioning systems for Fuel consumption and Electric Vehicle	6
2.3.1 Fuel Consumption Vehicle	6
2.3.2 Electric Vehicle	7
2.4 Refrigeration Cycle in Automotive	8
2.4.1 Compressor and condenser	9
2.4.2 Expansion valve and evaporator	10
2.5 Common type of Compressor uses in automotive HVAC	11
2.5.1 Scroll compressor	11
2.5.2 Rotary Compressor	12
2.6 Swash Plate Compressor	13
2.6.1 Fixed swash plates	14
2.6.2 Variable swash plate	15
2.7 Common air conditioning compressor failure	16
2.7.1 Refrigerant Leak	16

2.7.2	Expansion valve failure	17
2.7.3	Electrical component failure	17
2.8	Automotive climate control system.	18
2.8.1	Single-zone climate control	19
2.8.2	Dual-zone climate control	19
2.8.3	Tri-zone climate control	20
2.9	Refrigerant properties	21
2.10	Refrigerant leak detection test for automotive HVAC	23
2.10.1	Electronic leak detection	23
2.10.2	Contrast agent and Ultraviolet (UV).	24
2.10.3	Forming gas	24
2.11	Performance evaluation for Automotive HVAC system	25
2.11.1	Automotive HVAC cooling capacity	26
2.12	Design of Experiment	27
2.12.1	Type of Design of Experiment	28
2.13	Vehicle HVAC diagnostic	29
2.14	Summary table	32
2.14	Summary of research gap	35
METHODOLOGY		36
3.1	Introduction	36
3.2	Research Design	37
3.2.1	Schematic structure	38
3.2.2	Experimental Setup	39
3.2.3	Parameters	41
3.2.4	Development of Test Rig	42
3.2.5	Equipment	43
3.2.6	Development of the car air-conditioning test rig	45
3.2.6.1	System Leak Testing and Operation Testing	43
3.2.7	Developed Test rig operation process and Data Collection	45
3.2.7.1	Temperature and Pressure sensor placement	47
3.2.8	Experiment Structure	49
3.2.8.1	Experimental parameters	50
3.2.8.2	Alternative test rig	52
3.2.8.3	Alternative Test Rig Component	54
3.2.8.4	Experimental and Analysis Flow	57
3.2.8.5	Vibration data acquisition setup using online monitoring.	60
3.2.8.6	Coefficient of performance test rig	61
3.2.8.7	Type of condenser fault	63
3.2.8.8	Table of the analysis data	65
3.4	Design of experiment (Taguchi Method)	67
3.5	Summary	69
RESULTS AND DISCUSSION		70
4.1	Introduction	70
4.2	Overview Car Air-conditioning test rig	71
4.2.1	Car Air -Conditioning test rig Output	73
4.2.2	Developed CACTR Coefficient of Performance (COP)	74
4.3	Validation of test rig	75

4.4	Experimental Data Results	77
4.4.1	Coefficient of performance of the alternative test rig	78
4.4.2	Vibration analysis on a compressor related to condenser fault.	84
4.4.2.1	Horizontal Axis with Variable data	84
4.4.2.2	Vertical axis with variable data	86
4.4.2.3	Comparison of vibration Pattern on Idle RPM with No fault and $\frac{3}{4}$ fault in condenser (Horizontal)	88
4.4.2.3	Comparison of vibration Pattern on Idle RPM with No fault and $\frac{3}{4}$ fault in condenser (Vertical)	91
4.5	Variable data on rms with different levels of rpm and condenser fault	94
4.6	Experiment result on output of a car-air conditioner with different rpm and condenser fault	96
4.6.1	Experiment result on output of a car-air conditioner with different rpm and condenser fault (Horizontal)	96
4.6.2	EXPERIMENT RESULT ON OUTPUT OF AN CAR-AIRCONDITIONER WITH DIFFRENT RPM AND CONDENSER FAULT (VERTICAL)	98
4.7	Verification of analysis result	99
4.8	Summary	101
CONCLUSION & RECOMMENDATIONS		102
5.1	Summary of Test Rig Development	102
5.2	Summary of Analysis	103
5.3	Limitation of the Research	103
5.4	Future Recommendations	104
REFERENCES		106
APPENDICES		109
APPENDIX A Project Gantt chart		109
APPENDIX B Project Gantt chart		110
APPENDIX C ISO 10816 (Vibration Severity)		111
APPENDIX D Electric Scroll Compressor Specification		112
APPENDIX E Pressure-Enthalpy Diagram of R134a		114
APPENDIX F R134a Tables		115

LIST OF TABLES

TABLE	TITLE	PAGE
Table 2. 1	Property of R-12 and R134a.....	22
Table 2. 2	Type of Design of Experiment	28
Table 2. 3	Vehicle HVAC diagnostic method	30
Table 2. 4	Summary table.....	32
Table 3. 1	Parameter that is being measured in the analysis of the test rig.....	41
Table 3. 2	List of major equipment for developing the car air-conditioning test rig	43
Table 3. 3	Sensor description.....	48
Table 3. 4	Characteristics of chosen experimental designs for analysis in alternative test rig	50
Table 3. 5	Variable data from experiment.....	50
Table 3. 6	Display Components.....	52
Table 3. 7	Alternative test rig list of component and function	55
Table 3. 8	Type of condenser fault	62
Table 3. 9	Taguchi Method analysis.....	67
Table 4. 1	CACTR Components Description.....	71
Table 4. 2	CACTR output.....	72
Table 4. 3	experiment data.....	77
Table 4. 4	COP for every condenser condition and RPM	74
Table 4. 5	Experiment results of horizontal axis vibration data	83
Table 4. 6	Experiment results of vertical axis vibration data	85

LIST OF FIGURES

FIGURE	TITLE	PAGE
Figure 2. 1	Process of refrigerant cycle in automotive system (Sharif, 2023).....	10
Figure 2. 2	Scroll compressor design.....	12
Figure 2. 3	Fixed swash plates	14
Figure 2. 4	Variable swash plat.....	15
Figure 2. 5	Automotive climate control system.....	19
Figure 3. 1	Schematic diagram of test rig equipment	38
Figure 3. 2	Experimental flowchart.	39
Figure 3. 3	3D model of the test rig	Error! Bookmark not defined.
Figure 3. 4	Test rig assembly work process.....	44
Figure 3. 5	Leak Testing using soap	45
Figure 3. 6	AC to DC converter	46
Figure 3. 7	Test rig data collection process.	47
Figure 3. 8	Temperature and pressure sensor placement	48
Figure 3. 9	experimental flowchart	50
Figure 3. 10	Alternative Car air-conditioning test rig.....	53
Figure 3. 11	Component use for experiment.....	55
Figure 3. 12	Automatic Recovery machine	55
Figure 3. 13	Compressor and vibration sensor position.....	56
Figure 3. 14	Experiment flow analysis	57
Figure 3. 15	Recovery and flushing machine using recovery machine	58
Figure 3. 16	Analysis result table.....	64
Figure 4. 1	Car Air-conditioning test rig.....	70
Figure 4. 2	Display value for each data point	72
Figure 4. 3	System pressure test day 1	73
Figure 4. 4	System pressure test day 2.....	74
Figure 4. 5	Graph based on the result from experiment.....	77
Figure 4. 6	Graph based on the result shows on table.....	80
Figure 4. 7	Horizontal axis vibration behavior of time and frequency domain on idle RPM during normal conditions on condenser	86
Figure 4. 8	Horizontal axis vibration behavior of time and frequency domain on idle RPM during $\frac{3}{4}$ fault on condenser	87
Figure 4. 9	Vertical axis vibration behaviour of time and frequency domain on 1900 RPM during no fault condition of condenser	89
Figure 4. 10	Vertical axis vibration behaviour of time and frequency domain on 1900 RPM during $\frac{3}{4}$ fault condition of condenser	90
Figure 4. 11	RMS Vibration for Horizontal for different rpm and condenser fault ...	92
Figure 4.12	RMS vibration for vertical for different rpm and condenser fault	92

Figure 4.13	Experiment result on output of a car-air conditioner with different rpm and condenser fault (Horizontal)	94
Figure 4.14	Experiment result on output of a car-air conditioner with different rpm and condenser fault (vertical)	95
Figure 4.15	R134a refrigerant performance(Bonifaccino, 2020).....	97



LIST OF SYMBOLS AND ABBREVIATIONS

CACTR	-	Car Air-Conditioning Compressor Test Rig
BTUH	-	British Thermal Units per hour
COP	-	Coefficient of Performance
DAQ	-	Data Acquisition System
FCEVs	-	Fuel Cell Electric Vehicles
GWP	-	Global Warming Potential
HVAC	-	Heating, Ventilation, and Air Conditioning
IEPE	-	Integrated Electronic Piezoelectric
MCT	-	Mechanical Engineering Technology (Maintenance Technology)
ODP	-	Ozone Depletion Potential
PMSM	-	Permanent Magnet Synchronous Motor
VDC	-	Variable Displacement Compressor
TXV	-	Thermal Expansion Valve
UV	-	Ultraviolet
ANOVA	-	Analysis of Variance
DoE	-	Design of Experiment
EV	-	Electrical vehicle
RPM	-	Rate Per Minutes
W	-	Watt
°C	-	Degree Celsius
CO ₂	-	Carbon Dioxide
kW	-	Kilo Watt

m/s ²	-	Meter per second square
dB	-	Decibel
R-12	-	Dichlorodifluoromethane
R-134a	-	Tetrafluoroethene



اونيورسيتي تېكنيكل مليسيا ملاك

UNIVERSITI TEKNIKAL MALAYSIA MELAKA

LIST OF APPENDICES

APPENDIX	TITLE
APPENDIX A	Project Gantt chart
APPENDIX B	Project Gantt chart
APPENDIX C	ISO 10816 (Vibration Severity)
APPENDIX D	Electric Scroll Compressor Specification
APPENDIX E	Pressure-Enthalpy Diagram of R134a
APPENDIX F	R134a Tables

اونیورسیتی تکنیکل ملیسیا ملاک

UNIVERSITI TEKNIKAL MALAYSIA MELAKA

CHAPTER 1

INTRODUCTION

1.1 Background

The creation of an automotive HVAC test rig passes through the hands of a very thorough process that involves several stages and considerations. One of the very important initial stages of development is forming a design, which includes three-dimensional modeling, selection, and procurement of components, structural fabrication, component integration, and its operational testing (Jusoh, 2024). These will ensure that the test rig is well structured and will ensure it can simulate the conditions required of an automotive HVAC evaluation test.

Recent studies have focused on developing advanced test rigs capable of simulating extreme weather conditions, such as high temperature and humidity (Li et al., 2020). These platforms are equipped with advanced sensors and data acquisition systems, allowing accurate data collection on air conditioning system performance (Chen et al., 2020). In addition, the researchers explored the use of artificial intelligence and machine learning algorithms to analyze test bench data to predict the performance of air conditioning systems under operating conditions. different practices.

The development of advanced test rigs has also led to the creation of more flexible and realistic test scenarios, allowing for a more comprehensive assessment of air conditioning system performance (Kim et al. 2021). Additionally, the use of test rigs has enabled the development of more efficient and environmentally friendly air conditioning systems, thereby reducing energy consumption and greenhouse gas emissions (Lee et al., 2020).

1.2 Problem Statement

One of the current problems on the car air conditioning test bench is the problem of low pressure on the low side of the AC and low pressure on the high side. This problem occurs when the pressure readings on the low side and high side of the air conditioning system do not match the expected value on the pressure chart. Specifically, if the low-side pressure is higher than expected and the high-side pressure is lower than expected, this can indicate a series of problems in the system.

For example, too much refrigerant flowing into the evaporator can cause this pressure difference. Additionally, a damaged heat bulb that cannot sense the temperature signal or a blocked TXV (thermal expansion valve) can also cause this problem.

These problems can be difficult to diagnose and repair and may require specialized tools and expertise. Additionally, if left unchecked, they can lead to reduced air conditioning performance, increased energy consumption, and even system failure. Therefore, it is essential to quickly identify and resolve these problems to ensure the reliable operation of the car air conditioning system.

1.3 Research Objective

The main aim of this research -

- a) To develop a car air conditioning test rig
- b) To study the performance of the developed test rig in terms of the performance.

1.4 Scope of Research

The study will concentrate on creating and building a test rig for a car air-conditioning compressor that will be used with the air-conditioning system of a 2016 Honda Jazz Hybrid. The precise dimensions of the car structure primarily influence the test rig's design. This involves creating the structure, choosing the right materials, and ensuring the strength and longevity of the rig.

The test equipment will include sophisticated sensors and measuring instruments to observe important factors like temperature, pressure, airflow, and energy usage. This guarantees precision and dependability in gathering data. An efficient data acquisition system (DAQ) will be incorporated to gather, analyze, and save data from the sensors. This system will have the ability to monitor in real time and log data for future analysis. The sensor also demonstrates the complex connection between system performance and component failure.

Finally, the test rig will function as a hands-on educational tool for students. A set of lab experiments will be designed to take advantage of the test rig's abilities. These activities delve into how different parameters affect the air-conditioning system's performance and include examining how diverse compressor designs and operational techniques can lower energy usage and improve cooling effectiveness.

CHAPTER 2

LITERATURE REVIEW

2.1 Introduction

In recent years, there has been a strong emphasis on the study of test rigs for vehicle air conditioning. The primary goal has been to improve the accuracy, efficiency, and dependability of these test settings to ensure the safety, performance, and efficacy of modern automotive air conditioning systems. Advances in renewable energy sources and measuring techniques have been crucial in the development of test rigs for automotive air conditioning.

One instance is a study performed by Wu et al. (2019) that showcased a test configuration fueled by sustainable energy, including PV panels for solar power production. Yang et al. (2017) conducted another study showcasing a technique that employs artificial neural networks to control the internal temperature and humidity of a test equipment via simulation.

Moreover, Xie and colleagues (2018) performed a study that demonstrated the development of an advanced gas sensor array for monitoring air quality in real time in automotive air conditioning test rigs. The advancements have significantly improved the accuracy, efficiency, and reliability of car air conditioning testing systems.

2.2 Development of automotive air conditioning test rig using a centrifugal compressor

In contrast to other types of compressors, the development and testing of centrifugal compressors in the automotive industry, including those designed for specific applications such as fuel cell vehicles, can greatly benefit from customized designs for optimal performance (Cho et al., 2019; Li & Gao, 2021; Jin et al., 2020). The creation of specialized test rigs for centrifugal compressors allows for more accurate performance analyses and evaluations, as these rigs can be tailored to the unique requirements and characteristics of centrifugal compressor systems.

The creation of an automotive air conditioner test rig serves as a valuable tool for performance evaluation, fault detection, energy efficiency optimization, component testing, and environmental impact assessment. By utilizing the test rig, researchers can enhance system functionality, optimize control strategies, and improve overall efficiency.

2.3 Automotive air conditioning systems for Fuel consumption and Electric Vehicle

Air conditioning systems in automobiles serve an important role in assuring passenger comfort and safety during travel. However, these technologies have a significant impact on fuel usage and energy efficiency, particularly for electric vehicles.

2.3.1 Fuel Consumption Vehicle

The air conditioning system in a car increases fuel consumption significantly in vehicles with internal combustion engines. These types of systems are things called parasitic losses, and they electronics chatter on a daily basis with more things that influence the fuel consumption of other components, and bam, you have the much more holistic picture of how modern cars consume fuel. Now, due to its higher requirement of fuel as it has to run the air conditioning system, its fuel consumption becomes even higher, which is most loud when you are standstill. The vehicle uses additional fuel at different speeds, but mostly high speed when the air conditioning compressor turns on during operation. Examples of this are energy management and feedback control systems that bring the air conditioner performance and the cabin comfort to the optimum level which results in lower fuel use.

In conclusion, automobile air conditioning plays a huge role to our fuel consumption, especially those who owns a gasoline internal combustion engine car. The air conditioning system has a compressor, at any speed gases are being compressed, subsequently working the compressor uses more fuel and at higher speeds, it uses even more of it. To lower fuel use while providing a suitable degree of interior comfort, the energy management and feedback control techniques can step in and raise air conditioning efficiency to a new level.

2.3.2 Electric Vehicle

Air conditioning systems operation in electric vehicles affects energy consumption and general vehicle efficiency. In vehicles powered by electric energy, Eco-driving technologies such as driving mannerisms and cruising path selection can lead to large scale reduction of fuel usage and emission (Fafoutellis et al., 2020). Air conditioning systems in electric vehicles (EVs) serve an important role in preserving passenger comfort and efficiency. Research was carried out on cooling systems based on heat pumps with regard to their effectiveness in cooling fuel cell electric vehicles. This involves the use of heat pump technology to cool the cabin effectively. This new way of cooling EVs can help in the reduction of energy consumption and enhancements of thermal comfort.

Researchers have been investigating the use of heat pump technology to improve the air conditioning systems' cooling efficiency in Fuel Cell Electric Vehicles (FCEVs). Use of heat pump systems to cool the cabin of electric cars is a new strategy. This technology may help save some energy when used on EVs thus contributing to enhanced thermal comfort in the vehicle hence energy savings while improving its overall effectiveness. This could be a way out.

The cooling performance of air conditioning systems in fuel-cell electric vehicles is crucial for maintaining vehicle efficiency and range. Cooling systems in fuel cell electric vehicles have been widely investigated to understand their characteristics in terms of cooling performance, which motivated the evaluation of heat pump-sourced cooling systems in such vehicles. The possibility to incorporate heat pump technology into electric vehicles provides an opportunity for automotive engineers and manufacturers to come up with air conditioning systems that are both more sustainable and more energy efficient. This way may contribute to better fuel economy and the car's overall performance by reducing on board energy

utilization especially when it comes to maintaining thermal comfort.

2.4 Refrigeration Cycle in Automotive

Heating and cooling systems or more broadly known as the refrigerant cycle in both electric vehicle air conditioning and air conditioning system of fuel consumption car prevents the inside of the vehicle for uncomfortable temperatures. It operates through a fluid known as a refrigerant which is passed through four chief components of the system; the compressor, condenser, the valve and the evaporator. Here is how it works: the compressor compresses the refrigerant and this puts the heat into it while pressurizing it. The condenser then cools it down into a liquid state, where after coming out of the condenser it mixes with refrigerant oil and becomes a mixture. The expansion valve regulates the contents in a manner that its pressure is reduced so that it expands.

Last of all, the evaporator gains heat from the air and retransforms the refrigerant back to its gaseous state. This cycle is crucial for keeping cars cool and is important for making air conditioning systems more energy-efficient and environmentally friendly. In one study, researchers analyze the prospects of utilizing automobile Ac systems charged with low-GWP refrigerants (Alhendal et al. , 2020). These results involve energy and exergy analysis which is calculated using the first and second laws of thermodynamics that works to outline energy efficiency in the course of the refrigeration cycle.

2.4.1 Compressor and condenser

The compressor in the refrigeration system is used in compressing the refrigerant and helping in its circulation within the system (Sharif, 2023). Among the main apparatuses of the refrigerant cycle in air conditioning systems, the two indispensable parts are the compressor and the condenser. The purpose of compressor is to make the gas which is the refrigerant hot and high pressure at same time or in other words, the role of compressor is to use mechanical energy to put the gaseous refrigerant through cycle of high pressure and high temperature. The hot gas formed is now cooled in the condenser in a way to becoming a high pressure liquid through imparting heat to the surrounding air. This change is important as it helps the refrigerant to transfer the heat it absorbed throughout the cooling process. In the best of its operation, the condenser serves as a heat exchanger where heat is exchanged from refrigerant and turned into liquid.

Based on figure 2.1 During compression, the refrigerant is compressed by the pressure of the compressor, therefore increasing its temperature. The hot gas that is produced is cooled in the condenser in a manner to make it a very high-pressure liquid by transferring heat to the surrounding air. This change is crucial because during the cooling process, the refrigerant accumulates heat which it has to release to be reused. The heat absorbed during the cooling process is further rejected in this phase change from the gas to a liquid in the condenser. Which in simple terms can be described as a heat exchanger where the refrigerant is allowed to release heat and changes state to the liquid phase.

2.4.2 Expansion valve and evaporator

The evaporator, situated in the calometry water bath, receives liquid refrigerant from the expansion valve. It expands and enables the refrigerant to evaporate thus providing cooled air to the convection passing through the cabin. The thermal expansion valve is placed between the condenser and the evaporator; its primary function is to control the flow of the high-pressure liquid refrigerant into the low side. This controlled expansion leads to rapid evaporation, resulting in further cooling (Sharif, 2023).

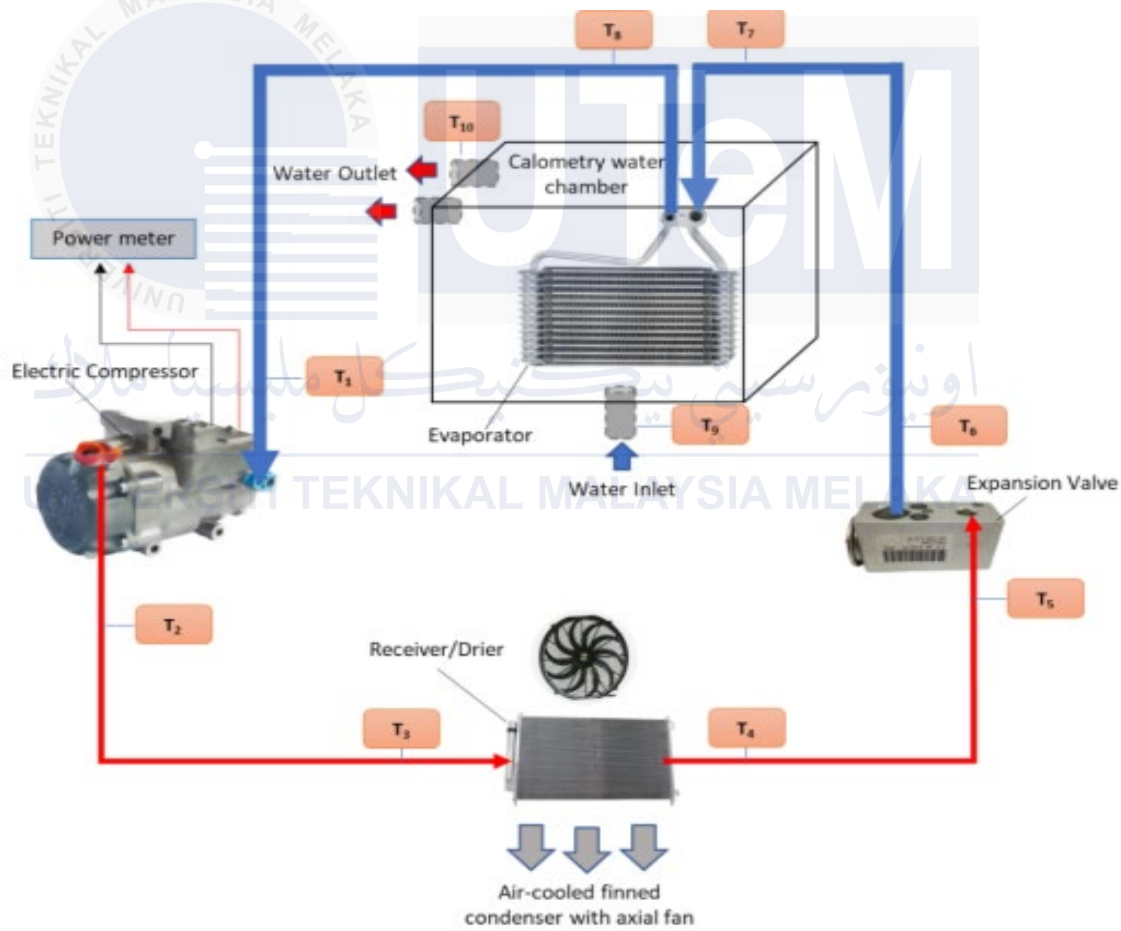


Figure 2. 1 Process of refrigerant cycle in automotive system (Sharif, 2023)

2.5 Common type of Compressor uses in automotive HVAC

Scrolls have become popular in automobiles due to their efficiency, reliability, and versatility in supporting a wide range of refrigerants, carbon dioxide inclusive. These compressors are part and parcel of refrigeration systems and are useful in matters to do with the flow and performance of fluids. Extensive theoretical and experimental research have been directed to refining the design and performance of the scroll compressor that is used in automobiles; issues include flow characteristics, instability, and proper finite control of innovative discharge port layout in electric vehicle HVAC systems. Regarding the subject, it is accurate to state that the scroll-type compressor has central importance in refrigeration systems relying on carbon dioxide as the natural refrigerant (Song et al. , 2023).

2.5.1 Scroll compressor

In scroll compressor working methodology, pockets of air got trapped between two scrolls which rotates in parallel fashion in opposite directions. When the scrolls are switched over the amount of air having been trapped between them reduces hence a build-up of pressure. This pressure compels the compressed air to be expelled via an outlet port at a greater pressure than it was when they entered the compressor. In specific research activities in scroll compressor within automotive contexts, features like flow behaviour, pulsating characteristics, and newly designed discharge port have been stressed especially in EVs-Air conditioning systems.

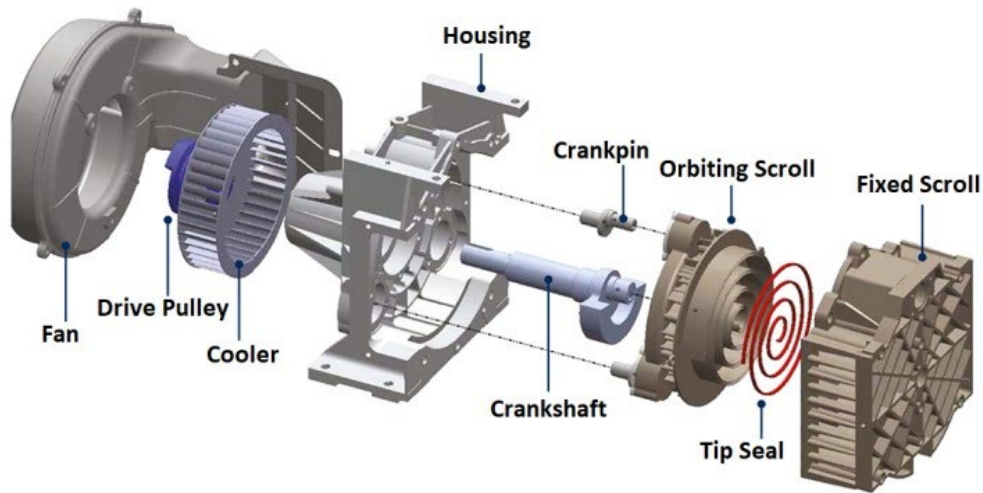


Figure 2. 2 Scroll compressor design

2.5.2 Rotary Compressor

Rotary compressors play a very important role in many applications, with the highest number being in the automotive industry for HVAC systems. These compressors operate based on rotary positive-displacement action, and this aspect ensures that they are both efficient and reliable for gas compression. The tribological behavior of materials in compressors has been explored with respect to the lubricants and their influence on different factors such as viscosity, the pressure-viscosity coefficient, and the consumed power on the whole when changing refrigerants (Bhutta et al,2018). Rotary compressors have an important position in HVAC systems in the automotive industry, and their research, for enhancement on the design, performance, and environmental impact, is under consideration with the requirement for energy efficiency and reliability.

2.6 Swash Plate Compressor

Swash plate compressors form an important component in most applications, especially the automotive HVAC systems. A swash plate compressor uses a mechanism made up of a swash plate to transform the rotary motion of the drive shaft into reciprocal motion, which can compress the refrigerant gases. Several studies have sought to optimize swash plate compressors design and dynamics in view of enhanced performance and efficiency. In this regard, research has focused on the lubrication characteristics of the piston/cylinder interface in swash plate compressors as well as the effect of load pressure and swash plate tilting angle on oil film thickness and friction force (Sun et al. 2019). There are two kinds of swash plates: the fixed and the variable. In a fixed swash plate, the latter is retained from rotating by some anti-rotation gears, and behind the swash plate, a cam is made to rotate. This gives rise to the up and down motion of pistons, in a plane parallel to the drive shaft of the compressor. Such fixed swash plate compressors have either six or ten pistons. In opposed axial compressors, the pistons are coupled by a solid piece that ensures they maintain a fixed distance from each other. All the pistons move in a direction parallel to the compressor's drive shaft.

2.6.1 Fixed swash plates

A swash plate compressor is used in vehicle air conditioning systems. It basically consists of an elliptical disc mounted at an angle to the drive shaft. It is held by gears, and a rotating cam behind the disc makes the pistons move in a straight line parallel to the drive shaft. The pistons are held in place by a solid piece, which ensures the pistons remain an equal distance apart. In such an arrangement, they can, therefore, move smoothly and effectively, resulting in uniform compression. Normally, the compressors have either 6 or 10 pistons, each of which is connected to a moving disc known as a slipper disc. There is a ball joint linking the piston and the slipper disc. This linkage is purposely provided to allow the pistons to move smoothly and accurately in either direction. This is how effective, and efficiency of the compression is done.

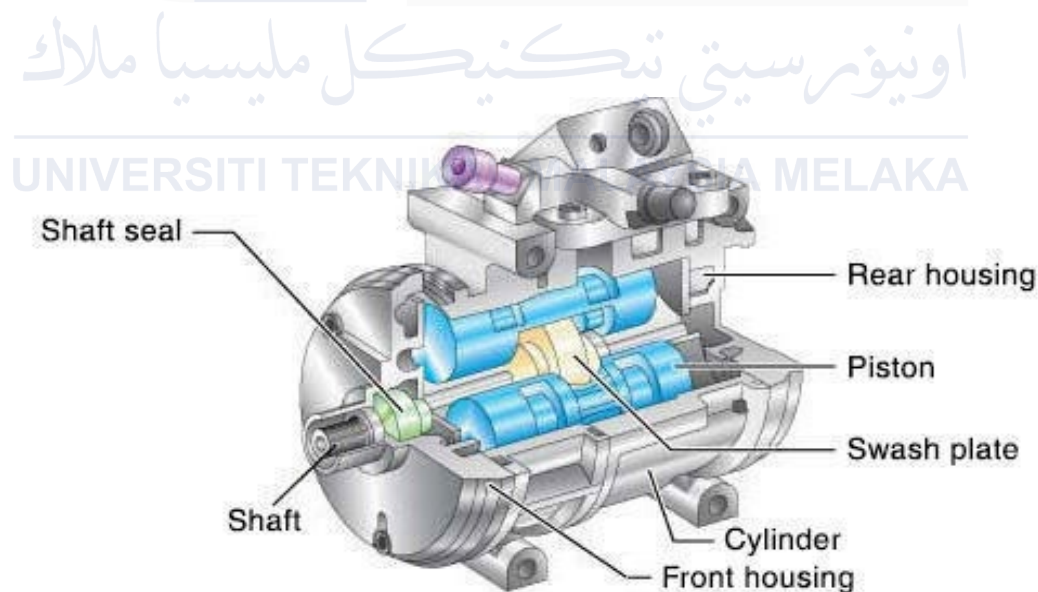


Figure 2. 3 Fixed swash plates

2.6.2 Variable swash plate

Variable swash plates form a key component of compressor systems, especially in automotive air conditioning systems. The VDC uses a variable swash plate mechanism to control its capacity by altering the swash plate angle, which is in response to the surrounding conditions, including temperature and humidity. In so doing, it modulates its output capacity, which allows precision in the cooling process, hence saving on energy. Variable swash plates allow adjustment to the diversity of different operating conditions for compressors to run efficiently. Researchers are trying to improve the design and operation of such compressors to meet the requirements of energy efficiency.

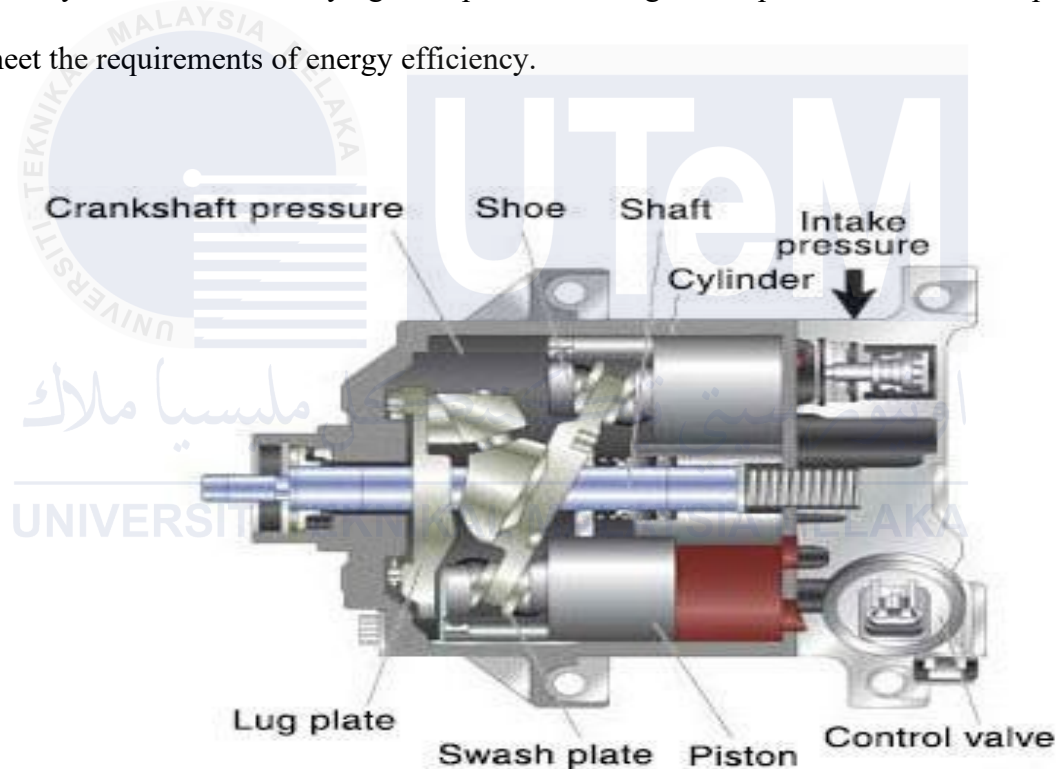


Figure 2. 4 Variable swash plat

2.7 Common air conditioning compressor failure

Air conditioning compressor failures in automotive HVAC systems can result from inadequate lubrication, blockages, leaks, or the use of improper lubricant. Inadequate lubrication can result from low refrigerant levels since it is necessary for the refrigerant to also carry the oil to the compressor. Other blockages, such as a clogged orifice tube, can restrict refrigerant and oil flow to the compressor. Leaks in the system cause the lubricant to be removed and the compressor will fail. Further, using the wrong kind of lubricant can also damage the compressor.

You can troubleshoot air conditioning compressor failures by checking the system pressure with a set of A/C service gauges. If the pressure is low on the high and low sides according to the gauges, most likely the system is low on refrigerant and needs to be recharged. But before adding refrigerant, it's important to inspect the system for leaks that are causing the refrigerant to escape.

2.7.1 Refrigerant Leak

The causes for the refrigerant leak in the air conditioning unit are a malfunctioning compressor or a leaking hose or connection. One way to diagnose this problem is by using a set of A/C service gauges for measurement of the system pressure. If the readings of both the high and low side pressure gauges are low, the system is low on refrigerant and needs to be recharged. But before recharging, the technician must check for leaks.

The technician will add a fluorescent leak tracer dye to the system. After running the air conditioning, the technician will use a blacklight to check the air conditioning system for the location of the leak. Once located, the technician will do the necessary repairs and then evacuate and recharge the system to prevent future refrigerant leaks. This procedure ensures the proper functioning of the air conditioning system and that there will not be any further leaks.

to damage the system.

2.7.2 Expansion valve failure

Warm air blowing from the air-conditioning gadget may be a sign of the failure of the expansion valve. The valve is answerable for the control of the amount of refrigerant that flows to the evaporator. As a end result of failures, refrigerants can be not able to reach the evaporator, subsequently allowing the gadget to blow heat air. Another probable cause may be moisture that accumulates within the device and then freezes the expansion valve, therefore blockading the passage of the refrigerant. When the growth valve blocks the route of the refrigerant, the evaporator is no longer able to taking up warmness from the cabin, and the air con device ceases to feature within the way of cooling the air. In other phrases, when the growth valve has failed or gotten blocked due to moisture, the refrigerant can not attain the evaporator; hence, the air con gadget is unable to chill the air. A expert in this subject is able to diagnosing the device and fix any malfunction thru the visible check of the machine and replacement of any faulty elements.

The technician will pressurize the device to test it for flaws and, if wished, to clear any obstructions inside the expansion valve with a unique tool. This method will make certain the consumer that the car air con is first-rate, and the air that blows is cool.

2.7.3 Electrical component failure

This can prevent the motor fan from rotating, usually because of a blown fuse or a bad relay that is stopping strength from accomplishing the motor blower. The blower motor pushes the air through the vents. Therefore, a broken or malfunctioning motor may cause it no longer to function nicely. Fan faults, which include strolling at the incorrect speed, are some other troubles that could be because of a difficult blower resistor. Another reason for no airflow may

additionally include a blocked air intake. This is caused by particles, leaves, and different matters that could obstruct the normal air access into the machine. Malfunctions of the aircon machine due to broken belts and hoses also can cause no drift of air through the vent.

2.8 Automotive climate control system.

Automotive climate management structures are critical for preserving passenger consolation with the aid of regulating the temperature within the automobile cabin. These structures offer heating, ventilation, and air conditioning (HVAC) functionalities to make certain a most desirable indoors climate irrespective of outside climate conditions. Key additives of automobile climate management structures consist of the compressor, condenser, evaporator, and diverse sensors, all running collectively to gain the preferred temperature and airflow.

Automotive air conditioning systems aim to enhance thermal comfort by utilizing advanced technology. One such example is the development of reinforcement learning-based thermal comfort control systems, which optimize the temperature inside the vehicle's cabin based on the preferences of the passengers and external factors. These systems use machine learning algorithms to continuously learn and adapt to the passengers' comfort levels, leading to a more personalized and enjoyable driving experience. Overall, the integration of innovative technology in automotive air conditioning systems is improving the comfort and convenience of modern vehicles. Additionally, advancements in system design, such as developing systems that can operate with the internal combustion engine off, have been explored to improve energy efficiency and reduce emissions (ALBERTI & MATIAS, 2022).



Figure 2. 5 Automotive climate control system

2.8.1 Single-zone climate control

A one-area climate control device is the term for any person of a mess of methods to maintain uniform temperature at some stage in the whole automobile. It is, actually, quite easy—the temperature is ready via the motive force or the front passenger, and that's what every person gets. There is a temperature sensor near the driver that measures the temperature, then heats or cools the auto accordingly.

You would usually locate single-area structures in small or basic automobiles. They are cheaper and easier to use and operate than a number of the greater high-priced and superior systems. Not exceedingly, they don't offer all the fancy customization options offered via the greater superior structures, however they may be able to offering a cushy trip to all and sundry inside the car, particularly in small automobiles where it is simpler to govern the temperature.

2.8.2 Dual-zone climate control

Dual-zone climate control makes it possible for the driver and front passenger to set individual temperatures with respect to their own likings, so everybody can be comfortable without stepping on the other's toes. The system does its work with two sensors, one located

near the driver and another close to the passenger, which compute temperatures and manage heating and cooling based on that measurement.

A lot of mid-size to luxury cars come equipped with this feature, and it provides much more customization and comfort compared to single-zone systems. The feature particularly comes in handy when drivers and passengers have varying preferences for temperature or when one vehicle is shared by many people. Dual-zone climate control allows both the driver and the front passenger to achieve a more personalized and comfortable ride.

2.8.3 Tri-zone climate control

The feature of the tri-zone climate control allows drivers, front passengers, and passengers in the rear to get their own preferred temperatures without affecting the other. The system uses three sensors to detect the temperature in each zone, regulating the heating or cooling accordingly.

This feature is common in large vehicles, such as SUVs, minivans, and luxury models. It gives a higher level of individuality and comfort, especially when there might be different climate preferences among the riders or when the same car is shared among users. Some tri-zone systems also let you adjust the airflow by controlling the air vents and fan speed to customize your comfort even more. In general, the tri-zone climate control system provides a more customized and comfortable ride for everyone inside the vehicle.

2.9 Refrigerant properties

The automotive world used R-12 as a refrigerant for air condition systems in the automobiles before the 1990s. R-12 is a CFC refrigerant highly categorized in the ODP and GWP, thus phased out. R-134a, a refrigerant in the HFC category, was developed as a substitute of the R-12, this with less ODP and GWP. It is, as a result, used in the replacement of R-12 automotive air conditioning systems.

Although the environmental impact of R-134a is less than that of R-12, it is still a greenhouse gas in production and use. Consequently, research and development of refrigerants with much lower ODP and GWP must continue so that their environmental damage is minimized. Even R-134a was a giant leap ahead over R-12, it is by no means perfect. In this respect, the research of more eco-friendly refrigerants for the decrease of car air-conditioning systems is important.

Table 2. 1 Property of R-12 and R134a

PROPERTY	R-12 (DICHLORODIFLUOROMETHANE)	R-134A (1,1,1,2-TETRAFLUOROETHANE)
BOILING POINT	-29.8°C (-21.6°F)	-26.3°C (-15.3°F)
OZONE DEPLETION POTENTIAL (ODP)	1.0 (high)	0 (ZERO)
GLOBAL WARMING POTENTIAL (GWP)	10,900 (high)	1,300 (MEDIUM)
TOXICITY	Low toxicity, but can cause asphyxiation	LOW TOXICITY, BUT CAN CAUSE ASPHYXIATION
FLAMMABILITY	Non-flammable	NON-FLAMMABLE
APPLICATION	Original refrigerant used in automotive air conditioning systems	WIDELY USED IN AUTOMOTIVE AIR CONDITIONING SYSTEMS
ENVIRONMENTAL IMPACT	PHASED OUT DUE TO HIGH ODP AND GWP	BEING PHASED OUT DUE TO HIGH GWP

The table shows the properties of two refrigerants: R-12 and R-134a. The boiling point, ozone depletion potential, global warming potential, toxicity, flammability, application and environmental impact are tabulated for comparisons of both refrigerants. R-12 has a higher global warming potential and ozone depletion potential compared to R-134a, but both refrigerants exhibit low toxicity and are non-flammable. R-12 was previously used in air conditioning systems in cars, but it has been phased out due to the high ODP and GWP. R-134a has been widely used in air conditioning systems for automobiles, but it is also being phased out due to its high GWP.

2.10 Refrigerant leak detection test for automotive HVAC

Refrigerant leak detection tests are crucial to ensuring that the automotive air conditioning system maintains its performance, safety, and environmental protection. A reduced cooling effect, increased energy consumption, and possible environmental hazards can be caused by leaks in the system. If not checked in time, refrigerant leakage can spoil the function of the system by causing inadequate cooling, increasing energy bills, and potentially damaging the environment.

Periodic leak detection testing is necessary to uncover and fix leaks that exist in the system and cause potential breakdowns, which prevent excess energy from being wasted and lower the potential to damage the environment.

2.10.1 Electronic leak detection

Electronic leak detection is the location of refrigerant leaks in the automobile air conditioning system by means of special electronic tools. These tools can detect minute quantities of halogen gases, a typical component in refrigerants, and are able to locate leaks in areas such as an evaporator. The different types of electronic leak detectors available are heated diode detectors, infrared detectors, and ultrasonic detectors.

Since electronic leak detection is highly accurate and sensitive in nature, it's always widely used by auto technicians. This method is safe for the environment and does not harm the car's system.

2.10.2 Contrast agent and Ultraviolet (UV).

The contrast agent and UV lamp method is a reliable and eco-friendly technique used to detect refrigerant leaks in HVAC systems. This method involves injecting a specially designed contrast agent into the system, which then circulates throughout the refrigerant circuit. When a UV lamp is shone on the system, the contrast agent reacts by emitting a bright, fluorescent yellow-green colour, clearly indicating the location of even the smallest leaks.

This method is particularly useful for identifying hard-to-find leaks that may be missed by other detection methods. The contrast agent is safe to use and does not harm the system or the environment, making it an attractive option for technicians and facility managers. Additionally, the UV lamp is a non-invasive tool that does not require any disassembly or damage to the system, reducing downtime and repair costs.

The contrast agent and UV lamp method is a valuable tool for detecting refrigerant leaks, allowing technicians to quickly and accurately identify and repair leaks, ensuring the efficient and safe operation of HVAC systems.

2.10.3 Forming gas

The forming gas method in general is a sensitive and accurate technique for sensing refrigerant leaks in HVAC systems. In this method, nitrogen and hydrogen forming gas is used to flood the system after which a gas analyzer is used to determine whether there is hydrogen in the system. The choice of the method is high sensitivity since hydrogen is a small molecule and its diffusivity is very high such that it can pass through many leakage paths. In this method, some merits include high sensitivity, non-invasive sample analysis, simplicity, overall cost, and efficiency, and compatibility with the environment.

However, it is necessary to stress that this method necessitates the utilization of specific apparatus, and it is essential to perform this method only with the help of experienced technicians due to the possible explosion threat of hydrogen application. In sum, the forming gas method is beneficial to the technicians and facility managers because it allows for efficient identification and repair of leaks in an elegant and fast manner to guarantee the proper functioning of the HVAC system.

2.11 Performance evaluation for Automotive HVAC system

Performance evaluation of Automotive HVAC systems is important for several reasons. Firstly, the HVAC systems control the indoor environmental conditions of vehicles, thereby ensuring passenger comfort and safety. First of all, the system's efficiency should be evaluated in such a way that fuel consumption and emissions are minimized in an attempt to conserve the environment. Areas of weakness are detected to enable manufacturers to make amends to improve effectiveness and reduce fuel costs. In a second instance, where the HVAC system breaks down, there might be safety concerns that could arise if the HVAC system does not heat or cool the vehicle's cabin. Performance evaluation can aid in detecting and resolving these issues in a move that will ensure the safety of the driver and other passengers.

The other aspect of an HVAC system is to keep the interior of the vehicle at the most comfortable temperature possible, as part of the HVAC functions during all weather extremes. Performance testing ensures that the system works to provide the best comfort for the riders. This also helps in identifying potential problems that could affect the longevity of the system, allowing manufacturers to handle it in time and prolong the life of the system.

2.11.1 Automotive HVAC cooling capacity

Measuring disturbances in the cooling capacity of automobiles' heating, ventilation and air conditioning systems is very important in terms of efficiency and outcome. Cooling capacity is measured in BTUH (British Thermal Units per hour), or in Watts, and it defines the capacity of an automotive conditioning system to extract heat from the cabin where passengers are seated (Sharif, 2023). The ideal cooling capacity and energy efficiency of the cooling system remain crucial as it ensures that passengers remain comfortable while also reducing energy consumption (Sharif, 2023).

The ideal temperature of an outlet air conditioning in automotive industry for perceived cool comfort and efficiency in a hot day varies between 40°F (4°C) and 45°F (7°C). This affects the temperature control so as to address the needs of the system as well as the comfort of individuals within the premises.

In practical applications, the cooling capacity of an HVAC system is generally expressed by the number of BTUs it is capable of removing within a span of sixty minutes, the higher the BTU rating, the stronger the cooling system. For instance, a compact car may offer a cooling power in the region of 20,000 BTUs/hour whereas, an SUV may have a cooling power of 30,000 BTU/h or more. Another important factor to evaluate is the one provocative temperature, which relates to the contrast between outside temperatures and the outlet temperature. As mentioned with regards climate control, the automotive HVAC has to be able to lower the temperature by about 30°F to 40°F (16°C to 22°C) in a hot day successfully.

To sum up, the proper range for temperature control of automotive HVAC cooling depends on its capability to provide an appropriate cooling capacity ranging from 40°F to 45°F/ 4°C to 7°C and the utilization of BTUs per hour as a control measure. Also, the temperature differences are often used for measuring automotive HVAC systems performance, and therefore are very important.

2.12 Design of Experiment

DOE is an essential strategy in diverse fields, especially in automotive applications for HVAC systems. The use of experimental design in automotive HVAC is the achievement of performance objectives including efficiency, air quality, and user comfort. (Russi et al. 2022), provided a study with insight into air quality and thermal environment in an electric vehicle cabin under heating and cooling operations alongside measurements of HVAC energy use. This research therefore underscores the role of experimental characterization in determination of the behavior of HVAC systems in automotive application.

Design of Experiment or DoE in a nutshell can be described as a rational and efficient way of conducting experiments to establish the association between the factors under study and the consequences they bring about. DoE deals with planning, executing, and evaluating experiments to establish the cause-and-effect of some variables that influence reactions or results. DoE principles aim at establishing a daring way of collecting the highest amount of information with the least number of experiments or tests. You should also note that DoE defines the factors that influence the response; it establishes the different levels of the factors and defines the design that provides the most desirable and accurate results known to man.

DoE is widely used in industries like engineering, manufacturing, pharmaceuticals and agriculture industries, to mention but a few, for process improvement, product enhancement and other related objectives such as reduction of costs. DoE is a method by which an organization determines and proves the critical input variables, enhances the situation of the processes, and forecasts the performance of a structure. Thus, there will be increased performance, reduced spread, and ultimately more competitiveness. In sum, DoE is a versatile tool in experimentation and decision-making processes, and expansion in the use of DoE is continuous if only organizations want to enhance the features, products, processes, and services.

2.12.1 Type of Design of Experiment

Table 2. 2 Type of Design of Experiment

METHOD	DESCRIPTION	ADVANTAGES	DISADVANTAGES
FULL FACTORIAL	Tests all possible combinations of factors.	Provides complete information about factor effects.	Requires many experiments for complex systems.
FRACTIONAL FACTORIAL	Efficiently explores factor interactions by testing a subset of all possible combinations.	Reduces the number of experiments while still capturing key interactions.	May miss some interactions due to fractional design.
TAGUCHI METHOD	Focuses on robustness by minimizing variation and identifying optimal settings.	Robust to noise factors.	Assumes linear effects and may not capture complex interactions.
PLACKETT-BURMAN	Screens factors to identify significant ones using a minimal number of experiments.	Efficient for screening purposes.	Limited to main effects; doesn't capture interactions.
CENTRAL COMPOSITE	Combines full factorial and response surface designs to explore factor effects and curvature.	Efficiently explores factor effects and quadratic behaviour.	Requires additional experiments beyond the factorial design.

The table 2.2 gives various experimental design categories and their benefits and disadvantages. Full Factorial is a comprehensive design but costly in terms of the number of experiments, especially for complex systems. Fractional Factorial explores interactions with fewer experiments, providing efficiency but missing some interactions. Taguchi Method focuses on robustness and minimizes variation. This method is limited, provided the effects are linear in nature, while the complex effects are missed. Plackett-Burman is efficient for screening significant factors and is limited to main effects. Central Composite is a combination of full factorial and response surface designs, hence quite comprehensive with good efficiency. However, it may require additional experiments beyond the factorial design. The correct design that suits you will depend on your nature of work, goals, and resources available to you.

2.13 Vehicle HVAC diagnostic

The diagnostic of automotive air conditioning is significant to maintain and operate HVAC systems of the vehicles. Diagnostic and technology tools help the technicians diagnose and solve problems quickly; systems work properly, consume less energy, and provide comfort to users. The works by (Chen et al. 2021) proposed a comprehensive taxonomy of HVAC system faults, focusing on the application of FDD tools to improve the functionality and efficiency of HVAC systems, thus reducing the adverse effects in buildings and inhabitants.

automotive air conditioning diagnostics should be done taking into consideration advanced diagnostic methodologies, fault categorization frameworks, rapid cool-down techniques, and different refrigerant assessments together with machine learning techniques. These approaches help the technicians work more efficiently, in identifying problems with the HVAC systems and rectifying these problems as well as in enhancing the efficiency of the systems in giving optimum comfort to the individuals inside the vehicles while at the same time promoting energy efficiency.

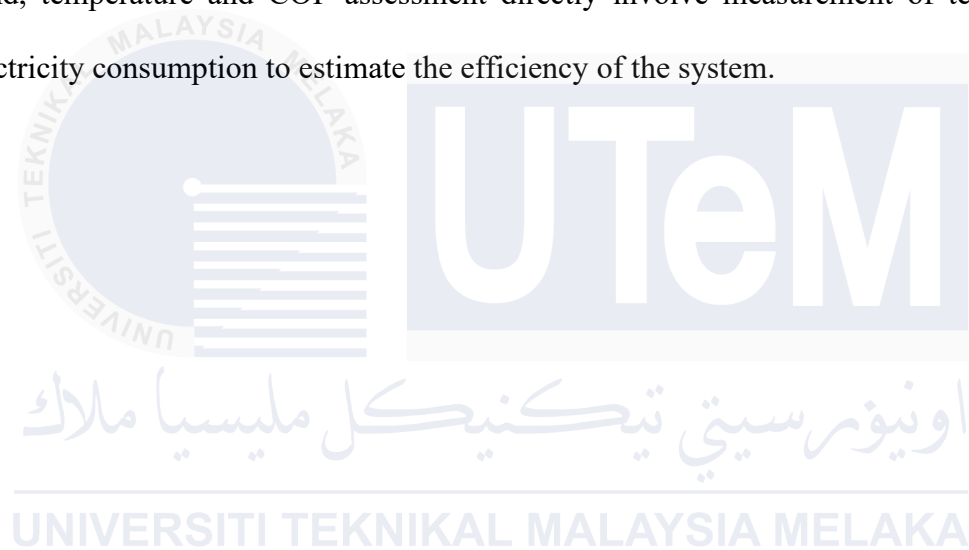
UNIVERSITI TEKNIKAL MALAYSIA MELAKA

Table 2. 3 Vehicle HVAC diagnostic method

ASPECT	ANALYSIS METHODS AND TECHNIQUES	DIAGNOSTIC TOOLS USED	RELEVANT SCIENTIFIC FORMULAS
PRESSURE	Measure pressure pulsations using pressure sensors. Understand characteristics of pressure pulsations generated by an automotive compressor.	- Pressure sensors	- N/A
NOISE SOURCE IDENTIFICATION	- Analyze compressor noise mechanism. - Four identification methods: - Transfer Path Analysis: Estimate forces on compressor parts. - Airborne Source Quantification: Clarify noise transfer paths. Use microphones and accelerometers for measurements ² .	- Microphones - Accelerometers	- N/A
VIBRATION AND NOISE REDUCTION	- Modify compressor structure to reduce vibration and aerodynamic noise. - Consider expansion mufflers. - Use accelerometers and microphones for vibration and noise measurements.	- Accelerometers - Microphones	- N/A
TEMPERATURE AND COP	- COP (Coefficient of Performance): Measure efficiency using temperature sensors and power consumption sensors. Higher COP indicates better efficiency.	- Temperature sensors - Power consumption sensors	$= \frac{\text{cooling output(watt)}}{\text{Electrical output(watt)}}$

The table outlines the parameters of a compressor system and the methods used in characterizing and quantifying the aspects. It includes chapters on pressure, source identification, noise and vibration control, and temperature and COP. Regarding each of the

aspects, they clearly indicate the analysis method and techniques used, the diagnostic tools applied and any scientific formulas that have been used. For instance, when observing pressure, pressure sensors are employed in detection of pressure fluctuations and their behaviour. Compressor noise causation analysis involves considering the mechanism of the compressor noise and using such approaches like the transfer path analysis to identify the source of the noise. Vibration and noise reduction, as their name implies, involve redesigning the structure of the compressor with an aim of minimizing vibration and aerodynamic noise, on the other hand, temperature and COP assessment directly involve measurement of temperature and electricity consumption to estimate the efficiency of the system.



2.14 Summary table

Table 2. 4 Summary table

Title	Objective	Author	Advantage	Limitations
Eco-Driving and Its Impacts on Fuel Efficiency	- Analyze eco-driving literature and models for fuel consumption estimation.	-E.I.V., E.G.M., P.F. contributed to the research paper.	- Data quality issues due to device limitations and errors. - Relatively low data availability with limited driver participation.	- Black box models use driving behavior data for fuel consumption estimation. - Machine Learning models enhance fuel consumption estimation accuracy.
The study analyzes automotive air conditioning systems with R1234yf refrigerant.	- Analyze AAC systems with R1234yf refrigerant for performance characteristics.	-Redhwan, Azmi, Sharif, Hagos - Sharif, Azmi, Zawawi, Ghazali	-R1234yf has lower COP compared to R134a in AAC systems. - Energy efficiency decreases with higher refrigerant charge and compressor speed. - Trade-off between cooling capacity and energy efficiency in AAC systems.	- R134a outperforms R1234yf with 25% higher COP at all speeds. - R134a is more efficient in the specific compressor setup.
Environmental impact assessment of a rotary compressor in Thailand.	Evaluate environmental performance of fixed speed rotary compressor in Thailand.	- Chantima Rewlay-ngoen - Seksan Papong	- Lack of completed on-site data for disposal stage assumptions - Limited technology for recycling R22 refrigerant in Thailand	- Inverter twin rotary compressor reduces environmental impact by 21.7-53.1%. - High energy efficiency in new compressor types minimizes environmental impact.
Considerations on design, development, and testing of Electrical Machines for automotive HVAC	- Design, analyze, and test PMSM for HVAC applications in vehicles. Develop machine for electric vehicle HVAC at low voltage.	- Martis Radu - The Authors	- Torque reduction with skew technique, but within acceptable limits. - HVAC impact on driving range in fully electric vehicles.	- PMSM offers high power density for automotive HVAC applications. - PMSM provides efficient variable speed operation for HVAC systems.

Development of an automotive embedded system for energy efficiency.	- Development of an embedded system for automotive industry efficiency enhancement.		<ul style="list-style-type: none"> - System requires conventional AC; Low Heat Flow; Low Efficiency. - Low weight increase; Limited heat flow compared to AC. 	- Low energy consumption, increased comfort, reduced emissions, and higher efficiency.
Numerical investigations on asymmetric inlet conditions in centrifugal compressor performance variations.	- Analyze centrifugal compressor performance with different inlet pipes using simulations.		<ul style="list-style-type: none"> - Performance degradation with Pz and Pu inlet bent pipes analyzed. - Power law relation between pressure ratio degradation and PCD observed. - Exponential relationship between efficiency degradation and PCD identified. 	<ul style="list-style-type: none"> - Investigated performance variations of centrifugal compressor with different inlet pipe structures. - Analyzed flow field characteristics to understand performance degradation extent.
Development and Evaluation of an Automotive Air-Conditioning Test Rig	- Evaluate air-conditioning system performance in limited space automotive environments.	- F. Yu and K. Chan conducted experimentation on home air conditioning.	<ul style="list-style-type: none"> - Limited space in car engine complicates air-conditioning system evaluation. - Increasing blower speed reduces COP of refrigeration system. 	<ul style="list-style-type: none"> - Evaluating automotive refrigeration system performance. - Analyzing COP, cooling load, and compressor power consumption.
Development of Automotive Air-Conditioning System Test Rig for Hybrid Electric Vehicles	- To develop AAC test rig for HEV AC system enhancement.	- The author is Redhwan et al.	- No specific limitations were mentioned in the provided contexts.	<ul style="list-style-type: none"> - Nanolubricants enhance AAC system efficiency and reduce compressor load. - Improved thermal transport properties increase condenser and evaporator efficiency. - Nanoparticles in lubricant improve system performance and energy efficiency.
Design and Characterization of a Centrifugal Compressor Surge Test Rig	- Study surge phenomenon in centrifugal compression systems.	- Christopher P. Goyne	<ul style="list-style-type: none"> - Surge initiation frequency range estimation near Helmholtz resonance frequency. - Limited axial and radial misalignment margin for motor coupling. 	<ul style="list-style-type: none"> - Surge control feasibility demonstrated using active magnetic bearings. - Experimental setup identifies surge phenomena, supporting utility of test rig.

Study on mixed lubrication characteristics of piston/cylinder interface of variable length	<ul style="list-style-type: none"> - Analyze lubrication performance in piston /cylinder interface with varying parameters. 	<ul style="list-style-type: none"> - The author is not explicitly mentioned in the provided contexts. 	<ul style="list-style-type: none"> - No specific limitations were mentioned in the provided contexts. 	<ul style="list-style-type: none"> - Study reveals effects of load pressure and swash plate tilting angle. - Increasing lubrication area reduces piston inclination and peak oil pressure. - Load pressure and swash plate angle affect oil film thickness.
A Historical Review on Tribological Performance of Refrigerants in Compressors	<ul style="list-style-type: none"> - The objective is to study lubricant properties with different refrigerants. 	<ul style="list-style-type: none"> - M.U. Bhutta et al. 	<ul style="list-style-type: none"> - CO2 requires higher pressure than other refrigerants for operation. - CO2 has limitations in operating temperatures and pressures. 	<ul style="list-style-type: none"> - CO2 refrigerant offers tribological advantages over R410a in compressor applications. - HFO-1234yf atmosphere enhances tribological performance with PAG lubricant.
Renewable and Sustainable Energy Reviews.	<ul style="list-style-type: none"> - To evaluate eco-driving training effectiveness and factors influencing fuel consumption. 	<ul style="list-style-type: none"> - Yuhan Huang - Elvin Ng - John Zhou - Nic Surawski - Edward Chan - Guang Hong 	<ul style="list-style-type: none"> - Driving simulator lacks real-world data, suitable for short-term studies. - PEMS has limited repeatability, lower accuracy due to real-world conditions. - Data loggers have limited accuracy, suitable for long-term studies. 	<ul style="list-style-type: none"> - Eco-driving reduces fuel consumption and emissions significantly. - Immediate impact with slightly increased travel time. - Training programs and in-vehicle devices are commonly used.
International Journal of Refrigeration	<ul style="list-style-type: none"> - To compare real-gas and ideal-gas models for swashplate compressors. 	<ul style="list-style-type: none"> - M. Arqam - Liu et al. - Ishii et al. - Tojo et al. - Tian et al. 	<ul style="list-style-type: none"> - Ideal gas model underperformed in discharge temperature prediction. - Sensitivity to suction valve flow coefficient affects volumetric efficiency prediction. 	<ul style="list-style-type: none"> - Improved predictions of compressor performance with real-gas properties and flow restriction. - Influence of valve model on compressor performance predictions at different speeds.

2.14 Summary of research gap

As a specialty within the automotive engineering sector, the design and construction of automotive air conditioning test rigs has been an important area of investigation for those interested in enhancing the precision and dependability of the technology. Recent achievements in the field of the renewable energy and measurements are the pioneer for the development including photovoltaic modules for generation of the solar energy (Wu, et al. , 2019), Control by Simulation with artificial neural networks (Yang, et al. , 2017). Advanced gas sensor arrays have also enhanced the reliability, time, and quality of these test rigs (Xie et al. ,2018).

Vehicle climate control mechanisms affect the fuel economy, especially vehicles with internal combustion motor (Cho et al., 2019; Li & Gao, 2021; Jin et al. 2020). It is evident that fuel consumption increases thereby the main cause for main consumption being the air conditioning system is fueled when in idle conditions. Measures like energy delivery and feedback control enable the reduction of fuel consumption required to operate air condition by aiming at minimizing it without causing inconvenience to passengers through an uncomfortable cabin environment.

In this context, A/C systems have consequences in electrical vehicles due to their effect on energy demand and car efficiency (Fafoutellis et al., 2020). Recent studies explored the cooling efficacy of fuel cell electric vehicles (FCEV) using heat pump-sourced cooling systems. This revolutionary concept integrates heat pumping into a vehicle and boosts thermal efficiency and energy management in EVs.

Testing and rating of automotive HVAC systems are significant to guarantee that they provide comfort and safety to the passengers, save fuel, and thereby reduce emissions; also, safety risks that may arise (Martis et al., 2020). Of the car air conditioning system cooling capacity condenses heat from the interior part of the cabin to keep the passengers comfortable (Sharif, 2023).

CHAPTER 3

METHODOLOGY

3.1 Introduction

It is therefore the purpose of this research to design and develop an enhanced and sophisticated MCT AC Fault Diagnostic Simulator which will only be able to produce ramifications of faulty component on different critical parameters of various categories of AC compressor. Such variables include temperature, pressure, current and, the vibration levels of the system, and all of these are important parameters that are likely to show the current health of the system. In this way, this simulator will act as an educational and diagnostic tool for students to demonstrate the effect which faulty components have on the rest of the AC system more efficiently. In addition, the described training simulator will include targeted sensors for tracking such parameters in real-time to engage students as effectively as possible. This research is set to assist the section of HVAC coaching and development by enlightening students on methods of recognizing how systems function as well as techniques for troubleshooting errors. The specifications of test rig will be designed using model of Honda jazz hybrid 2016.

3.2 Research Design

The method on this take a look at can be integrated and complete in terms of a blended-techniques layout. Quantitative and qualitative methods can be embraced inside the framework of studies techniques which will better seize multifaceted attributes on the targets of this mission. The quantitative part of this research paintings will be based on the following problem, specifically, the systematic series and analysis of the information to be obtained from the sensors integrated in the MCT AC Fault Diagnostic Simulator. Through the application of statistical techniques and facts visualization, tendencies, patterns, and correlations can be discovered within the sensor information, and because of the surfaced knowledge, treasured insights will be perceived on how AC compressors are impacted through defective components. The qualitative thing of this research, then again, can be realized based totally on staring at and deciphering the consequences of numerous defects on air conditioning machine operations.

This will be primarily based on systematically examining the simulator's performance beneath one-of-a-kind eventualities mimicking a illness and analysing college students' responses and interactions with the simulator for the duration of that. The qualitative findings will consequently be used to complement the quantitative facts in portray a richer, greater nuanced photo of how defects might effect the overall performance of the machine, in addition to the effectiveness of the usage of the simulator as an educational device. Generally, the mixed-methods approach will help make certain a extra balanced and complete exploration of the studies objectives for which greater validity and reliability of the findings may be claimed.

3.2.1 Schematic structure

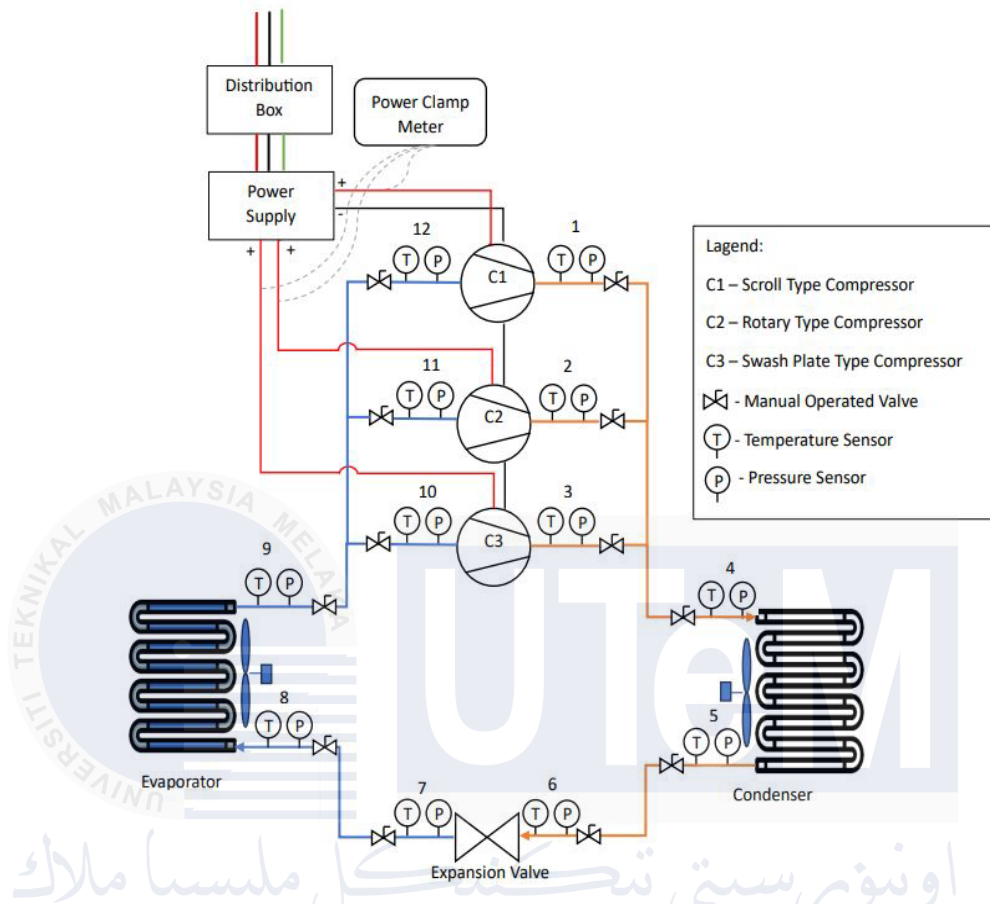


Figure 3. 1 Schematic diagram of test rig equipment

Figure 3.2 MCT AC Fault Diagnostic Simulator Setup that can be used to simulate faulty component effects on key variables in different AC compressors. Key sensors in the simulator include temperature, pressure, current, and vibration. Key components include: a computer system, sensors, and controllers - altogether mounted and designed to mimic the real AC compressor in the actual world. The software will conduct the data analysis and any calculations while the control system will be responsible for the proper operation and setting of the simulation. The software will bring out effective and accurate data analysis since it will work on the data and the computer system. The simulator is to be a high level and effective opportunity for learning for students in the HVAC education and training industry sector.

3.2.2 Experimental Setup

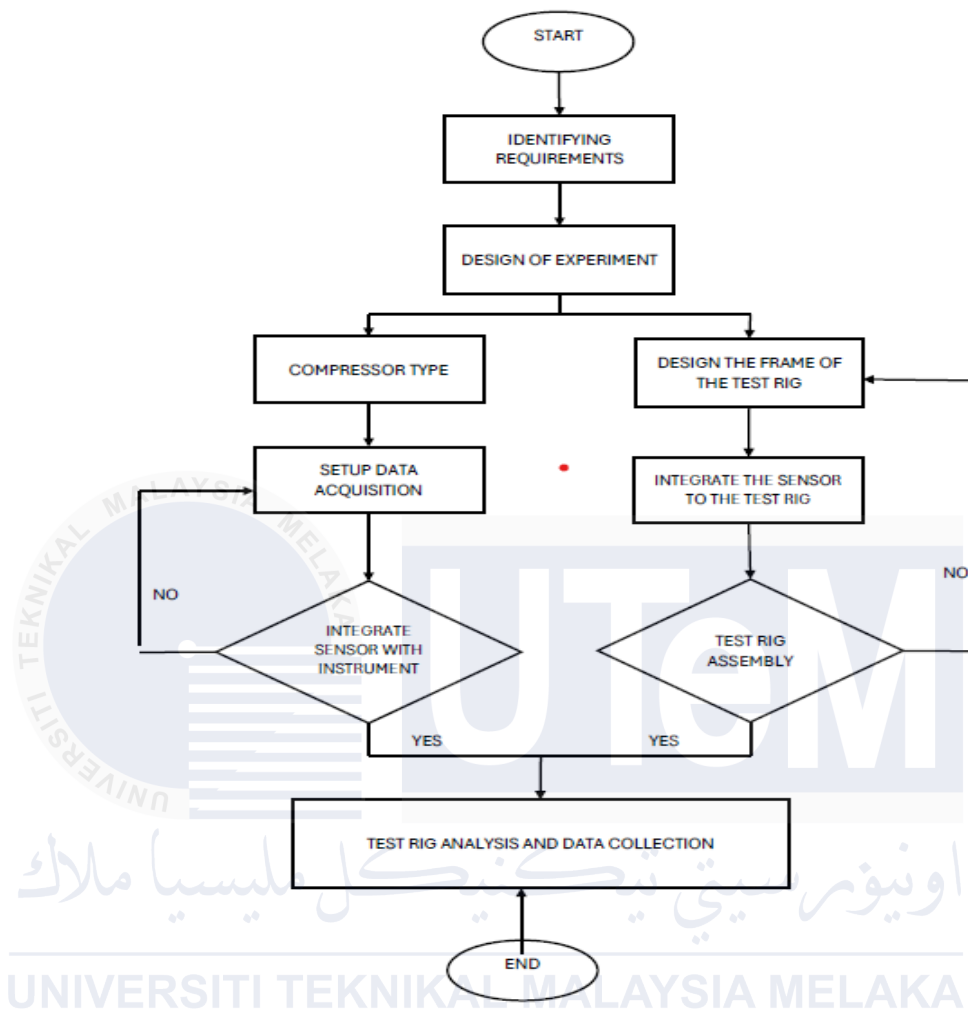


Figure 3. 2 Experimental flowchart

The use of the flowchart describes the process of establishing a test rig that would help in assessing the performance of a compressor. It starts with knowing the specifications that are to be put in the experiment and then comes the part of constructing the experiment. A compressor type is later selected, whereafter the way data collection will be done is arranged. At the same time, design of the frame of the test rig and eventual embedding of the sensor into the rig is done.

Finally, after setup the sensor is interfaced with required instruments and the test rig is fabricated. Subsequent to the assembly, it is employed for data capturing and evaluation and, therefore, marks the end of the experiment. The flowchart presented below can be considered ideal in this case since it is straightforward and precise and follows the ideal process of compressor performance analysis that needs to be followed in the establishment of the analysis. They are requirements analysis, experiment design or specification, selection of the compressor type, and data acquisition. They are then installed into the test rig and wired to required instruments before the sensor is incorporated into it. The test rig is constructed, a data acquisition system is used to record data, and finally results are being concluded about the compressor performance.

Along the way, it directs the user, making certain that all elements required in the experiment are accounted for and that the experiment will indeed be well-performed and credible. Through such a systematic display, the users will be confident that the needed analysis of compressor performance is well done and is very helpful in deciphering the compressor's functioning.

3.2.3 Parameters

Table 3. 1 Parameter that is being measured in the analysis of the test rig

NO	PARAMETER	UNITS	DESCRIPTION
1.	Temperature	°C	Temperature is monitored at compressor , Evaporator output, condenser input and output.
2.	Power Consumption	W	Electrical power supply to the compressor with different type of rpm
3.	Amount of Compressor Oil	g	Amount of compressor oil being inject to the compressor using machine.
4.	Amount of Refrigerant	Psi or g	Amount of refrigerant used that being supply to the test rig.
5.	Vibration	m/s	Vibration levels of the compressor based on different type of faults that being monitored.

Table 3.1 A collection of five important parameters, denoting the unit decibel, the ways in which to collect data, and definitions of understanding these in compressor system parameters. The first parameter is temperature measured in degrees centigrade at different locations at the compressor, the evaporator output and inlet and outlet condenser, which is to be able to assess how well the system performs. The power consumption (W) represents the electric power consumed by the compressor at various RPM intervals. The mass of compressor oil is the mass (in grams) of oil injected into the compressor through specialized equipment, which is here represented as the amount of refrigerant in Psi or grams, i.e., the refrigerant supplied to the test rig to run the system. Then vibration is a mechanical measurement necessary for the determination and analysis of the faults in the compressor, presented by m/s. All these are brought together as parameters to define the whole compressor performance health control.

3.2.4 Development of Test Rig

The development of the Car Air-Conditioning Compressor Test Rig includes conducting a specific study and determining every critical factors. This design has adequate space to contain the basic components of the air-conditioning system and sensors while also allowing for simple testing and maintenance.

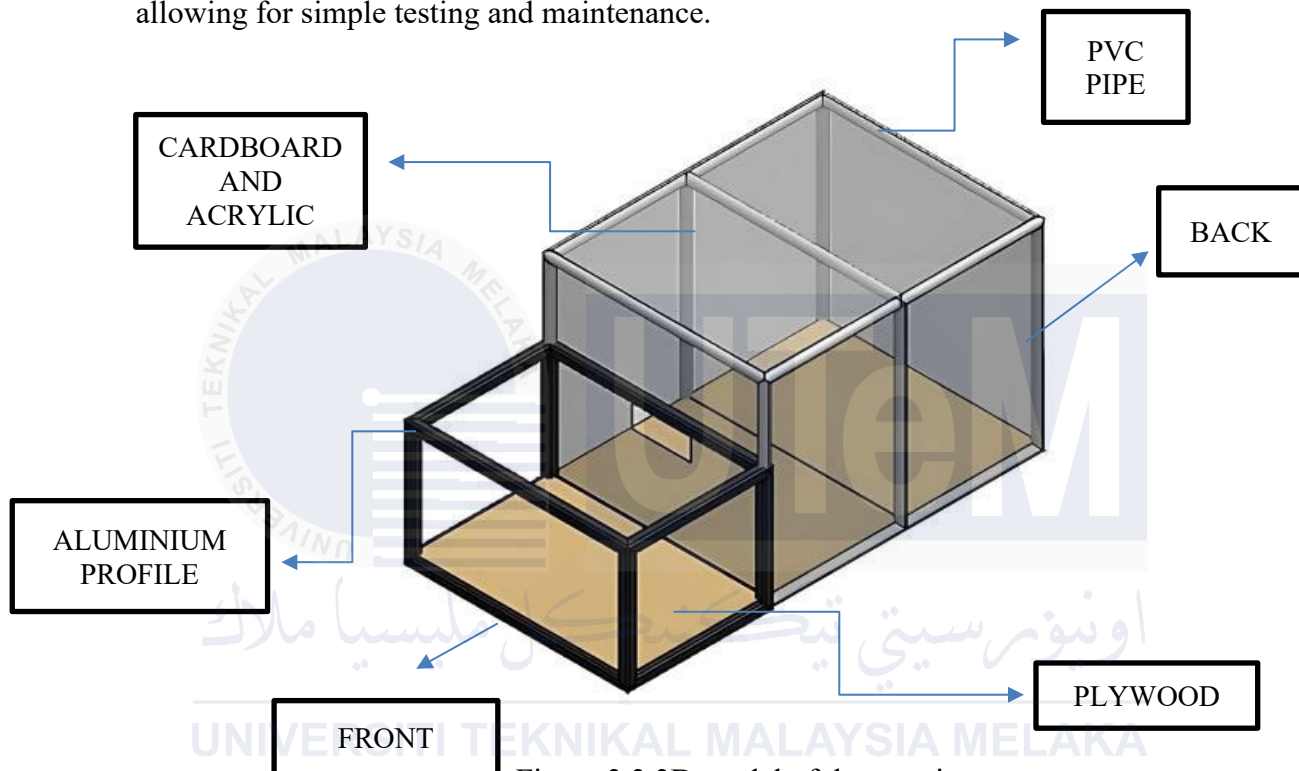


Figure 3.3 3D model of the test rig

The test rig construction was created utilizing a variety of materials to build a strong and practical enclosure. The structure's base is composed of plywood, which provides a solid and robust basis. The front of the structure is made of aluminium profiles, which characteristics is lightweight yet sturdy support to the whole car air conditioning full system. The back compartment walls are made of a mix of cardboard and acrylic, which provides protection while allowing for visual inspection of the inside. PVC pipes are utilized in cabins as connections or supplementary support for the upper part, ensuring that the structure is safe and solid.

3.2.5 Equipment

Table 3.2 List of major equipment for developing the car air-conditioning test rig

No.	Equipment	Basic Specifications
1.	12V Air Conditioning Compressor (Scroll Compressor)	<ul style="list-style-type: none"> Type : DC 12V / 24 V Cooling capacity: 1.688KW / 2.465KW (5731BTU / 8410BTU) Speed range : 1000 - 3000 rpm Rated power: 550W / 850w Rated
2.	Cooling Coil Honda Jazz Hybrid 2016	38mm × 220mm × 223mm
3.	Airconditioning Condenser Honda Jazz Hybrid 2016	770mm × 332mm × 16mm
4.	Aluminium Profile, Plywood, Acrylic, Roller	<ul style="list-style-type: none"> 30cm × 30cm Test Rig Structure
5.	Manifold Gauge, Low and High Pressure Head, R134A, R1234yf Gas	Dual gauge set for high and low-pressure readings that suit for R134A & R1234yf.
6.	DC to AC Converter	<ul style="list-style-type: none"> Input: 12V/24V DC Output: 120V/240V AC Power capacity: 100-500W
7.	Flare Connection Pipe	Size 1/4" to 3/8"
8.	Vacuum Machine	Flow rate with 3CFM and 15 Microns
9.	<ul style="list-style-type: none"> Wireless Vibration Sensor Gateway Router Wireless WiFi 	Type: ICP® (IEPE) Measurement Range: ±50 g to ±500 g Frequency Response: 0.5 Hz to 10 kHz Output Signal: Dynamic voltage proportional to acceleration
10.	Infrared temperature-measuring device with integrated aiming laser	
11.	Automatic Recovery Machine	Fully automatic mode with programmable settings for air-conditioner maintenance procedure.
12.	Thermocouple sensor	Measuring temperatures between -50°C to 500°C
13.	Testo Smart Pressure Sensor	Measuring compressor pressure on discharge and suction in Bar.

Table 3.3 includes a list of necessary equipment for creating the Car Air-Conditioning Compressor Test Rig, such as different types of compressors, cooling components from a

Honda Jazz Hybrid 2016, aluminum profiles for the frame, and multiple sensors



3.2.6 Development of the car air-conditioning test rig

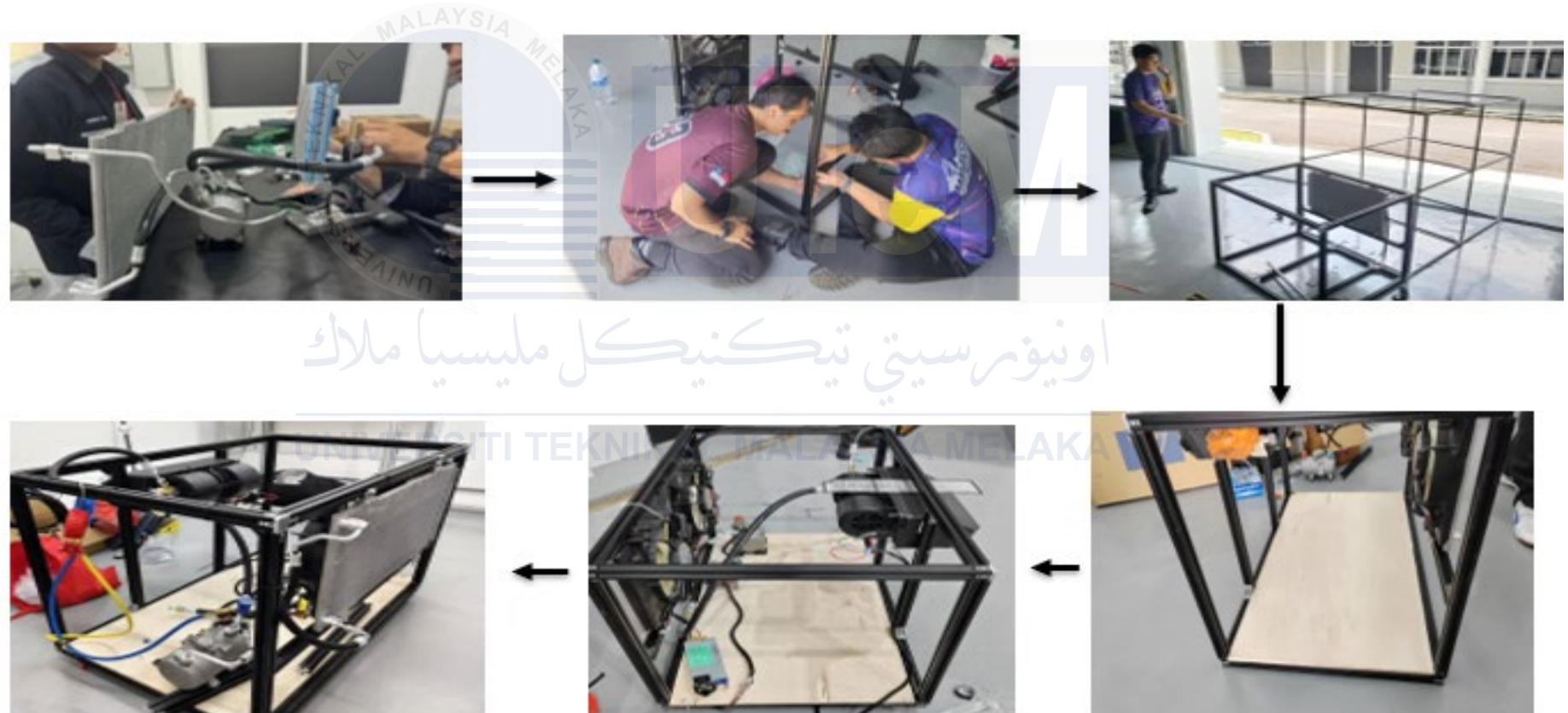


Figure 3.4 Test rig assembly work process

Tests of automobile air conditioning rigs are assembled by preparing and inspecting each component independently, such as the condensers, evaporators, compressors, and all electrical parts to ensure working apparatus. Then, the structural frame is made to give a solid foundation for mounting the individual parts of the test rig. Once the frame is completed, the major components of the conditioning arrangement, that is, the compressor, hoses, and electrical wiring, are incorporated into the test rig and fastened well enough to hold itself steady during operation. Wiring and piping are done to give proper refrigerant sensing, control, and flow. After that, the entire system is very carefully tested, checking for leaks, operating efficiency, and performance under simulated conditions, making changes when necessary, in order to suit requirements. Finally, all remaining panels or safeguard features are added, and quality control inspection is thoroughly to ensure that the rig is fully operational and ready for use.

3.2.6.1 System Leak Testing and Operation Testing



Figure 3.5 Leak Testing using soap

Soap leak testing is simple and inexpensive. It is used to find leaks in pressurized systems like air conditioning or refrigeration. The technique involves applying a soapy water solution to suspected areas like pipe joints, fittings, or valves. When the system is pressurized with air,

refrigerants, or some other gas, gas leaking through a hole will make the soap solution bubble at the region of the defect making it easy to identify the actual site of the leak. The method is simple: prepare the soapy solution; apply it well on the testing area; pressurize the system; and then observe for bubbles, marking off any leak point for repair. After repair, the same is done to ensure no leakage is detected. Once the leak testing was completed and the pipe or hose is confirmed leak free then move on to try run the test rig.



Figure 3.6 AC to DC converter

During this stage of operation test, the system added to being operationally tested using DC to AC converter (figure 3.7) power was tested in terms of correct electrical connections and functioning in the system. This ensured checking that all the electrical connections were secure and working correctly, including the fans and compressor. After passing these tests, the system was declared ready for further testing and performance check.

3.2.7 Developed Test rig operation process and Data Collection

This whole operation initiating the vacuum process stage is where this machine draws in air and moisture out of the whole refrigeration system by the use of a vacuum pump: at this stage, it lays the system perfect for receiving refrigerant charging as it is freed from impurities (A). After that, the charging phase will occur by weighing the refrigerant on a refrigerant scale to add it properly based on weight so that the perfect amount of refrigerant fills the system for its best performance. Along key locations in the whole system, thermocouple sensors will be positioned to monitor temperature and pressure in every component. These sensors are responsible for obtaining the needed data that will then be analysed with the use of the specific devices used for measurement in temperature and pressure. The collected data can be viewed within a manual thermocouple apparatus or via a data logger, allowing real-time observations of the system and an accurate assessment of performance detail.

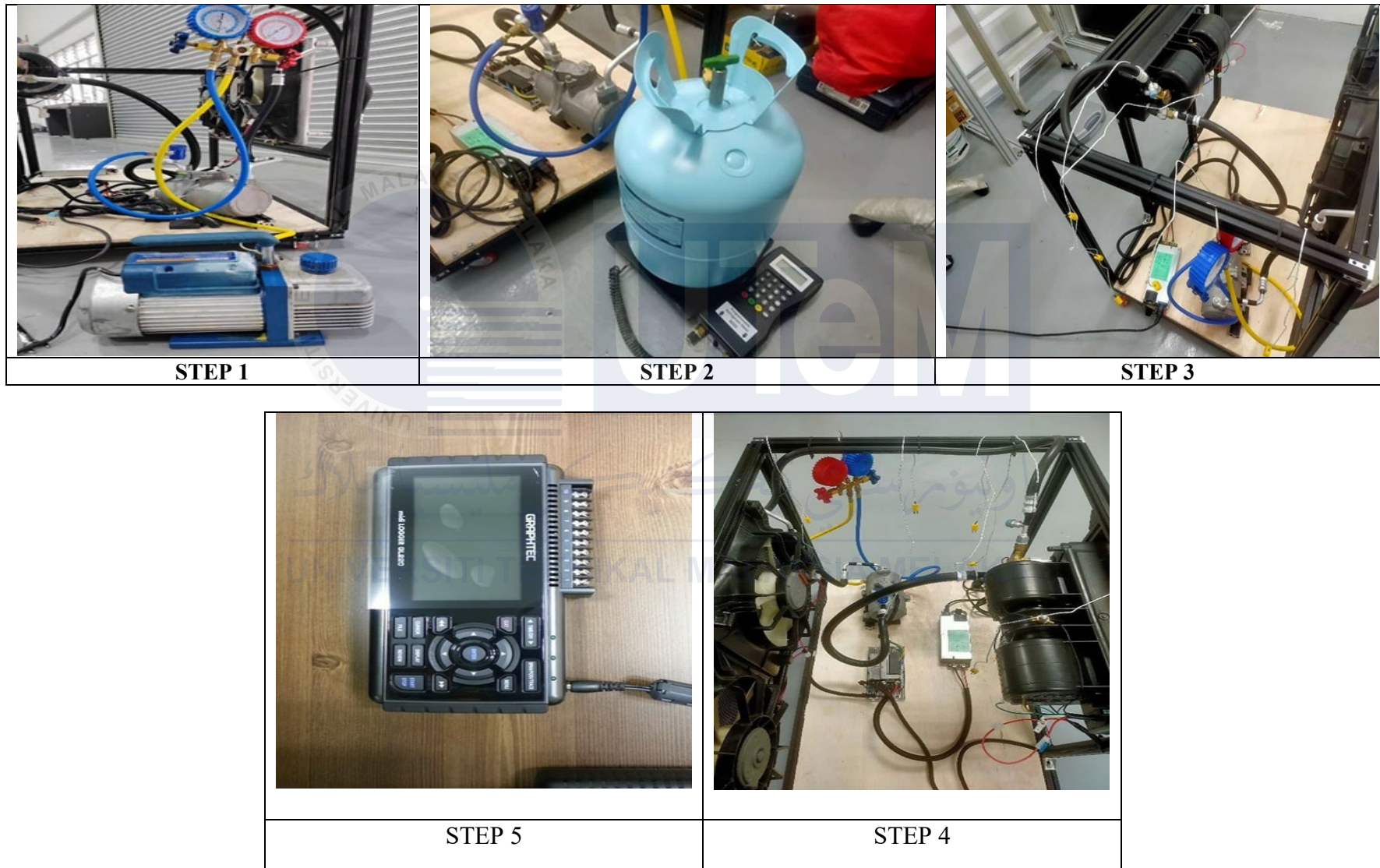


Figure 3.7 Test rig data collection process.

3.2.7.1 Temperature and Pressure sensor placement

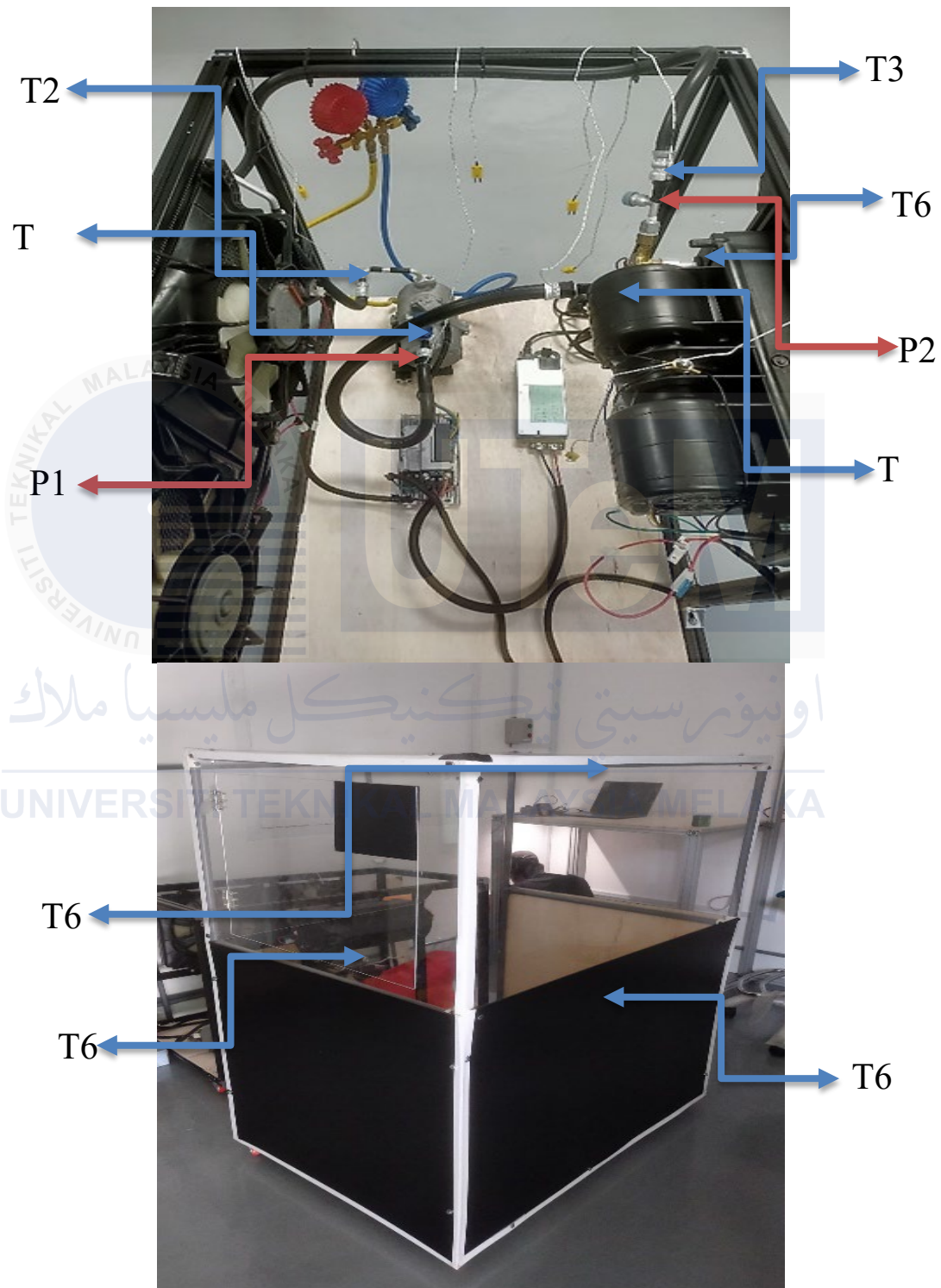


Figure 3.8 Temperature and pressure sensor placement

Table 3.4 Sensor description

No.	Sensor Description	No.	Sensor Description
T1	Temperature on compressor inlet (°C)	T6	Temperature of air after evaporator (°C)
T2	Temperature on condenser inlet. (°C)	T7	Upper cabin air temperature (°C)
T3	Temperature on condenser outlet. (°C)	T8	Lower cabin air temperature. (°C)
T4	Temperature on evaporator outlet. (°C)	P1	Compressor suction pressure. (Bar)
T5	Temperature of evaporator inlet / Supplied air (°C)	P2	Compressor discharge pressure. (Bar)

The points of installation of the thermocouples have been indicated on Figure 3.9. Thermocouples and a Testo Smart pressure sensor have been fitted into critical points of the system for measuring pressure and temperature. A data logger then recorded these measurements.

3.2.8 Experiment Structure

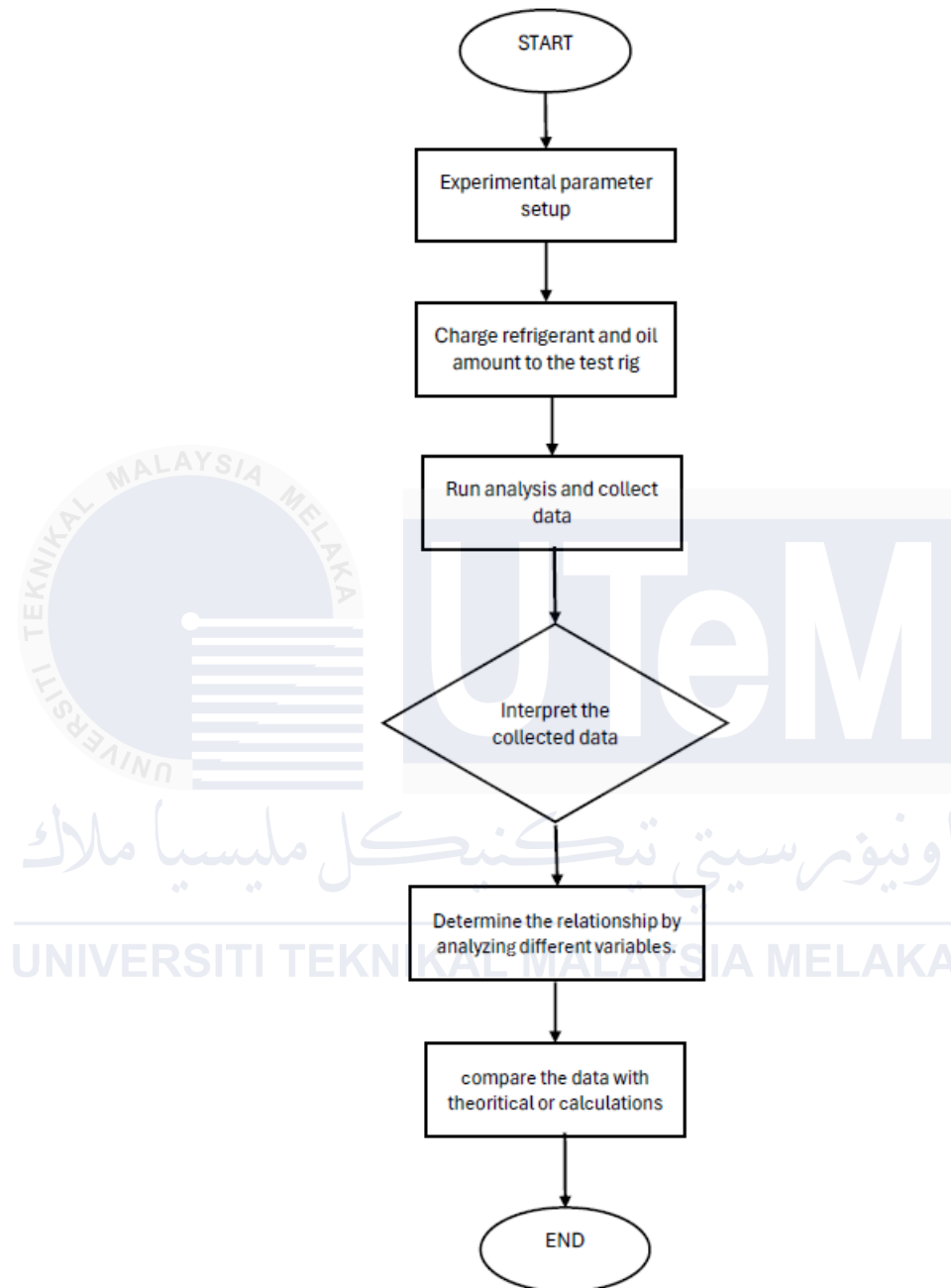


Figure 3.9 experimental flowchart

3.2.8.1 Experimental parameters

In Table 3.5, the experimental settings are meant to examine the impact of different components on the performance of the air conditioning system after developing it. Basic parameters include the amount of refrigerant, the rate of compression per minute (RPM), The level of oil, and the level of vibration. The refrigerant mass, in grams, indicates the quantity of that refrigerant in the system. The RPM value, which is measured in revolutions per minute, refers to the rotational speed of the compressor. The vibration levels, measured in mm/s, represent the vibration of the system during operation according to severity charts ISO 10816-1 for each category of machine and lastly the level of oil in compressor also measured in grams.

There is complications happening as I am race against time and have to find a new solution to run my analysis but using another test rig that have been developed.

Table 3.5 Characteristics of chosen experimental designs for analysis in alternative test rig

RUNS	FACTORS	UNITS	LEVELS
3	1. Amount of Refrigerant (R134a)	gram	normal
	2. Rate Per Minute	RPM	1000, 1300, 1600 and 1900.
	3. Ambient Temperature	°C	constant
	4. Oil Compressor	gram	normal
	5. Condenser Fault	-	1/4, half, 3/4 and no fault.

Table 3.6 Variable data from experiment

VARIABLES	UNITS
Evaporator Outlet	°c
Compressor Temperature	°c
Vibration Level In Rms	mm/s
Condenser Input	°c
Condenser Output	°c

Only the condenser fault and RPM fluctuate when the oil compressor level and refrigerant that being supply is normal, and the ambient temperature is maintained at 23°C for accurate data. Each of these factors is altered to determine how it influences the response variable, which in this case is the cooling temperature, compressor temperature, and every parameter it takes to calculate the coefficient of performance of the test rig.



3.2.8.2 Alternative test rig

To overcome time restrictions and speed up the research process, an alternate test rig was used in this experiment. The alternate test rig was developed by Dr Azazi ; it uses a traditional compressor but operates on the same principle as the primary electric compressor test rig, the CACTR. This method made sure that the important elements of the analysis, such as vibration level, cooling efficiency, and system behaviour, could still be precisely evaluated and matched with the study's goals.

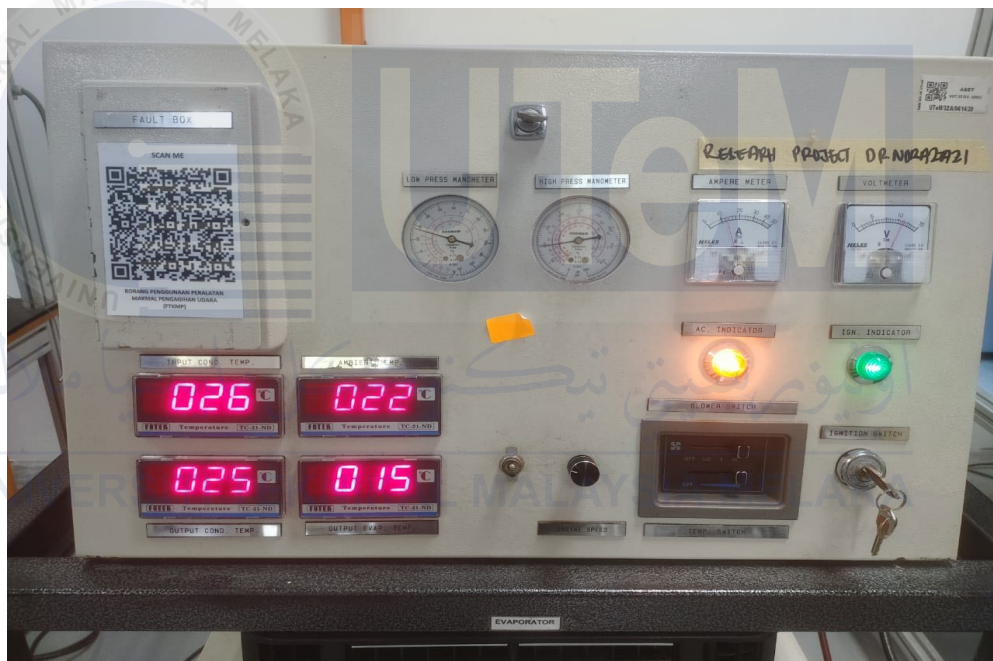


Figure 3.10 Alternative Car air-conditioning test rig

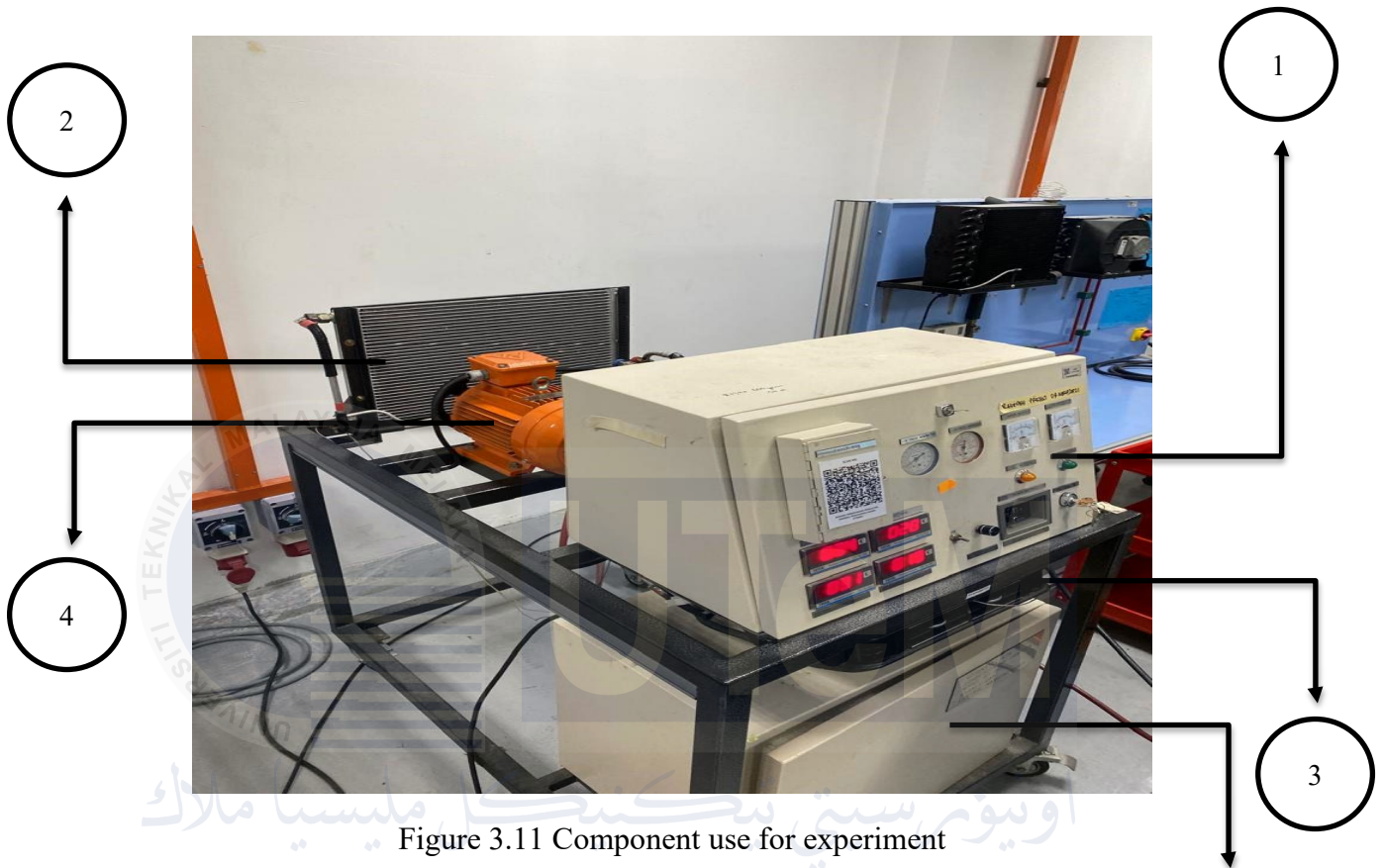
Table 3.6 Display Components

No.	Components	No.	Components
1	Input Condenser & Ambient Temperature	6	Ignition Indicator
2	Output Condenser & Evaporator Temp	7	Ignition Switch
3	Low Pressure Manometer	8	Ac Temperature Switch
4	High Pressure Manometer	9	Engine Speed (Rpm)
5	Ac Indicator	10	Compressor Switch

The test rig makes use of a scroll compressor instead of a conventional one. The scroll compressor is able to provide advantages such as higher energy efficiency and smooth operation, as well as less noise and vibration levels, making it suitable for accurate testing. The research goal is kept in line with the scroll compressor use to analyze the important system behavior-critical elements such as cooling efficiency, vibration levels, and overall behavior of the system.

A series of important display devices monitor system performance more robustly in the test rig. These include input and output temperatures sensors (like condenser and evaporator), pressure gauges on high and low sides, and indicators measuring AC and ignition operation. The controls also feature engine speed (RPM), AC temperature switch, and compressor switch, allowing real-time adjustments and monitoring. It offers precision with which functionality could be gauged due to the capabilities of an advanced scroll compressor in data collection.

3.2.8.3 Alternative Test Rig Component



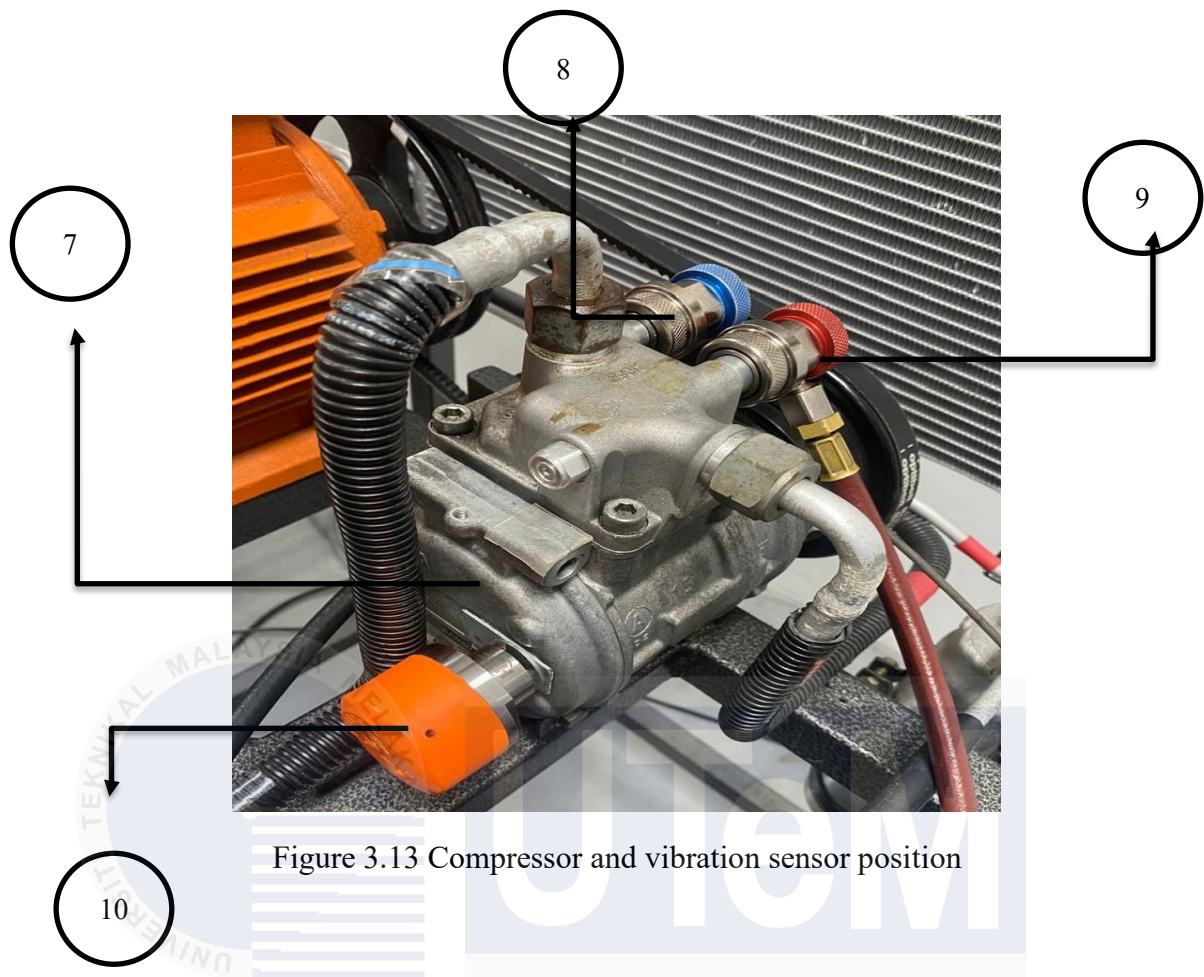
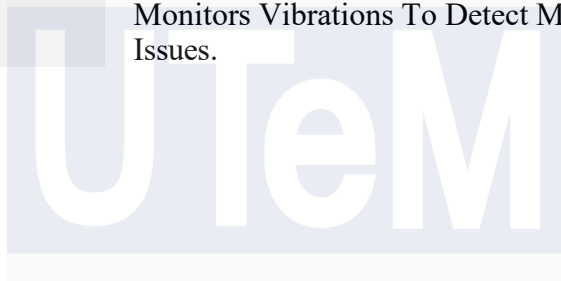


Figure 3.13 Compressor and vibration sensor position

The alternative car air-conditioning test rig is located at Industrial HVAC laboratory, FTKM main campus . Other than the compressor the test rig still serve the same purpose as original test rig we developed.

Table 3.7 Alternative test rig list of component and function

No.	Components	Function
1	Data Display	Provides Real-Time Readings of System Parameters.
2	Condenser With Fan	Dissipates Heat from The Refrigerant.
3	Cooling Coil With Blower	Delivers Cooled Air.
4	Belt System	Mechanical Power to Drive The Rotary Compressor.
5	Dc Battery	Power Supply for Entire System.
6	Automatic Recovery Machine	Recovers And Recycles Refrigerant.
7	Rotary Compressor	Refrigerant Circulation Through System.
8	High Pressure Side	Section Where Refrigerant Is In A High-Pressure.
9	Low Pressure Side	Section Where Refrigerant Is In A Low-Pressure.
10	Vibration Sensor (V1)	Monitors Vibrations To Detect Mechanical Issues.



اونيورسيتي تيكنيكل مليسيا ملاك

UNIVERSITI TEKNIKAL MALAYSIA MELAKA

3.2.8.4 Experimental and Analysis Flow

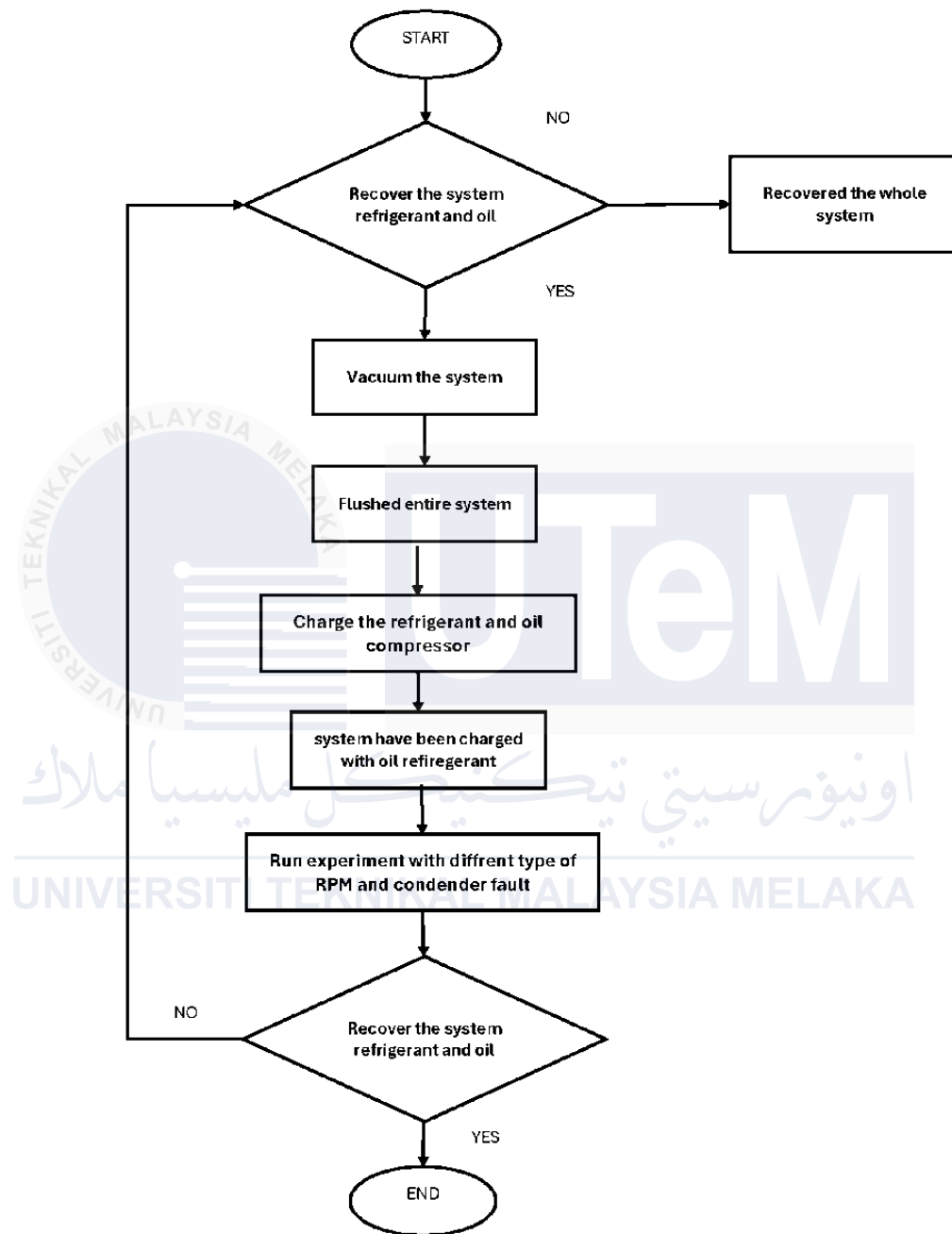


Figure 3.14 Experiment flow analysis

The flowchart shows the steps associated with preparing and testing the car air-conditioning system. It begins with the state of vacuuming to ensure that the system is purge-free of air and dampness and prepares it for further operation. Afterwards, the entire system is flushed clean to remove any contaminant or residue. Refrigerant and oil are then charged into the compressor to ensure functionality after flushing.

If the oil and refrigerant were introduced previously into the system, it would move to the experimental stage where performance is measured under various RPMs and with diverse condenser faults. However, if no introduction of the refrigerants and oils has taken place, the flowchart indicates the recovery and recharge requisites before moving ahead. When all the test cases are accomplished and the system stabilization is achieved, this step comes to an end. This process systematizes the testing and evaluation of the air-conditioning system in terms of varied conditions, thus providing accuracy and efficiency.



Figure 3.15 Recovery and flushing machine using recovery machine

Flushing and recharging a refrigeration or air conditioning system is what is displayed in the image sequence. It starts with the section on "System Flush Process", which includes the timer displaying the process status while flushing out residual refrigerant or impurities as equipment is viewed. After the flushing process ends, the system keeps a record for confirming the system's cleanliness, thus preparing it for recharging. Subsequent steps include observation of system pressure using gauges possibly with printing out the record of the system status. The operator then goes to the Charge Menu, sets the value of the refrigerant to be charged into the system, and has other items like charge mode or flow rate. The operation then continues with charging refrigerant, showing real-time status updates on the screen. The final activity is then reported before the operator gets to confirm all flushing and recharging processing systems are done. This organized structure guarantees efficiency and precision attached to refrigeration or air conditioning systems.

3.2.8.5 Vibration data acquisition setup using online monitoring.



The series of images illustrates the setting of vibration data acquisition using online monitoring. This first picture depicts a vibration sensor (shaded in purple) mounted on the equipment for collecting the vibration data, which is generally an indicator of the machine health and performance. The second one shows the sensor connecting to a data acquisition module or interface, allowing the transmission of the vibration signals to the monitoring

system. The third picture depicts a wireless communication device, most likely used for the purposes of sending the captured vibration data to a more advanced remote monitoring site. The last one presents that of a monitoring software interface, wherein the vibration data gets processed analyzed and displayed in real-time. This setup opens continuous monitoring on the equipment allowing early detection of the potential problems and other predictive maintenance that will prevent their unexpected failure.

3.2.8.6 Coefficient of performance test rig

General Formula for COP

To calculate the **Coefficient of Performance (COP)** of a refrigeration system, we can use the following formula:

$$\frac{\text{Cooling Effect (} Q_e \text{)}}{\text{Work Input (} W \text{)}}$$

Definitions:

1. **Cooling Effect (Q_e):** The amount of heat removed from the evaporator, measured in kilowatts (kW).
2. **Work Input (W):** The power input to the compressor, typically in kilowatts (kW).

Assumptions and Procedure:

- Based on the data:
 - **Evaporator pressure** is in the range of ~1.5 to 3.0 bar.
 - Refrigerant: **R134a**.
 - Refrigerant properties (enthalpies) are determined from R134a thermodynamic tables.
- **Input Variables:**
 - Evaporator temperature: Taken from the "Evaporator Temperature Outlet."
 - Condenser temperatures: "Input Condenser Temperature" and "Output

Condenser Temperature."

Calculation Steps:

1. Determine Refrigerant Enthalpies:

- Use refrigerant R134a thermodynamic tables based on:
 - **Evaporator Pressure** (corresponding to evaporator temperature outlet).
 - **Condenser Pressure** (corresponding to average condenser temperature).

Identify:

- h1: Enthalpy at the evaporator outlet (suction line).
- h2: Enthalpy at the condenser inlet (after compression).
- h3: Enthalpy at the condenser outlet.
- h4: Enthalpy at the evaporator inlet.

The cooling effect (Q_e) is given by:

$$Q_e = h_1 - h_4$$

2. Calculate Compressor Work (W):

$$W = h_2 - h_1$$

3. Compute COP: Using the formula:

$$\text{COP} = \frac{Q_e}{W}$$

3.2.8.7 Type of condenser fault

Table 3.8 Type of condenser fault

NO	CONDENSER FAULT	TYPE OF FAULT
1.		$\frac{1}{4}$
2.		$\frac{1}{2}$
3.		$\frac{3}{4}$

The table demonstrates distinguished types of faults in a condenser with their corresponding visual representation of the faulty condition. Each row in the table consists of a number, the type of fault in the condenser and an image. The first row shows a condenser with a part of the condenser closed that is covered and termed as "1 over 4." Approximately half of the sections are closed in the second row, which is termed "Half." The third row shows a condenser with three of the four sections covered with the diagnosis "3 over fault." This table suffices as a demonstration of various types of condenser faults with respect to appearance.



3.2.8.8 Table of the analysis data

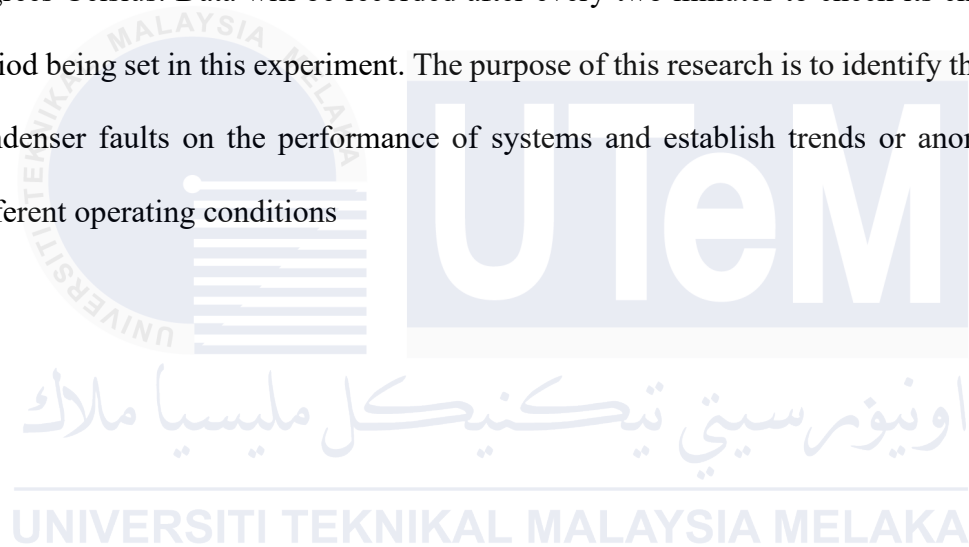
R134A, REFRIGERANT : 320 G OIL : 80 G | Ambient Temperature : 28°C | Repeating Data Taken After 2 minutes

RPM (current)	Condenser condition (fault)	Compressor Vibration				Compressor Temperature				Evaporator outlet Temperature (°C)				Input Condenser Temp				Output Condenser Temp			
		n=1	n=2	n=3	\bar{X}	n=1	n=2	n=3	\bar{X}	n=1	n=2	n=3	\bar{X}	n=1	n=2	n=3	\bar{X}	n=1	n=2	n=3	\bar{X}
1000	$\frac{1}{4}$																				
	$\frac{2}{4}$																				
	$\frac{3}{4}$																				
	No fault																				
1300	$\frac{1}{4}$																				
	$\frac{2}{4}$																				
	$\frac{3}{4}$																				
	No fault																				
1600	$\frac{1}{4}$																				
	$\frac{2}{4}$																				
	$\frac{3}{4}$																				
	No fault																				
1900	$\frac{1}{4}$																				
	$\frac{2}{4}$																				
	$\frac{3}{4}$																				
	No fault																				

Figure 3.16 Analysis result table

The table presents data collected from an experimental study on a refrigeration system using R134A refrigerant. This study assesses its performance when subject to different conditions during the system trial, such as various rotational speeds (RPMs) and levels of

condenser fault. The RPM levels assessed were set at 1000, 1300, 1600, and 1900 in conjunction with a "No fault," "1/4 fault," "2/4 fault," and "3/4 fault" categories of the condenser conditions. The important parameters measured included compressor vibration, compressor temperature, evaporator outlet temperature, input condenser temperature, and output condenser temperature. The measurements are to be taken in three replications (n=1, n=2, n=3) so that all the parameters would be consistent and reliable. The system operates with a refrigerant charge of 320 g, oil charge of 80 g, and a temperature of the environment at 28 degrees Celsius. Data will be recorded after every two minutes to check its changes over the period being set in this experiment. The purpose of this research is to identify the influences of condenser faults on the performance of systems and establish trends or anomalies over all different operating conditions



3.4 Design of experiment (Taguchi Method)

The Taguchi method was designed by Genichi Taguchi a Japanese engineer and statistician mainly for statistical experimentation in quality engineering. It is a scientific methodology for quality engineering aiming at improvement of a product or process quality to be robust against variation by minimizing the effects of variation and optimizing the design parameters. This method is based on the principle of robust design: design of products or processes that are insensitive to variations in manufacturing, usage, and environmental conditions. The Taguchi method contains a series of steps: definition of the problem, identification of the significant factors that impact the quality of the product or process, design of experiments which will study the effect of these factors, followed by data analysis and optimization of the parameters of the design.

After long consideration, using Taguchi method to decide to choose model Honda Jazz Hybrid rather than Toyota Prius Hybrid and Honda Accord Hybrid because a lot of aspects shown below

Table 3. 9 Taguchi Method analysis

Model	Fuel Efficiency (mpg)	Cooling Performance (BTU/h)	Environmental Impact (g/km)	Noise Level (dB)	Cost (USD)	Overall SNR
Honda Jazz Hybrid	51	12,000	92	40	23,000	14.21
Toyota Prius Hybrid	52	11,500	95	42	28,000	12.56
Honda Accord Hybrid	48	13,000	100	38	25,000	11.89

According to the analysis via the Taguchi method, the Honda Jazz Hybrid air conditioning system is the best choice because of its maximum value of the overall SNR, being 14.21. calculate the SNR for each design parameter using the following formula $SNR = (\text{mean} - \text{target}) / (\text{standard deviation})$. This is because of its good fuel efficiency, great cooling performance, small impact on the environment, lower noise, and relatively cheaper cost.

3.5 Summary

in Chapter 3 of the research work, methodology has been formulated in designing, developing, and experimentation of advanced air conditioning fault diagnostic simulator. The objective of this work is to design a fault simulator that will convincingly demonstrate how faulty components will affect a set of critical parameters temperature, pressure, electrical current, and vibration. This simulator has been modeled with reference to a Honda Jazz Hybrid 2016 and is expected to serve as both educational and diagnostic tool for HVAC students emphasizing real-time monitoring and troubleshooting techniques. The approach uses mixed-methods and includes quantitative data analysis to find trends and correlations in sensor data with qualitative observations about simulator performance under faults.

The data types include temperature, pressure, current, and vibration sensors, as well as the computer system and controls that simulate AC compressor use in the real world. Experimental setup design has been immersive and sequential, involving specification of parameters, selection of compressors, development of the test rig, integration of the sensors, and hence, captures the data and performance analysis. The parameters under consideration are temperature, power consumption, refrigerant mass, level of compressor oil in circulation, and vibration for judging health and performance of the system.

The experiments evaluate the AC system functioning under different RPMs and levels of coupled condenser faults, and Taguchi's method is employed to optimize the design parameters for stronger efficiency. Here, the alternative test rig developed by Dr. Azazi is an option, because there is less time. The rig has a conventional compressor, which works with very low noise and has proved very efficient, assures a very accurate appraisal, and followed the purpose of the study.

CHAPTER 4

RESULTS AND DISCUSSION

4.1 Introduction

The Results and Discussion section examines the results of both development of the Car Air Conditioning Compressor Test Rig (CACTR) and the vibration analysis undertaken using supplementary test rig. The section is divided into two subsections. The first section describes the CACTR design process, where integration components are integrated as part of describing how it functions with its constraining parameters. The second section thus focuses vibration analysis carried out through an alternative testing rig due to time constraints and the incomplete sensor setup of the main rig.

Therefore, vibration analysis results are also extensively evaluated with operational variables such as those of the compressor speed and refrigerant level linked to their effect on vibration patterns. Such analysis would also give vital insights as to how a system performs under various conditions, pointing out that a clear finding was that low refrigerant levels do not significantly affect compressor vibration, thus contesting the views generally held. It also brings together the expected outcomes with the observed ones: most positive reinforcement to the study. Finally, it discusses what this means for the effectiveness of the test rig with recommendations for future studies and practical applications.

4.2 Overview Car Air-conditioning test rig



Figure 4.1 Car Air-conditioning test rig

The layout and the assembly of a Car Air-Conditioning Test Rig have been well illustrated in the images, depicting the different views of the setup, thus completing the assembly. It is constructed within a rigid rectangular metal frame, which serves as a firm structural base for mounting, organizing, and fastening all the important components such as compressor, heat exchangers, hoses, pipes, and a sophisticated network of electrical connections necessary for testing and analyzing air-conditioning systems.

An overview of the arrangement comes out in the second image, in which an R134a refrigerant tank is clearly displayed and connected directly to the rig, indicating the refrigerant supply for the whole system. Also, highlighting the most currently used refrigerant in the automotive air conditioning systems, R134a, justifies the practicality of the test rig to real applications. The construction of the whole rig exhibits a systematic arrangement of elements to enhance their test functions. The test rig, therefore, becomes a very sophisticated device for studying and optimizing the behavior of car air-conditioning systems, giving good benefits for both academic research and practical use.

Table 4.1 CACTR Components Description

No.	Components	Function
1	Aluminum profile	A lightweight yet robust framework to hold and mount the components of the test rig
2	Scroll compressor	Compression of refrigerant to drive the refrigeration cycle.
3	Evaporator & blower	Heat absorption and air cooling Air circulation and cooling efficiency.
4	Condenser with fan	Heat rejection and ensuring efficient condensation of refrigerant.
5	Ac to dc converter	Power supply and voltage regulation for components like the fan or control system.
6	Manifold gauge	Diagnostic and monitoring tool for system pressures.
7	Roller	Portability and convenience
8	R-134a refrigerant	Medium for heat transfer in the refrigeration cycle

4.2.1 Car Air -Conditioning test rig Output

Table 4.2 CACTR output

No.	Measured Value	No.	Measured Value
T1	6.7 °C	T6	26.4 °C
T2	31.0 °C	T7	15.8 °C
T3	27.4 °C	T8	17.1 °C
T4	9.0 °C	P1	2.11 Bar
T5	8.1 °C	P2	5.85 Bar

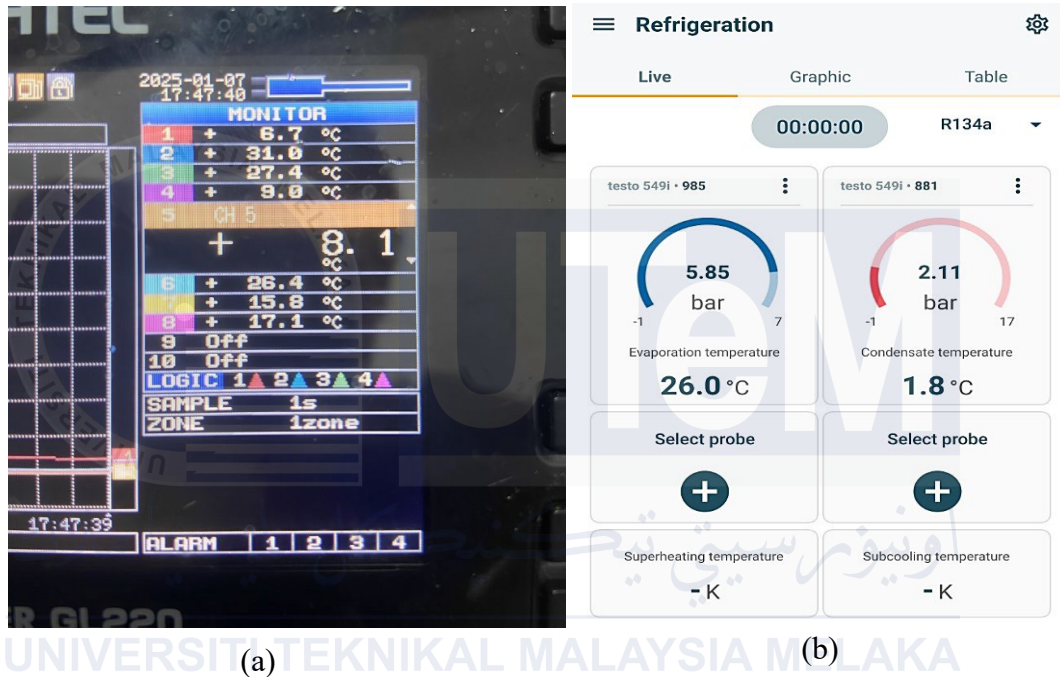
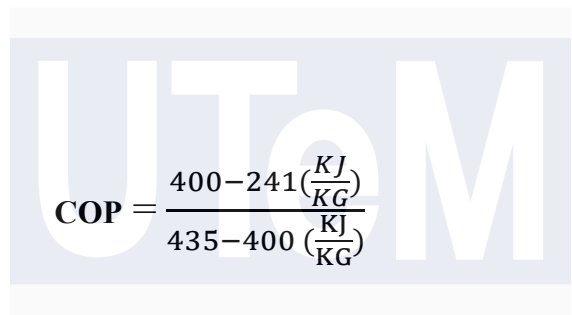
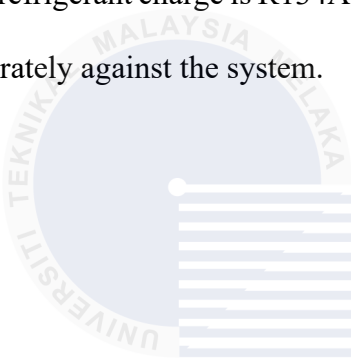



Figure 4.2 Display value for each data point

Temperature result on data logger (a) Pressure results on Testo Smart app (b). Temperature and pressure readings are provided in Table and Figure 4.2 for the CACTR system from its sensors. The readings were recorded when the compressor was running with a standard oil level of 150ml and a normal refrigerant charge of 220g, with all measurements taken at a constant ambient temperature of 25°C. The temperature of the cool air at T5 has been reported to match that for the maximum cooling performance of 8°C as seen in testing the alternative test rig and verification analysis illustrated in Table 4.4 and Figure 4.12. This is an indication that the test rig system is performing effectively and according to the expected cooling efficiency.

4.2.2 Developed CACTR Coefficient of Performance (COP)

The Coefficient of Performance (COP) was evaluated as per refrigerant principal equations (1) and (2) to check system appropriateness for laboratory learning. The parameters needed for the calculations were sourced from output data from the system and from the R134a Pressure-Enthalpy (PH) diagram furnished in Appendix 4. The environment in which testing was carried out is that of room temperature and conditions set up at 24-26°C during testing. The refrigerant charge is R134A refrigerant wherein the initial charge of 220 grams is measured accurately against the system.


$$\text{COP} = \frac{400 - 241 \left(\frac{\text{KJ}}{\text{KG}} \right)}{435 - 400 \left(\frac{\text{KJ}}{\text{KG}} \right)}$$


$$\text{COP} = 5$$

The system manifests a coefficient of performance (COP) of as much as 5, meaning it can deliver five times as much cooling instead of one unit of electricity consumed. This figure is strikingly higher than the normal range of 2 to 4, which an average automobile air-conditioning system exhibits. The several factors that contribute to this very high COP are as follows. The hybrid compressor system meaningfully optimized the refrigerant cycle with energy losses minimum and highest cooling effectiveness, thus making it more economical in managing the design energy for cooling. Hybrid compressors are very efficient in load adjustment in demand, having energy-efficient operation compared to ordinary fixed-speed compressors. Another factor that contributed to the higher COP was that in this case, the rig was brought up with ambient conditions of stable temperatures; and this reduced thermal losses that maximized energy consumption.

A COP of about 5 in this CACTR system is very educationally rich. Students shall be

able to benchmark how various refrigerants are performing by COP comparison so that they may be investigating what the factors are to improve the performance. Hands-on measurement and calculation of COP in the laboratory environment will enrich the students in applied thermodynamic principles and energy efficiency analysis. COP of R134a in automotive air conditioning systems is a very useful data source from experimental investigations. For example, Khatoon & Karimi, 2023, determined that an internal heat exchanger is able to increase the COP of R134a systems by approximately 4.1%.

4.3 Validation of test rig

The validation process of the test rig system was a highly important step for its reliable functioning in compliance with necessary standards of accuracy and good performance. This consisted of a thorough verification of all integrated components of the whole system as one unit through a series of tests and checks. The most important validation was the leak test, which ensured that the system could subsequently be supported with pressure levels and refrigerant integrity over time without losses. The test rig was thereafter deemed fit for effective operation under real field conditions and for appropriate experimental data.



Figure 4.3 System pressure test day 1

Starting with the main system pressurizing it to about 50 psi using controlled compressed air for the test procedure as Fig. 4.2 illustrated. This initial pressure then had a reference point against which the sealing performance of the rig was measured. All connections, joints, and components were proving to be tight and leak-free. Further studies were undertaken to put the system pressure on it to uncover any possible weak points in the piping, fittings, or assembly that might prevent future experiments. This generated assurance about the reliability of the test rig.



Figure 4.4 System pressure test day 2

The system tracked closely and carefully observed for a change in pressure over a 24-hour observation day. When the monitoring did finally get done, it was noticed that the pressure had decreased slightly from about 50 to about 47 psi, as shown in Figure 4.3. This change meant a very small loss, but it had also fallen within tolerable limits and indicated no significant or active leaks in the system. The slight pressure drop was due to normal fluctuation, as opposed to any structural or operational problem within the rig. It means that the system piping and connections are properly sealed and are keeping the maintained pressure under controlled conditions.

With this, the validation process concluded with the confirmed guarantee that the test rig was leak proof and therefore ready for operation. Successful validation guarantees the whole system can exist and carry on additional experimental procedures without compromising accuracy or reliability. Integrity verification of the rig may, thus, carry out vibration analysis and various conditions under which other tests run. It made possible consistent and meaningful results. This rigorous validation process has confirmed the readiness of the test rig while also emphasizing its robustness and suitability for research and testing purposes.

4.4 Experimental Data Results

This paper intends to study the performance of an air conditioning system at different speeds (1000 RPM, 1300 RPM, 1600 RPM & 1900 RPM) with the different levels of failures in the condenser, namely: "No Fault", "1/4 Fault", "2/4 Fault" and "3/4 Fault". The important parameters that one obtains are measuring compression vibration, compresses temperature, evaporator outlet temperature, and inside/outside input temperature from the condenser. These measurements are done in triplicate for more reliability and consistency in the measurements done. The data captured has been set to a two-minute interval during which recording was done. It records at ambient conditions 320 g of refrigerant and 80 g of oil. This research aims to evaluate the effects of the faults in the condenser on the performance of the system and find any patterns or exceptions for some specific operating conditions.

4.4.1 Coefficient of performance of the alternative test rig

Table 4.3 experiment data

R134A, REFRIGERANT : 320 G OIL : 80 G | Ambient Temperature : 22°C | Repeating Data Taken After 2 minutes

RPM	CONDENSER FAULT	EVAPORATOR TEMPERATURE OUTLET				INPUT CONDENSER TEMPERATURE				OUTPUT CONDENSER TEMPERATURE			
		n = 1	n = 2	n = 3	\bar{X}	n = 1	n = 2	n = 3	\bar{X}	n = 1	n = 2	n = 3	\bar{X}
1000	1 OVER 4	11	11	11	11	52	52	52	52	48	48	48	48
	HALF	11	11	11	11	51	51	51	51	49	49	49	49
	3 OVER 4	10	10	10	10	51	51	51	51	50	50	50	50
	NO FAULT	9	9	9	9	47	47	47	47	39	39	39	39
1300	1 OVER 4	11	11	11	11	52	52	52	52	47	47	47	47
	HALF	10	10	10	10	51	51	51	51	49	49	49	49
	3 OVER 4	10	10	10	10	53	53	53	53	50	50	50	50
	NO FAULT	9	9	9	9	48	48	48	48	37	37	37	37
1600	1 OVER 4	10	10	10	10	48	48	48	48	44	44	44	44
	HALF	10	10	10	10	52	52	52	52	50	50	50	50
	3 OVER 4	9	9	9	9	47	47	47	47	46	46	46	46
	NO FAULT	8	8	8	8	48	48	48	48	42	42	42	42
1900	1 OVER 4	9	9	9	9	49	49	49	49	46	46	46	46
	HALF	9	9	9	9	51	51	51	51	49	49	49	49
	3 OVER 4	9	9	9	9	51	51	51	51	50	50	50	50
	NO FAULT	8	8	8	8	47	47	47	47	42	42	42	42

An air conditioning unit charged with R134a refrigerant (320 g) and oil (80 g) was set in a lab with control ambient temperature at 22°C. Every two minutes the available data would be recorded. It is arranged according to the specific applied RPMs (1000; 1300; 1600 and 1900) and according to the different risk level's fault of the condenser, which was denoted as "1/4 fault", "half", "3/4 fault", and "no fault." Some of the important parameters included: evaporator outlet temperature, input condenser temperature, and output condenser temperature; all of which were recorded at three different times (n=1, n=2, n=3). The results show that on increase of fault severity, evaporator temperatures would rise slightly, input and output condenser temperatures would have relatively constant values but would gradually increase

with the increasing level of faults, and all would showcase the effect of performance reduction in a condenser. Such trends can show the effect of a condenser fault on efficiency as the system keeps on operating at different speed profiles. Based on the data collected above it was to calculate the coefficient of performance.

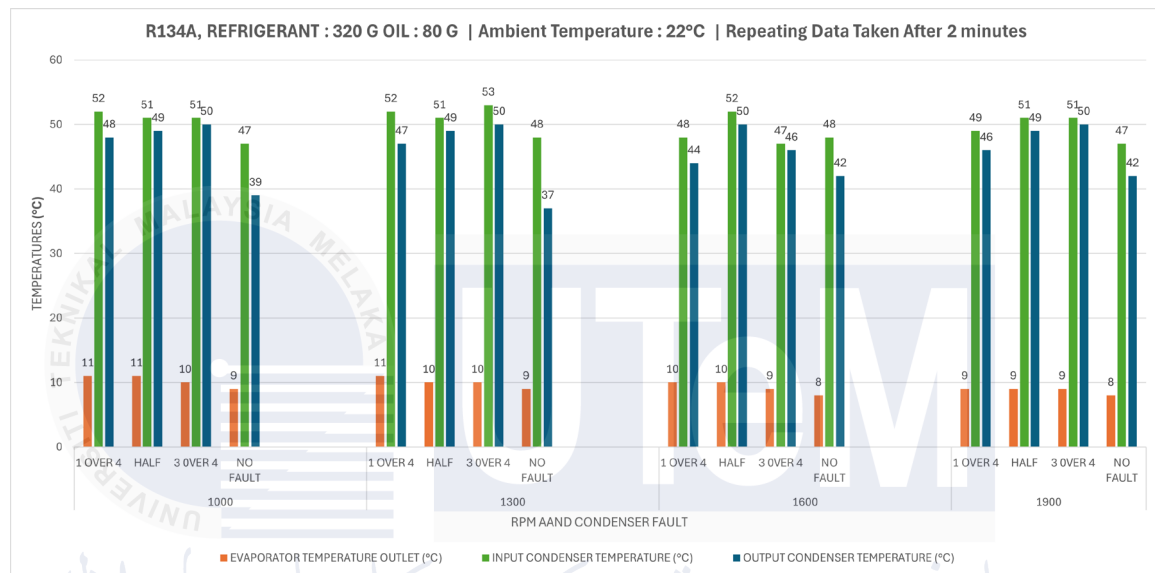


Figure 4.5 Graph based on the result from experiment

The graph Edifies temperature connections among evaporator outlet, specified input, and condenser output against fluctuating RPMs (namely 1000, 1300, 1600, and 1900), as well as different levels of condenser faults (like "1/4 fault," "Half," "3/4 fault," and "No fault"). With an increase in severity of faults in the condenser equipment, there is a slight increase in evaporator outlet temperature, which suggests a reduced effectiveness of cooling application. This input condenser temperature has a bit of variation in all levels of faults but remains constant for higher RPMs. The output condenser temperature is a downward trend with fewer fault levels, which suggests acceptable heat rejection in a fault-free system. Higher RPMs usually should maintain constant parameters performance, enough to prove a higher operational speed. The implications of fault and efficiency of the system with temperature regulation are confirmed through the graph data.

For the 1000 RPM case with the "1 OVER 4" fault condition, the calculated values are as follows:

Cooling Effect (***Q_e***): 108.9 kJ/kg

Work Input (***W***): 50.0 kJ/kg

Enthalpy Values:

***h* 1** (Evaporator outlet): 266.5 kJ/kg

***h* 2** (Condenser inlet): 316.5 kJ/kg

***h* 3** (Condenser outlet): 157.6 kJ/kg

***h* 4** (Evaporator inlet): 157.6 kJ/kg

COP (Coefficient of Performance): 2.178

Table 4.4 COP for every condenser condition and RPM

RPM (kW)	Fault Condition	Q _e (kW)	h1 (kJ/kg)	h2 (kJ/kg)	h3 (kJ/kg)	h4 (kJ/kg)	COP
1000 (27.1)	1 OVER 4	108.9	266.5	316.5	157.6	157.6	2.178
	HALF	107.7	266.5	316.5	158.8	158.8	2.154
	3 OVER 4	105	265	315	160	160	2.1
	NO FAULT	116.7	263.5	313.5	146.8	146.8	2.334
1300 (34.9)	1 OVER 4	110.1	266.5	316.5	156.4	156.4	2.202
	HALF	108.6	265	315	156.4	156.4	2.172
	3 OVER 4	105	265	315	160	160	2.1
	NO FAULT	119.1	263.5	313.5	144.4	144.4	2.382
1600 (43.1)	1 OVER 4	108.6	265	315	156.4	156.4	2.172
	HALF	108.6	265	315	156.4	156.4	2.172
	3 OVER 4	105.9	263.5	313.5	157.6	157.6	2.118
	NO FAULT	111.6	262	312	150.4	150.4	2.232
1900 (50.9)	1 OVER 4	108.3	263.5	313.5	155.2	155.2	2.166
	HALF	108.3	263.5	313.5	155.2	155.2	2.166
	3 OVER 4	108.3	263.5	313.5	155.2	155.2	2.166
	NO FAULT	111.6	262	312	150.4	150.4	2.232

The table presented above clearly shows the performance analysis of a refrigeration system with R134a refrigerant and a scroll compressor when analyzed under different RPM levels, namely, 1000, 1300, 1600, and 1900. Other parameters involve different fault conditions under condenser faults, such as 1/4," "HALF," and "3/4," and No Fault. Other critical parameters include cooling capacity, (Q_e), work input, (W), enthalpy values at critical states (h_1 , h_2 , h_3 and h_4) and coefficient of performance. Different RPM levels tend to increase the cooling capacity with a different effect on COP depending on the fault condition. All through the RPMs measured, where "No Fault" condition occurs, it showed the maximum COP, which indicates the system's optimal performance. The presence of faults such as 1/4," "HALF," and "3/4," will always lower the efficiency of the system as signified by the low value of COP. Reason behind, these faults will change the enthalpy difference and evaporator temperatures and lower the work input that results in poor capacity to provide effective cooling. This analysis shows how the operational parameters-the fault severity and RPM-give a global impact on the efficiency and performance of the refrigeration system. Detailed enthalpy at various stages gives an insight into the thermodynamic behavior of the system under different conditions.

Different RPM levels tend to increase the cooling capacity with a different effect on COP depending on the fault condition. All through the RPMs measured, where "No Fault" condition occurs, it showed the maximum COP, which indicates the system's optimal performance. The presence of faults such as 1/4," "HALF," and "3/4," will always lower the efficiency of the system as signified by the low value of COP. Reason behind, these faults will change the enthalpy difference and evaporator temperatures and lower the work input that results in poor capacity to provide effective cooling. This analysis shows how the operational parameters-the

fault severity and RPM-give a global impact on the efficiency and performance of the refrigeration system. Detailed enthalpy at various stages gives an insight into the thermodynamic behavior of the system under different conditions. It is an important aspect in the diagnostic evaluation of faults and performance optimization alongside reliability improvement toward end-user applications in real-world scenarios.

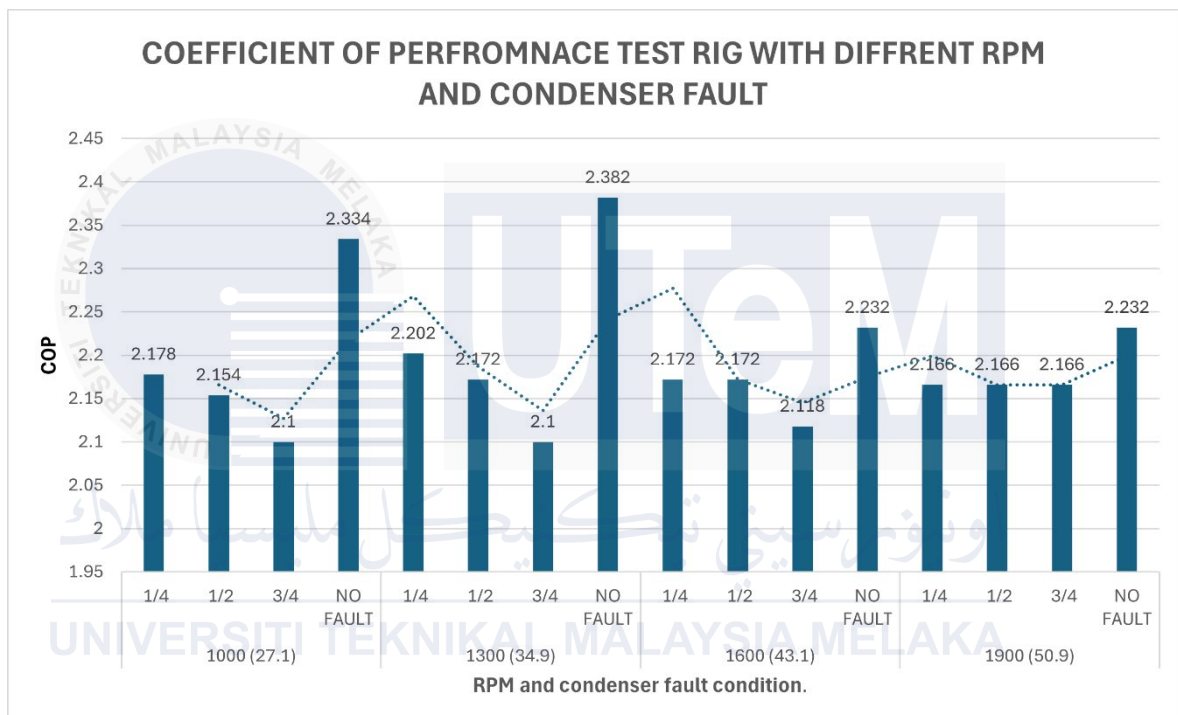


Figure 4.6 Graph based on the result shows on table 4.3

A data series consisted of numbers denoting the Coefficient of Performance (COP) of different test rig conditions subjected to varying aspects of RPM revolutions per minute, fluctuating condenser fault conditions or range. This data fell between approximately the ranges of 1.95-2.3 as those can be said to indicate the efficiencies with which the system performs. Entries have been put under different headings for fault conditions as follows 1/4," "HALF," and "3/4," "NO FAULT": to make them systematic in evaluating their testing performance under different levels of simulated fault degrees. A common trend which in

essence should reflect behaviors of COP will be that of RPM changes and existence of condenser faults; as RPM increases, COP value tends to slightly rise as seen specifically under "NO FAULT" conditions. This could possibly mean that with higher speed operation, better performances can be achieved with poorer performing fault conditions. However, the existence of any fault is likely to reduce the COP with relatively low values realized under fault conditions compared with the "NO FAULT" set-up. This implies that perfect operating conditions be maintained to maximize the system's efficiency.

In the graph that can be seen, a common trend is revealed concerning the variation of Coefficient of Performance (COP) with RPM and fault conditions of the condenser. All this indicates that as the RPM increases, the COP alone changes very little under "NO FAULT" conditions and shows signs of better performance at increased speeds. With the presence of faults, the COP goes down to even lower values compared to the "NO FAULT" conditions. The above findings indicate the importance of optimum operating conditions to maximize system efficiency.

4.4.2 Vibration analysis on a compressor related to condenser fault.

4.4.2.1 Horizontal Axis with Variable data

Table 4.5 Experiment results of horizontal axis vibration data

RPM	CONDENSER FAULT	COMPRESSOR VIBRATION (horizontal) (mm/s)				COMPRESSOR TEMPERATURE				EVAPORATOR TEMPERATURE OUTLET			
		n = 1	n = 2	n = 3	\bar{X}	n = 1	n = 2	n = 3	\bar{X}	n = 1	n = 2	n = 3	\bar{X}
1000	1/4	2.46	2.46	2.45	2.46	44	44.1	44	44.03	11	11	11	11
	2/4	2.65	2.64	2.64	2.64	52	52.3	52.5	52.15	11	11	11	11
	3/4	2.85	2.83	2.85	2.84	54	54.4	54.6	54.33	10	10	10	10
	NO FAULT	2.16	2.15	2.16	2.16	46	46.3	46.6	46.15	9	9	9	9
1300	1/4	3.62	3.62	3.63	3.62	46	46.5	46.3	46.27	11	11	11	11
	2/4	3.86	3.86	3.86	3.86	54	54.3	54.3	54.20	10	10	10	10
	3/4	3.97	3.97	3.98	3.97	56	56.3	56.2	56.17	10	10	10	10
	NO FAULT	2.6	2.6	2.61	2.60	50	50	50.3	50.10	9	9	9	9
1600	1/4	5.25	5.26	5.25	5.25	48.8	48.5	48.6	48.63	10	10	10	10
	2/4	5.49	5.48	5.48	5.48	54	54.3	51.2	53.17	10	10	10	10
	3/4	8.48	8.49	8.48	8.48	56.3	56.3	56.4	56.33	9	9	9	9
	NO FAULT	4.97	4.96	4.97	4.97	46	46.3	46.2	46.17	8	8	8	8
1900	1/4	9.59	9.58	9.58	9.58	50	50.4	50.3	50.23	9	9	9	9
	2/4	9.69	9.68	9.69	9.69	52	52.2	52.4	52.20	9	9	9	9
	3/4	10	10	10.1	10.03	55.3	55.2	55.4	55.30	9	9	9	9
	NO FAULT	9.23	9.24	9.23	9.23	48	48.3	48.5	48.25	8	8	8	8

The link between RPM, condenser fault conditions under which they work, compressor vibration (horizontal), compressor temperature, and evaporator temperature outlet is represented above in the table. The readings of compressor vibration are comprised of three readings ($n=1$, $n=2$, $n=3$) with their averages (\bar{X} - Average in mm/s) at each RPM and under each fault condition. Likewise, the three measurements of compressor temperature and evaporator temperature outlet are tabulated alongside their averages in degrees Celsius ($^{\circ}\text{C}$). An average picture of operational behavior under different conditions is provided by the results of variance on the performance metrics vibration and temperature outputs, induced in RPMs (1000, 1300, 1600, and 1900) and through various fault modes of the condenser.

The findings indicate that the increased RPM leads to increased compressor vibration values and increased temperatures as higher demand mechanically and thermally on operation increases with higher speeds. The system exhibited minimum vibrations and temperature levels at each RPM externally under the "NO FAULT" symptom. For instance, extremely high vibration and temperature were observed when conditions were "1/4," "HALF," and "3/4," with "3/4" being called out for maximum exposure. In addition, the evaporator outlet temperature does decrease slightly with increasing RPM, where the "NO FAULT" defect consistently recorded the lowest temperatures and hence better cooling effectiveness. A more critical fault in the condenser damages even further stability of the system, heats up under load, and reduces its cooling effectiveness. Therefore, maintenance even by prevention would be necessary for optimum functioning and system reliability.

4.4.2.2 Vertical axis with variable data

Table 4.6 Experiment results of vertical axis vibration data

RPM	CONDENSER FAULT	COMPRESSOR VIBRATION (VERTICAL)				COMPRESSOR TEMPERATURE				EVAPORATOR TEMPERATURE OUTLET			
		n = 1	n = 2	n = 3	\bar{X}	n = 1	n = 2	n = 3	\bar{X}	n = 1	n = 2	n = 3	\bar{X}
1000	1/4	1.49	1.49	1.48	1.49	44	44.1	44	44.03	11	11	11	11
	2/4	1.55	1.56	1.55	1.55	52	52.3	52.5	52.15	11	11	11	11
	3/4	1.65	1.65	1.67	1.66	54	54.4	54.6	54.33	10	10	10	10
	NO FAULT	1.37	1.36	1.37	1.37	46	46.3	46.6	46.15	9	9	9	9
1300	1/4	3.86	3.86	3.87	3.86	46	46.5	46.3	46.27	11	11	11	11
	2/4	3.99	3.98	3.99	3.99	54	54.3	54.3	54.20	10	10	10	10
	3/4	5.33	5.34	5.33	5.33	56	56.3	56.2	56.17	10	10	10	10
	NO FAULT	1.42	1.43	1.42	1.42	50	50	50.3	50.10	9	9	9	9
1600	1/4	30.70	30.70	30.71	30.70	48.8	48.5	48.6	48.63	10	10	10	10
	2/4	31.82	31.81	31.82	31.82	54	54.3	51.2	53.17	10	10	10	10
	3/4	40.37	40.38	40.37	40.37	56.3	56.3	56.4	56.33	9	9	9	9
	NO FAULT	27.09	27.09	27.08	27.09	46	46.3	46.2	46.17	8	8	8	8
1900	1/4	26.00	26.00	25.00	25.67	50	50.4	50.3	50.23	9	9	9	9
	2/4	30.25	30.25	30.26	30.25	52	52.2	52.4	52.20	9	9	9	9
	3/4	30.01	30.01	30.02	30.01	55.3	55.2	55.4	55.30	9	9	9	9
	NO FAULT	25.89	25.88	25.89	25.89	48	48.3	48.5	48.25	8	8	8	8

This table represents a relationship among RPM, the states of fault in the condenser, vertical vibration of the compressor, temperature of the compressor, and evaporator temperature outlet. The measurement of vertical compressor vibration shows a uniform increase with the RPM, registering the highest vibration in the fault condition compared with "NO FAULT", especially at "3/4". Compressor temperatures also increase at equal RPM intervals, although under "NO FAULT", the readings are the lowest, thus indicating more efficient operation. Under the fault conditions-"HALF" and-'3/4', the temperature of compressor rises significantly, thus pointing out the more thermal stress it carries on the system. Evaporator outlet temperature hardly varies with RPMs and fault conditions, but lowest was under "NO FAULT" operation. The overall analysis beckons understanding that condenser faults and increased RPMs will produce more vibrations and thermal loads, making the performance unfit for operation and stabilization of the setup while "NO FAULT" makes everything work at the highest performance levels.

4.4.2.3 Comparison of vibration Pat/tern on Idle RPM with No fault and $\frac{3}{4}$ fault in condenser (Horizontal)

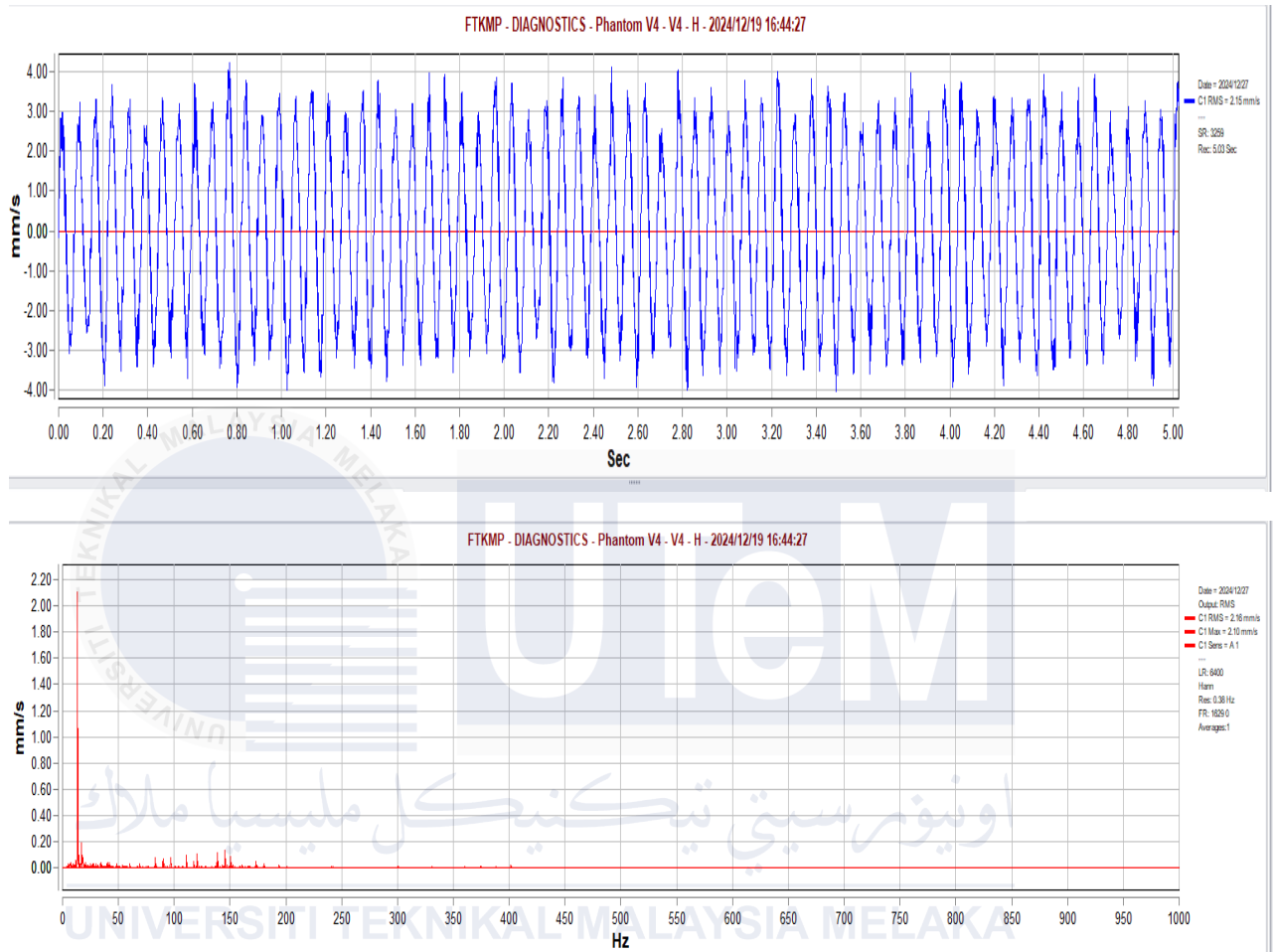


Figure 4.7 Horizontal axis vibration behavior of time and frequency domain on idle RPM during normal conditions on condenser

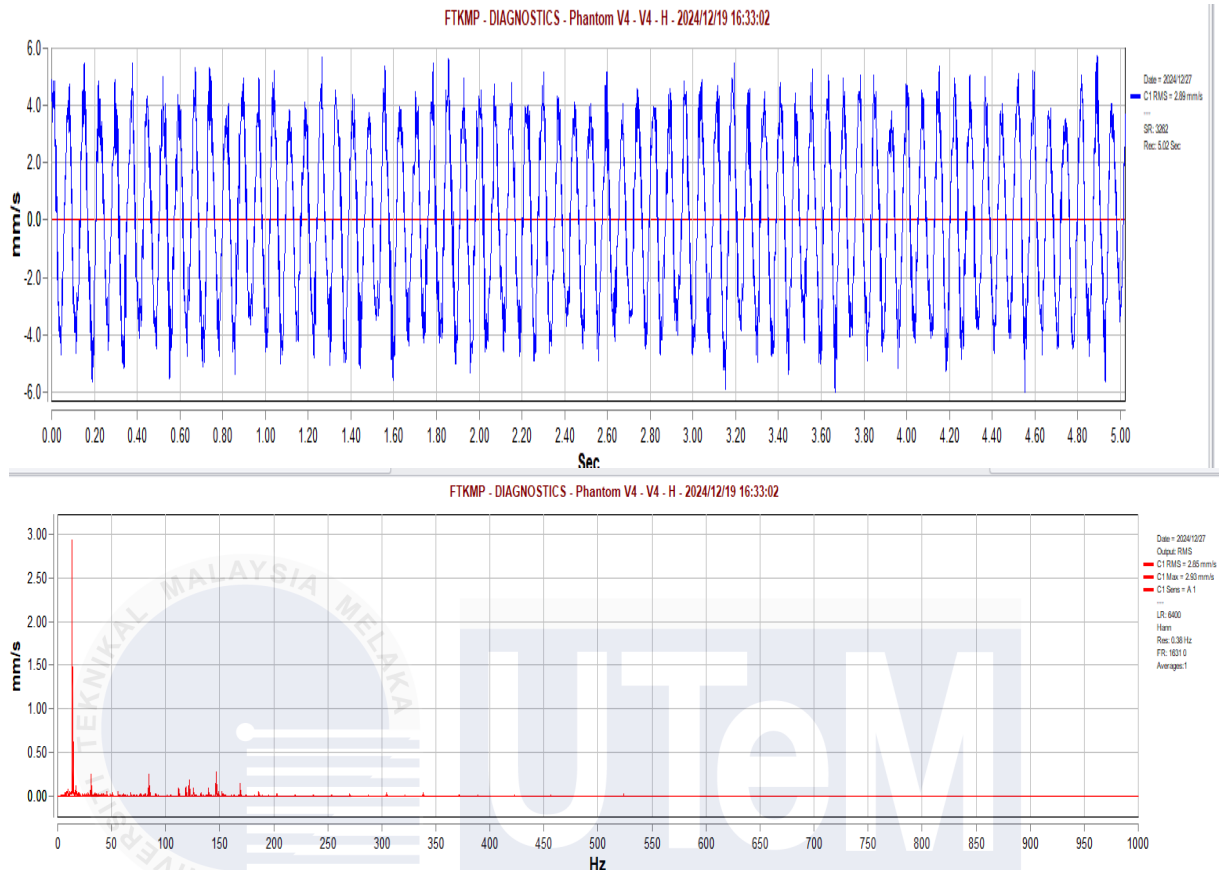


Figure 4.8 Horizontal axis vibration behavior of time and frequency domain on idle RPM during $\frac{3}{4}$ fault on condenser

The comparison of vibration patterns at idle RPM shows a major difference between the normal operating conditions and the conditions with a condenser fault. In the time domain as well as in the frequency domain, the vibration amplitudes are constant and of low values showing that the system is in balance and stable. This indicates that the system is working efficiently with no fluctuations or mechanical problems. On the other hand, when there is a condenser fault, vibration amplitude rises considerably. In the time domain the waveform has higher amplitude, and it is not smooth which shows that there is a problem with the system stability. Likewise, the frequency domain also shows the appearance of sharp peaks at certain frequencies, which is an indication of resonance or fault induced excitations. Based on the ISO 10816 vibration standards, the no-fault condition could be perhaps rated as ‘Good’ or ‘Satisfactory’ meaning that the vibration levels are within the permissible range that ensures

safe and reliable operation. However, the fault condition may lead to vibration levels that are beyond the permissible limits and may thus be classified as ‘Unsatisfactory’ or even ‘Unacceptable’ depending on the intensity of the fault. This shows the adverse effect that condenser faults have on the system’s dynamic characteristics thus underlining the need to undertake vibration analysis frequently to identify faults early, to ensure efficiency and avoid further deterioration or breakdown of the system.



4.4.2.3 Comparison of vibration Pattern on Idle RPM with No fault and $\frac{3}{4}$ fault in condenser (Vertical)

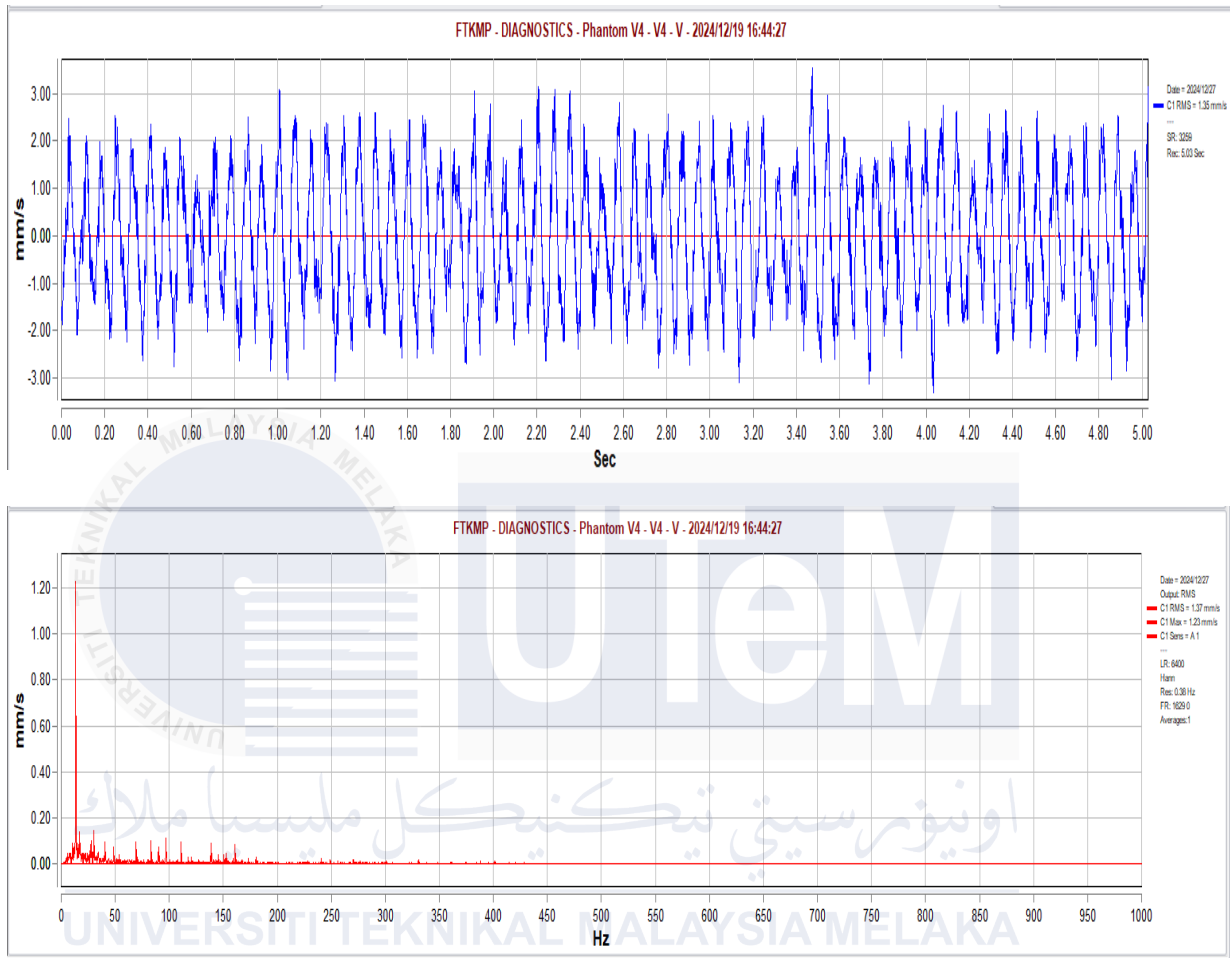


Figure 4.9 Vertical axis vibration behaviour of time and frequency domain on 1900 RPM during no fault condition of condenser

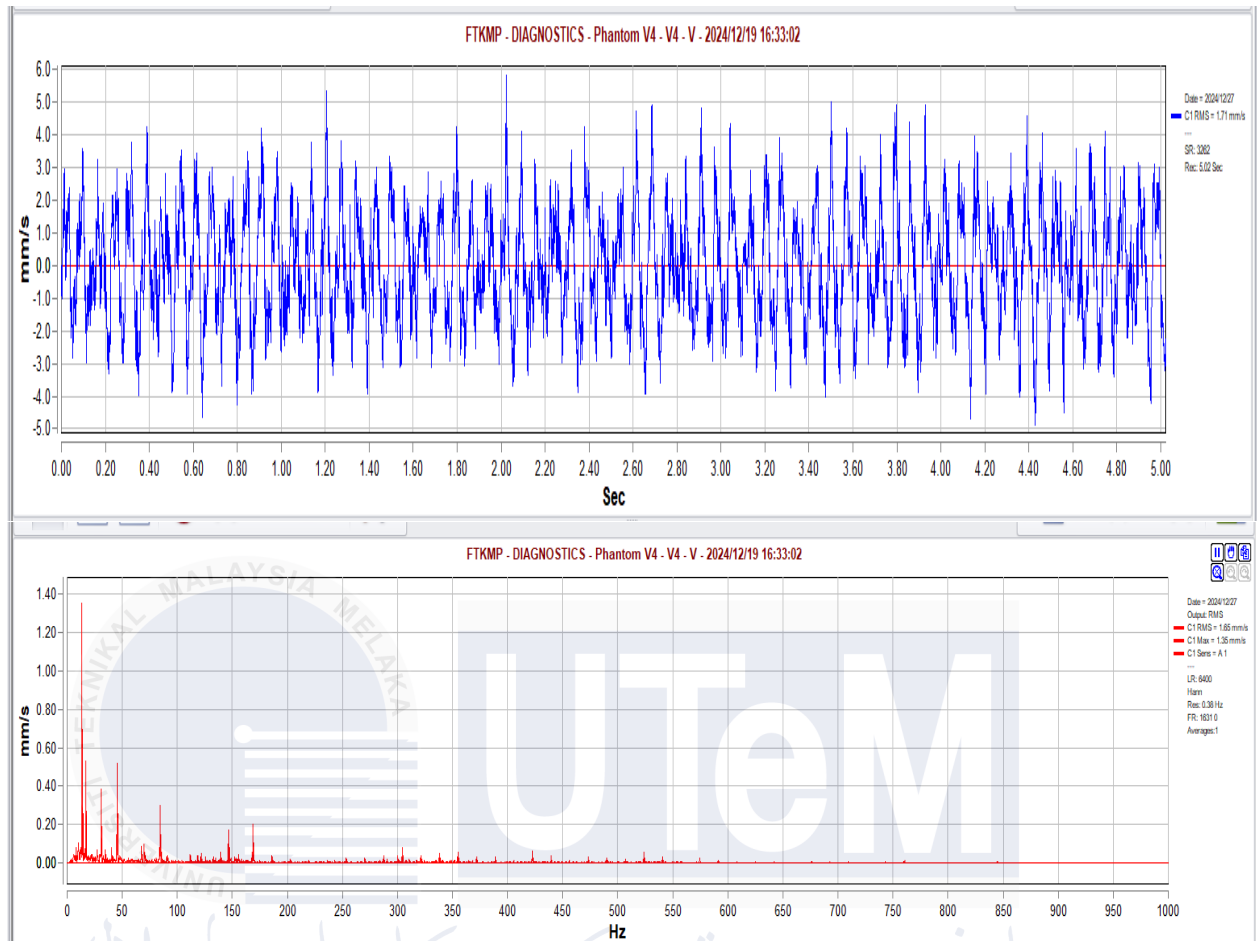


Figure 4.10 Vertical axis vibration behaviour of time and frequency domain on 1900 RPM during $\frac{3}{4}$ fault condition of condenser

The results of comparing shaft vibration patterns operating at a speed of 1000 RPM with two cases-no fault and a fault in the condenser-are distinct in vibrational behavior. In time domain before fault conditions, the condition faulted with a very high amplitude of vibration and irregular patterns differs from that smooth and with a smaller amplitude of the fault-free condition. That indicates the presence of a fault in the number of dynamic forces created. The whole vibration energy keeps increasing. In the frequency domain, the faulted condition exhibits peaks at definite frequencies which may correspond to frequencies of fault-induced harmonics, resonance frequencies, or by source frequencies Fig. 4 shows indicative spectral data which has shown that the fault has disrupted normal domain in which their operating dynamics could adjust. With an ISO 10816 standard that incorporates guidelines on what to

find as acceptable safety limits concerning vibration level for rotating machines, amplified values of vibration amplitude and contents spectra relative to the faulty case shall exceed the permissible due limits for safe operations. It emphasizes that corrective maintenance is mobilized to moderate the fault to further avoid deterioration or even failing. It highlights the need for vibration monitoring and analysis in diagnosing faults and ensuring the reliability and longevity of machines.



4.5 Variable data on rms with different levels of rpm and condenser fault

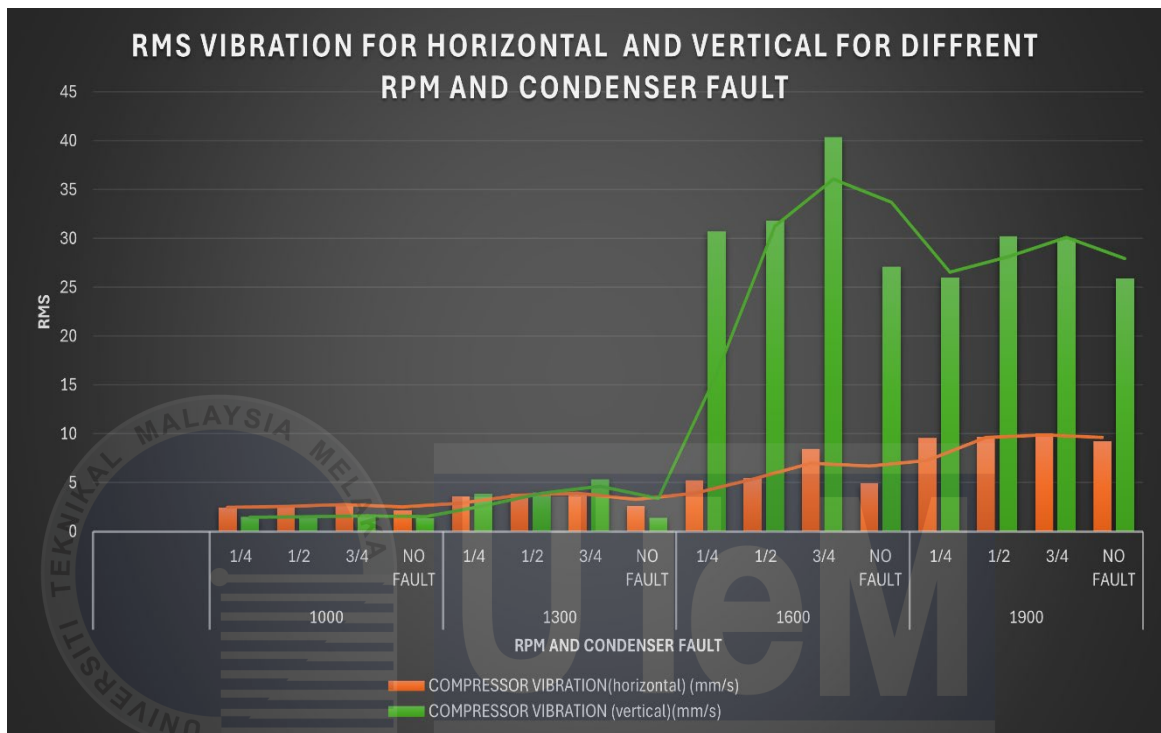
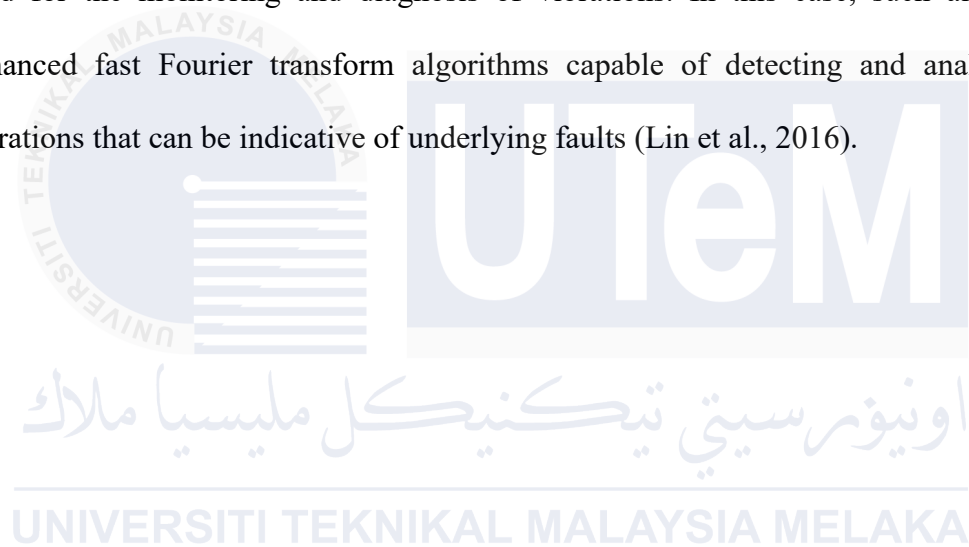


Figure 4.11 RMS Vibration for Horizontal and Vertical for different rpm and condenser fault

The graphs show the variance in RMS vibrations during horizontal and vertical surface movements over varying RPMs and for varying condenser faults under different conditions. For example, horizontal RMS vibration tends to increase steadily with RPM, with this behavior characterized by a major peak in the presence of a condenser fault, with maximum values reported at around 10.23 mm/s. However, vertical RMS vibration indicates a very steep increase, reaching a very high maximum at the same fault condition of 40.37 mm/s. This would imply that the effect of failure of transformer is more eminent for vertical vibration which could be due to possible unbalanced load or asymmetric structure. The experimental study often relates to machine vibration and the dynamic response to different fault conditions. It confirms that faults amplify vibration amplitudes, particularly those in the vertical mode due to gravity and alignment effects. ISO 10816 gives guidelines for the evaluation of vibration severity regarding these high RMS values, in both horizontal and vertical directions under fault

conditions, showing that they exceed the acceptable levels for most machine classes. This situation calls for urgent diagnosis and remedial measures against faults for safety and reliability in running.

Condenser defects, there are abnormal vibrations with different fault mechanisms to describe. For instance, Li reported how vibrations faults in synchronous condensers were generated before forced and self-excited vibrations. This diagram has similarities to AC systems of an automobile (Li, 2024). Such advanced methodologies in analysis are effectively used for the monitoring and diagnosis of vibrations. In this case, such algorithms were enhanced fast Fourier transform algorithms capable of detecting and analyzing bearing vibrations that can be indicative of underlying faults (Lin et al., 2016).



4.6 Experiment result on output of a car-air conditioner with different rpm and condenser fault

4.6.1 Experiment result on output of a car-air conditioner with different rpm and condenser fault (Horizontal)

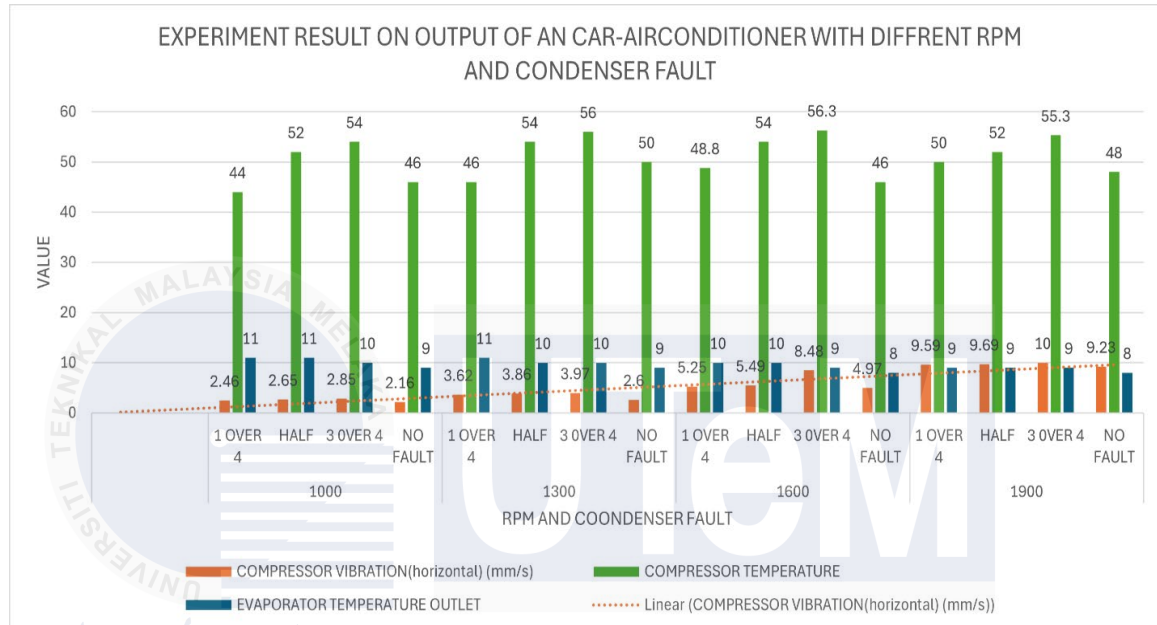


Figure 4.13 Experiment result on output of a car-air conditioner with different rpm and condenser fault (Horizontal)

This graph illustrates the test results of the air conditioner of the car, different RPMs, and condenser fault types which are three performance parameters; these parameters are compressor vibration-nominals in which they were measured using millimetres per second, evaporator temperature outlet, evaporator, and a compressor inlet temperature. As the RPM rise, the fault condition increases the compressor vibration; it was observed that at 1900 were the maximum point of 9.69 mm/s at 1900 RPM, and lower speeds and fault levels will have a maximum of 2.46 mm/s. The increased speed and severity of the fault are now represented by orange colours, where dynamic instability can be seen.

At a fault condition, compressor temperature, which is largely represented by the green

colours, will always be higher. Most definitely, under the worst condition created by the faults at the condenser, it reached up to a peak of 56.3°C. The statement quality reflects the additional thermal load and the inefficiency owing to both condenser faults. The evaporator temperature outlet appears bluish and is stable; however, somehow, it varies for fault and no-fault conditions. This is due to cooling efficiency.

Compressor vibration shows solid line trend of dotted linearity; that means vibration generation directly dependent on rpm and fault severity. It is according to ISO 10816 states that if the higher level is above 7mm/s, the vibration level will be detected. It might raise the alarm for unsafe operation or damage. This data interrelates the dynamic response in thermal relationship with the system itself through fault and, at the same time, affects vibration and temperature compromising the cooling and reliability of air conditioning unit.

4.6.2 EXPERIMENT RESULT ON OUTPUT OF AN CAR-AIRCONDITIONER WITH DIFFERENT RPM AND CONDENSER FAULT (VERTICAL)

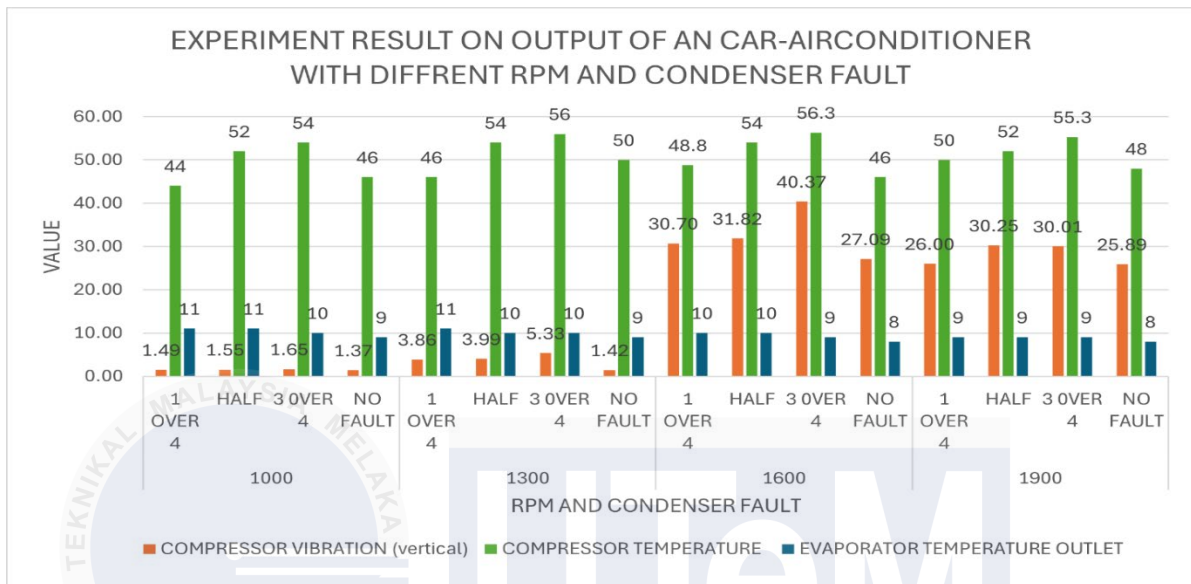


Figure 4.14 Experiment result on output of a car-air conditioner with different rpm and condenser fault (vertical)

It shows the experimental results from tests performed on a car air conditioner at varied values of RPMs (1000, 1300, 1600, and 1900) and various fault conditions (1/4 overcharged, 1/2 overcharged, 3/4 overcharged, and no fault) of the condenser. The three parameters are measured: compressor vibration (vertical), compressor temperature, and temperature of evaporator outlet. Values for compressor vibration are lower for almost all scenarios, showing many deviations when the fault of the condenser changes at a certain RPM. Here, a notable increase is observed due to the "3/4 overcharged" fault that would be followed by the other fluctuation downwards with "no fault" on 1600 RPM read.

Compressor temperature occupies the value in this graph completely because it is always higher than other parameters in all forms of RPM sizes and fault condition forms. At this point, it is highest in terms of RPM (for example, 1300 and 1600 RPM having overcharge faults) and is stable with slight drops at the 1900 RPM range. Similarly, outlet temperature of evaporator (blue bars) shows little difference with the conduction, maintaining value all

through the offseason experiment with variations produced above 8-11 in almost all cases.

In short, the conclusion of the effects of the faults in the condenser and the effect of different RPMs on the compressor performance and heat exchange efficiency has summed when this graph is viewed. The highest effect is there on the compressor temperature, which is a very sensitive factor in terms of RPM and fault conditions, which is actually the most important factor of system efficient performance. In fact, the temperature outlet of the evaporator remains almost constant, which would mean stability in cooling performance with respect to these parameters, while a high fluctuation in compressor vibration indicates that mechanical impacts are caused due to loading of the system and fault conditions. Helpful in the diagnosis of system inefficiencies and performance optimizations.

4.7 Verification of analysis result

The cooling performance of a Proton Persona car was put through tests to validate the analytical results for acceptability and likeness. The manufactured compressor has a standardized oil level and refrigerant charge of R134a gas with ambient temperature of 23 Celsius in the year 2022. The cooling temperature applied to the system for the test achieved a maximum efficiency of cooling valued at 8 Celsius very similarly with the ideal cooling performance for Alternative test rig well-maintained system. The results show that under these normal conditions, the system will be able to provide most of the cooling performance expected. This also proves that the compressor and refrigerant levels are working under supposed parameters. Thus, these results underline the fact that oil and refrigerant levels must be optimally maintained for effective cooling performance.

According to research, the performance of an AC compressor also depends on the performance of the condenser. According to Dahlan et al., the efficiency of electric compressors in automotive applications reaches as high as 97.5% under optimal speeds, thus

highlighting the importance of maintaining all components, including the condenser, in good order. Dahlan et al. (2014).

To summarize, a car air conditioning system depends greatly on the perfect operation of the different components, such as the condenser. A well-functioning condenser will boost the compressor's performance, improve energy consumption, and add to the fuel efficiency of the automobile. Because of the continuance improvement of compressor technology and general system design, there is also a strong case for keeping performance high standards in automotive AC systems.

Ambient Air Temperature	Relative Humidity	Service Port Pressure		Maximum Left Center Discharge Air Temperature
		Low Side	High Side	
13–16°C (55–65°F)	0–100%	175–206 kPa (25–30 psi)	340–850 kPa (49–123 psi)	7°C (45°F)
19–24°C (66–75°F)	Below 40%	175–215 kPa (25–31 psi)	430–930 kPa (62–135 psi)	6°C (43°F)
	Above 40%	175–254 kPa (25–37 psi)	570–1070 kPa (83–155 psi)	9°C (48°F)
25–29°C (76–85°F)	Below 35%	175–249 kPa (25–36 psi)	760–1410 kPa (147–205 psi)	9°C (48°F)
	35–60%	175–261 kPa (26–38 psi)	830–1180 kPa (120–171 psi)	10°C (50°F)
	Above 60%	185–286 kPa (27–42 psi)	880–1250 kPa (128–181 psi)	11°C (52°F)
30–35°C (86–95°F)	Below 30%	193–293 kPa (28–43 psi)	1010–1410 kPa (146–205 psi)	12°C (54°F)
	30–50%	228–269 kPa (30–44 psi)	1050–1440 kPa (153–209 psi)	13°C (55°F)
	Above 50%	221–324 kPa (32–47 psi)	1100–1470 kPa (160–213 psi)	14°C (58°F)
36–41°C (96–105°F)	Below 20%	241–337 kPa (35–47 psi)	1310–1700 kPa (190–246 psi)	16°C (61°F)
	20–40%	247–345 kPa (36–50 psi)	1320–1700 kPa (190–230 psi)	16°C (61°F)
	Above 40%	259–353 kPa (37–52 psi)	1350–1690 kPa (196–246 psi)	16°C (61°F)
42–46°C (106–115°F)	Below 20%	292–378 kPa (42–55 psi)	1630–1950 kPa (238–283 psi)	17°C (62°F)
	Above 20%	297–383 kPa (43–55 psi)	1620–1930 kPa (235–280 psi)	19°C (66°F)
47–49°C (116–120°F)	Below 30%	338–405 kPa (50–59 psi)	187–2080 kPa (271–302 psi)	20°C (68°F)

Figure 4.15 R134a refrigerant performance (Bonifaccino, 2020)

4.8 Summary

Chapters 4 entail the outcomes and analysis following the development and testing of a test rig for Car Air Conditioning Compressor. The testing of vibration has been done using another test rig due to constraints in terms of time. All said, the CACTR has its components in a very solid frame with a scroll compressor, evaporator, blower, and R134a refrigerant tank, mimicking the normal air-conditioning systems. The rig was validated under pressure tests, and it was realized that the rig became more reliable with only very negligible pressure drops within acceptable limits. Experimental tests enabled evaluation of system performance at variable RPMs-1000, 1300, 1600, and 1900-under various fault conditions in the condenser: No Fault, 1/4," "HALF," and "3/4,". Increased faults decreased the Coefficient of Performance (COP) and rose vibration and temperature of compressor which together belittled cooling efficiency. Horizontal and vertical vibration analyses do show that faults hugely increased vibration level. More prominently, due to structural factors, vertical vibrations become higher than horizontal vibrations.

Faulted and fault-free conditions reveal the maintenance of such integrity about systems as the performances without fault are stable and efficient. This includes further running results on the Proton Persona car, thus bringing real-world test validation of the results from the study. Together with that, maintaining the refrigerant and oil levels in the optimal ranges will contribute to effective cooling. Therefore, in general, this chapter talks about the impact of the condenser faults and the conditions of operation on the performance of the system and the need to do preventive maintenance, vibration monitoring, and placing the equipment under optimal operational settings to increase its reliability and efficiency.

CHAPTER 5

CONCLUSION & RECOMMENDATIONS

5.1 Summary of Test Rig Development

The thesis is titled "Design & Development of Car Air Conditioning Compressor Test Rig (CACTR) for 2016 Honda Jazz Hybrid." The rig was planned and executed on material selection criteria ensuring the rig would be durable and functional. A robust plywood construction, light aluminum profiles were used for structural strength in facilitating easy assembly and disassembly, that is the general outside wall of the test rig. It included a section of protective cardboard and acrylic for seeing inside parts, but also glass-covered or exposed outside surfaces for an easy-peep visual inspection and protection from direct foreign attack as it is made up of materials.

Some of the primary components making up the rig include a scroll compressor known for its reliability as well as efficiency, evaporators for heat absorption, and condensers for heat discharge. These components were specifically designed and located in the test rig in a manner that represents the real air conditioning system setup. The validation test rig underwent a series of rigorous tests including leak tests and pressure tests which confirmed that these tests were reliable for operation. The successful realization of CACTR would serve as a very crucial research tool both in academic terms and applied in real-life for industry reporting on performance and efficiency.

5.2 Summary of Analysis

The entire analysis is focused on evaluating the air conditioning performance concerning various operating conditions at different RPMs: 1000, 1300, 1600, and 1900. This was done considering the different levels of condenser fault, which were classified as No Fault, 1/4 Fault, Half Fault, and 3/4 Fault. Hence, looking at the performance through the above means made an exhaustive analysis regarding the performance of HVAC with respect to these different parameters. Various key characteristics were recorded, including, but not limited to, the Coefficient of Performance (COP), which is usually a good indicator of energy efficiency, and compressor vibration and temperature readings for both the compressor and evaporator.

The analysis showed good relationships existed between the various levels of faults of the condenser and performance of the system. The higher the faults, the more the COP decreased. While this happened, both the temperature and vibration levels of the compressor continued to increase, which points to mechanical stress and thermal load on the system. Further analysis concluded that, as far as conditions with faults were concerned, there were usually bigger vertical vibrations rather than horizontal ones. This might indicate stability problems concerning the system. The analysis thus can draw conclusions between operational parameters with structured tables through which conditions can easily be read toward understanding their efficiency and effectiveness.

5.3 Limitation of Research

Despite the Thorough study, there appeared to be numerous limitations that might affect the findings and conclusions in application. One such aspect is the very limited time that was given to the research, due to that, vibration analysis was done with the alternative test rig rather

than the main rig. This alone could have caused variations in the results as well as limited further analysis. The research, it is important to state, investigates just one type of vehicle, which turned out to be the Honda Jazz Hybrid 2016. This may limit the generalization of results to other vehicle models or even types.

Concentrating on just one model may also keep out unaccounted performance variation that could exist in different automotive air conditioning systems. The study did not consider the long-term aspect of continuously affected fault conditions on system performance, which could have given insight into automotive HVAC systems durability and maintenance aspects after a long period. The study did not consider the influence of external environmental factors such as ambient temperature and humidity on the performance of the air conditioning system, which may further influence the results.

5.4 Future Recommendations

For the future effectiveness and applicability of research to recommend several aspects, beginning study must be extended to more diverse vehicles and models, thus expanding the results beyond just a few automotive air conditioning systems into something that reveals much more a very strong understanding of how much of the diverse technology designs perform under comparatively similar testing situations. Further, long-term performance studies shall be useful as they would show the impact of repeated faults on the effectiveness and reliability of the air-conditioning system. Such assessments hold the potential to shine light on wear-and-tear issues that can manifest in the long run and help guide maintenance regimes while helping extend life cycles.

Access to advanced diagnostic tools and artificial intelligence algorithms would significantly improve fault detection and predictive maintenance strategies in automotive

HVAC systems while enhancing overall operation efficiency. Such technologies can bring about real-time monitoring and at-the-time analysis of system performance so as to avert faults for maintenance intervention before the problem aggravates into a fault condition. And finally, further study on alternative refrigerants and their effects on performance, as well as environmental sustainability ever more strongly recommended new ways toward development of greener automotive air conditioning solutions, can indeed be a great benefit. In this way, even in the recommendations, futuristic research can be built upon.



REFERENCES

- ALBERTI, R. and MATIAS, G. (2022). Ecs - sistema econômico de climatização..
<https://doi.org/10.5151/simea2022-pap06>
- Bhutta, M. U., Khan, Z. A., Garland, N. P., & Ghafoor, A. (2018). A historical review on the tribological performance of refrigerants used in compressors. *Tribology in Industry*, 40(1), 19-51. <https://doi.org/10.24874/ti.2018.40.01.03>
- Jusoh, M. A., Yusop, Z. M., Albani, A., Daud, M. Z., & Ibrahim, M. Z. (2024). An innovative dry-lab test rig for mechanical-hydraulic power take-off of wave energy conversion system. *International Journal of Power Electronics and Drive Systems (IJPEDS)*, 15(2), 715. <https://doi.org/10.11591/ijpeds.v15.i2.pp715-724>
- Khatoon, S. and Karimi, M. (2023). Thermodynamic analysis of two evaporator vapor compression refrigeration system with low gwp refrigerants in automobiles. *International Journal of Air-Conditioning and Refrigeration*, 31(1). <https://doi.org/10.1007/s44189-022-00017-1>
- Kim, J., Lee, S., & Kim, Y. (2021). Dynamic testing of automotive air conditioning systems using a advanced test rig. *Applied Thermal Engineering*, 184, 116933.
- Kumar, P., Singh, R., & Kumar, A. (2020). Experimental investigation of automotive air conditioning system performance using a test rig. *Journal of Thermal Science and Technology*, 10(2), 1-12.
- Lee, S., Kim, J., & Lee, J. (2020). Development of an eco-friendly automotive air conditioning system using a test rig. *International Journal of Automotive Technology*, 21(3), 537-546.
- Li, C. (2024). Analysis on mechanism and characteristic of vibration fault on new large capacity synchronous condenser. *Journal of Physics Conference Series*, 2731(1), 012002. <https://doi.org/10.1088/1742-6596/2731/1/012002>
- Li, Z., Chen, Y., & Zhang, J. (2020). Simulation of extreme weather conditions using an advanced test rig for automotive air conditioning systems. *International Journal of Simulation and Process Modelling*, 15(3), 233-244.
- Lin, H., Ye, Y., Huang, B., & Su, J. (2016). Bearing vibration detection and analysis using enhanced fast fourier transform algorithm. *Advances in Mechanical Engineering*, 8(10). <https://doi.org/10.1177/1687814016675080>
- Marco Bonifaccino. (2020, November 3). *How temperature and humidity affect the car's AC performance*. <https://www.acdiagnosis.com/post/how-temperature-and-humidity->

affect- car-ac-

performance?srsId=AfmBOorUuOuBRuwXWUk1OmWOBFYzh61IUeXiL9OhvDJh
O 6bphccGLVTT

- Martis, R., Pop-Pîgleșan, F., Cosman, S. I., & Marțiș, C. (2020). Considerations on design, development and testing of electrical machines for automotive hvac. *MATEC Web of Conferences*, 322, 01042. <https://doi.org/10.1051/mateconf/202032201042>
- Rahman, M.N., Abdullah, R., and Kamarudin, N., 2012. Work Study Techniques Evaluation at Back-End Semiconductor Manufacturing. *Proceedings of the 2012 International Conference on Design and Concurrent Engineering*, Melaka, Malaysia, 2, pp. 24-27.
- Russi, L., Guidorzi, P., Pulvirenti, B., Aguiari, D., Pau, G., & Semprini, G. (2022). Air Quality and Comfort Characterisation within an Electric Vehicle Cabin in Heating and Cooling Operations. *Sensors*, 22(2), 543. <https://doi.org/10.3390/s22020543>
- Sharif, M. Z., Azmi, W. H., Ismail, M. F., Awalludin, M. M. N., Ghazali, M. F., & Aminullah, A. R. M. (2023). Performance analysis of automotive air conditioning systems with electric compressors using r1234yf refrigerant: insights into power consumption, cooling capacity, and energy efficiency. *IOP Conference Series: Earth and Environmental Science*, 1267(1), 012069. <https://doi.org/10.1088/1755-1315/1267/1/012069>
- Song, P., Wu, D., Lu, Z., Zheng, S., Wei, M., Zhuge, W., ... & Zhang, Y. (2023). An improved geometric theoretical model and throughflow prediction method for a co2 scroll compressor of automotive air conditioning system. *International Journal of Energy Research*, 2023, 1-18. <https://doi.org/10.1155/2023/9382690>
- Sun, S., Sun, N., & Wang, X. (2019). Study on mixed lubrication characteristics of piston/cylinder interface of variable length. *AIP Advances*, 9(7). <https://doi.org/10.1063/1.5093925>
- Surampudi, B., Redfield, J., Montemayor, A., Ray, G., Ostrowski, G., McKee, H., ... & Lawrence, J. (2006). Electric air conditioning for class 8 tractors.. <https://doi.org/10.4271/2006-01-0165>
- Wang, X., Li, Z., & Chen, Y. (2020). Optimization of automotive air conditioning system design using a test rig. *Journal of Intelligent Information Systems*, 57(2), 257-271.
- Zhang, D., Gao, J., Ding, T., Wu, Y., Shi, J., Chen, J., ... & Zhang, S. (2021). Switching on auxiliary devices in vehicular fuel efficiency tests can help cut co2 emissions by

millions of tons. *One Earth*, 4(1), 135-145.

<https://doi.org/10.1016/j.oneear.2020.12.010>

Zhang, J., Li, Z., & Chen, Y. (2022). Prediction of automotive air conditioning system performance using machine learning algorithms and test rig data. *Applied Soft Computing*, 116, 108333.



APPENDICES

APPENDIX A Project Gantt chart

PROJECT PLANNING (GANTT CHART)														
Project activities	W1	W2	W3	W4	W5	W6	W7	W8	W9	W10	W11	W12	W13	W14
PSM 1 related research study														
Find project title and complete registration form														
Find the design structure and components on the project														
chapter 1 and chapter 2 project														
Study project related														
completing chapter 3 submitting draft														
correction on draft report														
submit report														
Presentation														

APPENDIX B Project Gantt chart

		PROJECT PLANNING AND EXECUTE (GANTT CHART)														
Project activities		W1	W2	W3	W4	W5	W6	W7	W8	W9	W10	W11	W12	W13	W14	W15
PSM 2 related research study	P															
	E															
Product development completed	P															
	E															
Sensor apply to the test rig	P															
	E															
Analysis and completing chapter 4	P															
	E															
Product Testing	P															
	E															
Updating changes from chapter 1,2 and 3	P															
	E															
Correction On draft report based on Supervisor Feedback	P															
	E															
Presentation and thesis evaluation	P															
	E															

LEGEND	
	P - Planning
	E - Executed

APPENDIX C ISO 10816 (Vibration Severity)

VIBRATION SEVERITY PER ISO 10816						
Machine			Class I Small Machines	Class II Medium Machines	Class III Large Rigid Foundation	Class IV Large Soft Foundation
	In/s	mm/s				
Vibration Velocity V _{ms}	0.01	0.28				
	0.02	0.45				
	0.03	0.71		GOOD		
	0.04	1.12				
	0.07	1.80				
	0.11	2.80	SATISFACTORY			
	0.18	4.50				
	0.28	7.10	UNSATISFACTORY			
	0.44	11.2				
	0.70	18.0				
	0.71	28.0	UNACCEPTABLE			
	1.10	45.0				

UNIVERSITI TEKNIKAL MALAYSIA MELAKA

APPENDIX D Electric Scroll Compressor Specification

Refrigerant (Gas): R134a
Speed range: 1000~2100 rpm
Working pressure: Suction pressure: 0.2~0.45Mpa
Discharge pressure: ≤ 2.0 Mpa / ≤ 2.2 Mpa
pressure ratio: ≤ 10 Ambient
temperature: -40°C - 80°C
Discharge temperature: ≤ 110 °C
Lubricating oil require: 8%-10% of whole system refrigerant (Gas)

Compressor data:

Compressor style: Semi-closed Horizontal Scroll
Compressor Material: Aluminum alloy Voltage: DC 12V / 24V
Working voltage range: 10.5VDC~15VDC / 19.5VDC~32VDC
Current: 45A+-2 / 35A+-2
Displacement: 21cm³/r
Cooling capacity: 1.688KW / 2.465KW (5731BTU / 8410BTU)
Speed range: 1000 - 2300rpm / 1000 - 3000rpm
Rated power: 550W / 850w Rated speed: 1800rpm / 3000rpm
Oil: POE / 130ml - 150ml (Oil has already in compressor)
Gas/Refrigerant: R134a
Condensing temperature range: 26.7~68°C
Evaporating temperature range: -10~12.5°C
Refrigerant leakage rate: <14g per year
Suction pipe inner size: Ø18.3mm
Discharge pipe inner size: Ø15.5mm COP W/W: 3.07 / 2.9
Compressor body not to be tilted (the angle between the main axis of the compressor and the horizon should not be greater than 5 °)

Brushless controller unit :

Brushless direct current controller
1. Over / Under voltage protection: DC 12V -- (21V / 10.5V) DC 24V -- (42V / 20.5V)
2. Max power: 600w / 1200W

Generator (battery) request :

12V compressor require generator ampere over 100A;
24V compressor require generator ampere over 70A.
About vehicle battery. If you want to use the electric compressor after parking, then your vehicle battery capacity should be large enough. For example, 12V compressor current about 45A. So one new and full charged 45A battery can run the compressor for one hour.

Led blinking:

Blinking 1 times, pause 1 second: Standby mode.

Fast blinking 2 times, pause 1 second: Excessive current, Over 50A.

Fast blinking 3 times, pause 1 second: Locked rotor protection.

Fast blinking 4 times, pause 1 second: Undervoltage protection.

Fast blinking 6 times, pause 1 second: Electric fan fault.

Fast blinking 7 times, pause 1 second: Motor lack of phase. Please check if the motor got burnt and connection is correct or not.

Fast blinking 8 times, pause 1 second: Compressor over heated protection.

Fast blinking 9 times, pause 1 second: Pressure switch protection.

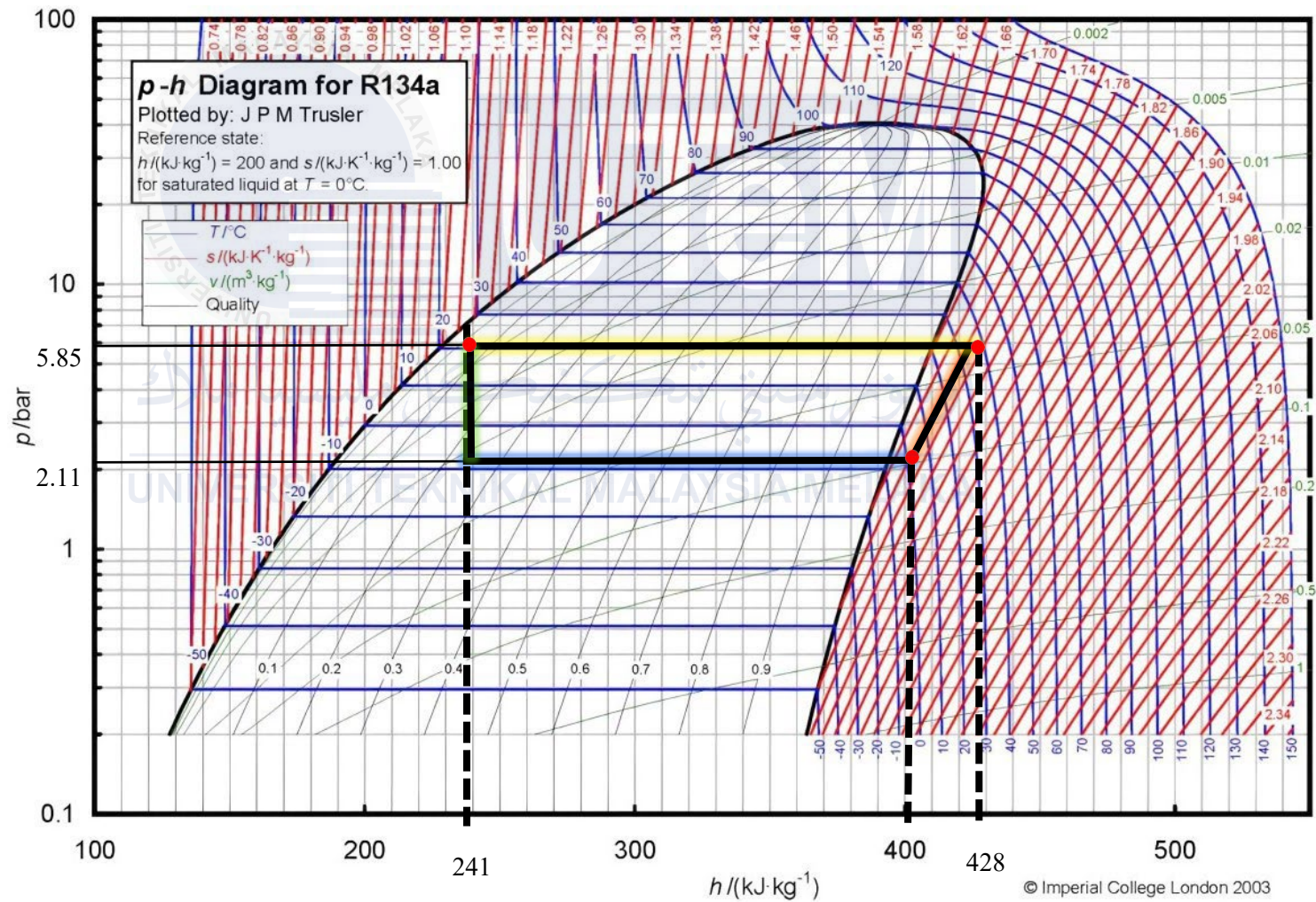
Package product list:

1. 1 x Compressor
2. 1 x Brushless controller unit
3. 1 x Power wire
4. 1 x Evaporator wire
5. 1 x Cooling fan extension lines
6. 1 x Direr (Pressure switch extension lines)

Khatoon, S. and Karimi, M. (2023). Thermodynamic analysis of two evaporator vapor compression refrigeration system with low gwp refrigerants in automobiles. *International Journal of Air-Conditioning and Refrigeration*, 31(1). <https://doi.org/10.1007/s44189-022-00017-1>

Experimental investigations have provided valuable data on the COP of R134a in automotive air conditioning systems. For example, a study by Khatoon & Karimi (2023) reported that the use of an internal heat exchanger (IHX) in R134a systems improved the COP by approximately 4.1%

APPENDIX E Pressure-Enthalpy Diagram of R134a



APPENDIX F R134a Tables

TABLE A-11

Saturated refrigerant-134a—Temperature table

Temp., T°C	Press., P _{sat} , MPa	Specific volume, m ³ /kg		Internal energy, kJ/kg		Enthalpy, kJ/kg			Entropy, kJ/(kg · K)	
		Sat. liquid, v _f	Sat. vapor, v _g	Sat. liquid, u _f	Sat. vapor, u _g	Sat. liquid, h _f	Evap., h _{fg}	Sat. vapor, h _g	Sat. liquid, s _f	Sat. vapor, s _g
-40	0.05164	0.0007055	0.3569	-0.04	204.45	0.00	222.88	222.88	0.0000	0.9560
-36	0.06332	0.0007113	0.2947	4.68	206.73	4.73	220.67	225.40	0.0201	0.9506
-32	0.07704	0.0007172	0.2451	9.47	209.01	9.52	218.37	227.90	0.0401	0.9456
-28	0.09305	0.0007233	0.2052	14.31	211.29	14.37	216.01	230.38	0.0600	0.9411
-26	0.10199	0.0007265	0.1882	16.75	212.43	16.82	214.80	231.62	0.0699	0.9390
-24	0.11160	0.0007296	0.1728	19.21	213.57	19.29	213.57	232.85	0.0798	0.9370
-22	0.12192	0.0007328	0.1590	21.68	214.70	21.77	212.32	234.08	0.0897	0.9351
-20	0.13299	0.0007361	0.1464	24.17	215.84	24.26	211.05	235.31	0.0996	0.9332
-18	0.14483	0.0007395	0.1350	26.67	216.97	26.77	209.76	236.53	0.1094	0.9315
-16	0.15748	0.0007428	0.1247	29.18	218.10	29.30	208.45	237.74	0.1192	0.9298
-12	0.18540	0.0007498	0.1068	34.25	220.36	34.39	205.77	240.15	0.1388	0.9267
-8	0.21704	0.0007569	0.0919	39.38	222.60	39.54	203.00	242.54	0.1583	0.9239
-4	0.25274	0.0007644	0.0794	44.56	224.84	44.75	200.15	244.90	0.1777	0.9213
0	0.29282	0.0007721	0.0689	49.79	227.06	50.02	197.21	247.23	0.1970	0.9190
4	0.33765	0.0007801	0.0600	55.08	229.27	55.35	194.19	249.53	0.2162	0.9169
8	0.38756	0.0007884	0.0525	60.43	231.46	60.73	191.07	251.80	0.2354	0.9150
12	0.44294	0.0007971	0.0460	65.83	233.63	66.18	187.85	254.03	0.2545	0.9132
16	0.50416	0.0008062	0.0405	71.29	235.78	71.69	184.52	256.22	0.2735	0.9116
20	0.57160	0.0008157	0.0358	76.80	237.91	77.26	181.09	258.35	0.2924	0.9102
24	0.64566	0.0008257	0.0317	82.37	240.01	82.90	177.55	260.45	0.3113	0.9089
26	0.68530	0.0008309	0.0298	85.18	241.05	85.75	175.73	261.48	0.3208	0.9082
28	0.72675	0.0008362	0.0281	88.00	242.08	88.61	173.89	262.50	0.3302	0.9076
30	0.77006	0.0008417	0.0265	90.84	243.10	91.49	172.00	263.50	0.3396	0.9070
32	0.81528	0.0008473	0.0250	93.70	244.12	94.39	170.09	264.48	0.3490	0.9064
34	0.86247	0.0008530	0.0236	96.58	245.12	97.31	168.14	265.45	0.3584	0.9058
36	0.91168	0.0008590	0.0223	99.47	246.11	100.25	166.15	266.40	0.3678	0.9053
38	0.96298	0.0008651	0.0210	102.38	247.09	103.21	164.12	267.33	0.3772	0.9047
40	1.0164	0.0008714	0.0199	105.30	248.06	106.19	162.05	268.24	0.3866	0.9041
42	1.0720	0.0008780	0.0188	108.25	249.02	109.19	159.94	269.14	0.3960	0.9035
44	1.1299	0.0008847	0.0177	111.22	249.96	112.22	157.79	270.01	0.4054	0.9030
48	1.2526	0.0008989	0.0159	117.22	251.79	118.35	153.33	271.68	0.4243	0.9017
52	1.3851	0.0009142	0.0142	123.31	253.55	124.58	148.66	273.24	0.4432	0.9004
56	1.5278	0.0009308	0.0127	129.51	255.23	130.93	143.75	274.68	0.4622	0.8990
60	1.6813	0.0009488	0.0114	135.82	256.81	137.42	138.57	275.99	0.4814	0.8973
70	2.1162	0.0010027	0.0086	152.22	260.15	154.34	124.08	278.43	0.5302	0.8918
80	2.6324	0.0010766	0.0064	169.88	262.14	172.71	106.41	279.12	0.5814	0.8827
90	3.2435	0.0011949	0.0046	189.82	261.34	193.69	82.63	276.32	0.6380	0.8655
100	3.9742	0.0015443	0.0027	218.60	248.49	224.74	34.40	259.13	0.7196	0.8117

Source for Tables A-8 through A-10: M. J. Moran and H. N. Shapiro, *Fundamentals of Engineering Thermodynamics*, 2nd ed. (New York: John Wiley & Sons, 1992), pp. 710–15. Originally based on equations from D. P. Wilson and R. S. Basu, "Thermodynamic Properties of a New Stratospherically Safe Working Fluid—Refrigerant-134a," *ASHRAE Trans.* 94, Pt. 2 (1988), pp. 2095–118. Used with permission.

TABLE A-12

Saturated refrigerant-134a—Pressure table

Press., P, MPa	Temp., T _{sat} , °C	Specific volume, m ³ /kg		Internal energy, kJ/kg		Enthalpy, kJ/kg			Entropy, kJ/(kg · K)	
		Sat. liquid, v _f	Sat. vapor, v _g	Sat. liquid, u _f	Sat. vapor, u _g	Sat. liquid, h _f	Evap., h _{fg}	Sat. vapor, h _g	Sat. liquid, s _f	Sat. vapor, s _g
0.06	-37.07	0.0007097	0.3100	3.41	206.12	3.46	221.27	224.72	0.0147	0.9520
0.08	-31.21	0.0007184	0.2366	10.41	209.46	10.47	217.92	228.39	0.0440	0.9447
0.10	-26.43	0.0007258	0.1917	16.22	212.18	16.29	215.06	231.35	0.0678	0.9395
0.12	-22.36	0.0007323	0.1614	21.23	214.50	21.32	212.54	233.86	0.0879	0.9354
0.14	-18.80	0.0007381	0.1395	25.66	216.52	25.77	210.27	236.04	0.1055	0.9322
0.16	-15.62	0.0007435	0.1229	29.66	218.32	29.78	208.18	237.97	0.1211	0.9295
0.18	-12.73	0.0007485	0.1098	33.31	219.94	33.45	206.26	239.71	0.1352	0.9273
0.20	-10.09	0.0007532	0.0993	36.69	221.43	36.84	204.46	241.30	0.1481	0.9253
0.24	-5.37	0.0007618	0.0834	42.77	224.07	42.95	201.14	244.09	0.1710	0.9222
0.28	-1.23	0.0007697	0.0719	48.18	226.38	48.39	198.13	246.52	0.1911	0.9197
0.32	2.48	0.0007770	0.0632	53.06	228.43	53.31	195.35	248.66	0.2089	0.9177
0.36	5.84	0.0007839	0.0564	57.54	230.28	57.82	192.76	250.58	0.2251	0.9160
0.4	8.93	0.0007904	0.0509	61.69	231.97	62.00	190.32	252.32	0.2399	0.9145
0.5	15.74	0.0008056	0.0409	70.93	235.64	71.33	184.74	256.07	0.2723	0.9117
0.6	21.58	0.0008196	0.0341	78.99	238.74	79.48	179.71	259.19	0.2999	0.9097
0.7	26.72	0.0008328	0.0292	86.19	241.42	86.78	175.07	261.85	0.3242	0.9080
0.8	31.33	0.0008454	0.0255	92.75	243.78	93.42	170.73	264.15	0.3459	0.9066
0.9	35.53	0.0008576	0.0226	98.79	245.88	99.56	166.62	266.18	0.3656	0.9054
1.0	39.39	0.0008695	0.0202	104.42	247.77	105.29	162.68	267.97	0.3838	0.9043
1.2	46.32	0.0008928	0.0166	114.69	251.03	115.76	155.23	270.99	0.4164	0.9023
1.4	52.43	0.0009159	0.0140	123.98	253.74	125.26	148.14	273.40	0.4453	0.9003
1.6	57.92	0.0009392	0.0121	132.52	256.00	134.02	141.31	275.33	0.4714	0.8982
1.8	62.91	0.0009631	0.0105	140.49	257.88	142.22	134.60	276.83	0.4954	0.8959
2.0	67.49	0.0009878	0.0093	148.02	259.41	149.99	127.95	277.94	0.5178	0.8934
2.5	77.59	0.0010562	0.0069	165.48	261.84	168.12	111.06	279.17	0.5687	0.8854
3.0	86.22	0.0011416	0.0053	181.88	262.16	185.30	92.71	278.01	0.6156	0.8735

R-134a

اونيورسيتي تيكنيكل مليسيا ملاك
UNIVERSITI TEKNIKAL MALAYSIA MELAKA

TABLE A-13

Superheated refrigerant-134a

T °C	v m ³ /kg	u kJ/kg	h kJ/kg	s kJ/(kg · K)	v m ³ /kg	u kJ/kg	h kJ/kg	s kJ/(kg · K)	v m ³ /kg	u kJ/kg	h kJ/kg	s kJ/(kg · K)
$P = 0.06 \text{ MPa } (T_{\text{sat}} = -37.07^\circ\text{C})$					$P = 0.10 \text{ MPa } (T_{\text{sat}} = -26.43^\circ\text{C})$				$P = 0.14 \text{ MPa } (T_{\text{sat}} = -18.80^\circ\text{C})$			
Sat.	0.31003	206.12	224.72	0.9520	0.19170	212.18	231.35	0.9395	0.13945	216.52	236.04	0.9322
-20	0.33536	217.66	237.98	1.0062	0.19770	216.77	236.54	0.9602				
-10	0.34992	224.97	245.96	1.0371	0.20686	224.01	244.70	0.9918	0.14549	223.03	243.40	0.9606
0	0.36433	232.24	254.10	1.0675	0.21587	231.41	252.99	1.0227	0.15219	230.55	251.86	0.9922
10	0.37861	239.69	262.41	1.0973	0.22473	238.96	261.43	1.0531	0.15875	238.21	260.43	1.0230
20	0.39279	247.32	270.89	1.1267	0.23349	246.67	270.02	1.0829	0.16520	246.01	269.13	1.0532
30	0.40688	255.12	279.53	1.1557	0.24216	254.54	278.76	1.1122	0.17155	253.96	277.97	1.0828
40	0.42091	263.10	288.35	1.1844	0.25076	262.58	287.66	1.1411	0.17783	262.06	286.96	1.1120
50	0.43487	271.25	297.34	1.2126	0.25930	270.79	296.72	1.1696	0.18404	270.32	296.09	1.1407
60	0.44879	279.58	306.51	1.2405	0.26779	279.16	305.94	1.1977	0.19020	278.74	305.37	1.1690
70	0.46266	288.08	315.84	1.2681	0.27623	287.70	315.32	1.2254	0.19633	287.32	314.80	1.1969
80	0.47650	296.75	325.34	1.2954	0.28464	296.40	324.87	1.2528	0.20241	296.06	324.39	1.2244
90	0.49031	305.58	335.00	1.3224	0.29302	305.27	334.57	1.2799	0.20846	304.95	334.14	1.2516
100									0.21449	314.01	344.04	1.2785
$P = 0.18 \text{ MPa } (T_{\text{sat}} = -12.73^\circ\text{C})$					$P = 0.20 \text{ MPa } (T_{\text{sat}} = -10.09^\circ\text{C})$				$P = 0.24 \text{ MPa } (T_{\text{sat}} = -5.37^\circ\text{C})$			
Sat.	0.10983	219.94	239.71	0.9273	0.09933	221.43	241.30	0.9253	0.08343	224.07	244.09	0.9222
-10	0.11135	222.02	242.06	0.9362	0.09938	221.50	241.38	0.9256				
0	0.11678	229.67	250.69	0.9684	0.10438	229.23	250.10	0.9582	0.08574	228.31	248.89	0.9399
10	0.12207	237.44	259.41	0.9998	0.10922	237.05	258.89	0.9898	0.08993	236.26	257.84	0.9721
20	0.12723	245.33	268.23	1.0304	0.11394	244.99	267.78	1.0206	0.09339	244.30	266.85	1.0034
30	0.13230	253.36	277.17	1.0604	0.11856	253.06	276.77	1.0508	0.09794	252.45	275.95	1.0339
40	0.13730	261.53	286.24	1.0898	0.12311	261.26	285.88	1.0804	0.10181	260.72	285.16	1.0637
50	0.14222	269.85	295.45	1.1187	0.12758	269.61	295.12	1.1094	0.10562	269.12	294.47	1.0930
60	0.14710	278.31	304.79	1.1472	0.13201	278.10	304.50	1.1380	0.10937	277.67	303.91	1.1218
70	0.15193	286.93	314.28	1.1753	0.13639	286.74	314.02	1.1661	0.11307	286.35	313.49	1.1501
80	0.15672	295.71	323.92	1.2030	0.14073	295.53	323.68	1.1939	0.11674	295.18	323.19	1.1780
90	0.16148	304.63	333.70	1.2303	0.14504	304.47	333.48	1.2212	0.12037	304.15	333.04	1.2055
100	0.16622	313.72	343.63	1.2573	0.14932	313.57	343.43	1.2483	0.12398	313.27	343.03	1.2326
$P = 0.28 \text{ MPa } (T_{\text{sat}} = -1.23^\circ\text{C})$					$P = 0.32 \text{ MPa } (T_{\text{sat}} = 2.48^\circ\text{C})$				$P = 0.40 \text{ MPa } (T_{\text{sat}} = 8.93^\circ\text{C})$			
Sat.	0.07193	226.38	246.52	0.9197	0.06322	228.43	248.66	0.9177	0.05089	231.97	252.32	0.9145
0	0.07240	227.37	247.64	0.9238								
10	0.07613	235.44	256.76	0.9566	0.06576	234.61	255.65	0.9427	0.05119	232.87	253.35	0.9182
20	0.07972	243.59	265.91	0.9883	0.06901	242.87	264.95	0.9749	0.05397	241.37	262.96	0.9515
30	0.08320	251.83	275.12	1.0192	0.07214	251.19	274.28	1.0062	0.05662	249.89	272.54	0.8937
40	0.08660	260.17	284.42	1.0494	0.07518	259.61	283.67	1.0367	0.05917	258.47	282.14	1.0148
50	0.08992	268.64	293.81	1.0789	0.07815	268.14	293.15	1.0665	0.06164	267.13	291.79	1.0452
60	0.09319	277.23	303.32	1.1079	0.08106	276.79	302.72	1.0957	0.06405	275.89	301.51	1.0748
70	0.09641	285.96	312.95	1.1364	0.08392	285.56	312.41	1.1243	0.06641	284.75	311.32	1.1038
80	0.09960	294.82	322.71	1.1644	0.08674	294.46	322.22	1.1525	0.06873	293.73	321.23	1.1322
90	0.10275	303.83	332.60	1.1920	0.08953	303.50	332.15	1.1802	0.07102	302.84	331.25	1.1602
100	0.10587	312.98	342.62	1.2193	0.09229	312.68	342.21	1.1076	0.07327	312.07	341.38	1.1878
110	0.10897	322.27	352.78	1.2461	0.09503	322.00	352.40	1.2345	0.07550	321.44	351.64	1.2149
120	0.11205	331.71	363.08	1.2727	0.09774	331.45	362.73	1.2611	0.07771	330.94	362.03	1.2417
130									0.07991	340.58	372.54	1.2681
140									0.08208	350.35	383.18	1.2941

TABLE A-13

Superheated refrigerant-134a (Concluded)

T °C	v m ³ /kg	u kJ/kg	h kJ/kg	s kJ/(kg · K)	v m ³ /kg	u kJ/kg	h kJ/kg	s kJ/(kg · K)	v m ³ /kg	u kJ/kg	h kJ/kg	s kJ/(kg · K)
$P = 0.50 \text{ MPa } (T_{\text{sat}} = 15.74^\circ\text{C})$					$P = 0.60 \text{ MPa } (T_{\text{sat}} = 21.56^\circ\text{C})$				$P = 0.70 \text{ MPa } (T_{\text{sat}} = 26.72^\circ\text{C})$			
Sat.	0.04086	253.64	256.07	0.9117	0.03408	238.74	259.19	0.9097	0.02918	241.42	261.85	0.9080
20	0.04188	239.40	260.34	0.9264								
30	0.04416	248.20	270.28	0.9597	0.03581	246.41	267.89	0.9388	0.02979	244.51	265.37	0.9197
40	0.04633	256.99	280.16	0.9918	0.03774	255.45	278.09	0.9719	0.03157	253.83	275.93	0.9539
50	0.04842	265.83	290.04	1.0229	0.03958	264.48	288.23	1.0037	0.03324	263.08	286.35	0.9867
60	0.05043	274.73	299.95	1.0531	0.04134	273.54	298.35	1.0346	0.03482	272.31	296.69	1.0182
70	0.05240	283.72	309.92	1.0825	0.04304	282.66	308.48	1.0645	0.03634	281.57	307.01	1.0487
80	0.05432	292.80	319.96	1.1114	0.04469	291.86	318.67	1.0938	0.03781	290.88	317.35	1.0784
90	0.05620	302.00	330.10	1.1397	0.04631	301.14	328.93	1.1225	0.03924	300.27	327.74	1.1074
100	0.05805	311.31	340.33	1.1675	0.04790	310.53	339.27	1.1505	0.04064	309.74	338.19	1.1358
110	0.05988	320.74	350.68	1.1949	0.04946	320.03	349.70	1.1781	0.04201	319.31	348.71	1.1637
120	0.06168	330.30	361.14	1.2218	0.05099	329.64	360.24	1.2053	0.04335	328.98	359.33	1.1910
130	0.06347	339.98	371.72	1.2484	0.05251	339.38	370.88	1.2320	0.04468	338.76	370.04	1.2179
140	0.06524	349.79	382.42	1.2746	0.05402	349.23	381.64	1.2584	0.04599	348.66	380.86	1.2444
150					0.05550	359.21	392.52	1.2844	0.04729	358.68	391.79	1.2706
160					0.05698	369.32	403.51	1.3100	0.04857	368.82	402.82	1.2963
$P = 0.80 \text{ MPa } (T_{\text{sat}} = 31.33^\circ\text{C})$					$P = 0.90 \text{ MPa } (T_{\text{sat}} = 35.53^\circ\text{C})$				$P = 1.00 \text{ MPa } (T_{\text{sat}} = 39.39^\circ\text{C})$			
Sat.	0.02547	243.78	264.15	0.9066	0.02255	245.88	266.18	0.9054	0.02020	247.77	267.97	0.9043
40	0.02691	252.13	273.66	0.9374	0.02325	250.32	271.25	0.9217	0.02029	248.39	268.68	0.9066
50	0.02846	261.62	284.39	0.9711	0.02472	260.09	282.34	0.9566	0.02171	258.48	280.19	0.9428
60	0.02992	271.04	294.98	1.0034	0.02609	269.72	293.21	0.9897	0.02301	268.35	291.36	0.9768
70	0.03131	280.45	305.50	1.0345	0.02738	279.30	303.94	1.0214	0.02423	278.11	302.34	1.0093
80	0.03264	289.89	316.00	1.0647	0.02861	288.87	314.62	1.0521	0.02538	287.82	313.20	1.0405
90	0.03393	299.37	326.52	1.0940	0.02980	298.46	325.28	1.0819	0.02649	297.53	324.01	1.0707
100	0.03519	308.93	337.08	1.1227	0.03095	308.11	335.96	1.1109	0.02755	307.27	334.82	1.1000
110	0.03642	318.57	347.71	1.1508	0.03207	317.82	346.68	1.1392	0.02858	317.06	345.65	1.1286
120	0.03762	328.31	358.40	1.1784	0.03316	327.62	357.47	1.1670	0.02959	326.93	356.52	1.1567
130	0.03881	338.14	369.19	1.2055	0.03423	337.52	368.33	1.1943	0.03058	336.88	367.46	1.1841
140	0.03997	348.09	380.07	1.2321	0.03529	347.51	379.27	1.2211	0.03154	346.92	378.46	1.2111
150	0.04113	358.15	391.05	1.2584	0.03633	357.61	390.31	1.2475	0.03250	357.06	389.56	1.2376
160	0.04227	368.32	402.14	1.2843	0.03736	367.82	401.44	1.2735	0.03344	367.31	400.74	1.2638
170	0.04340	378.61	413.33	1.3098	0.03838	378.14	412.68	1.2992	0.03436	377.66	412.02	1.2895
180	0.04452	389.02	424.63	1.3351	0.03939	388.57	424.02	1.3245	0.03528	388.12	423.40	1.3149
$P = 1.20 \text{ MPa } (T_{\text{sat}} = 46.32^\circ\text{C})$					$P = 1.40 \text{ MPa } (T_{\text{sat}} = 52.43^\circ\text{C})$				$P = 1.60 \text{ MPa } (T_{\text{sat}} = 57.92^\circ\text{C})$			
Sat.	0.01663	251.03	270.99	0.9023	0.01405	253.74	273.40	0.9003	0.01208	256.00	275.33	0.8982
50	0.01712	254.98	275.52	0.9164								
60	0.01835	265.42	287.44	0.9527	0.01495	262.17	283.10	0.9297	0.01233	258.48	278.20	0.9069
70	0.01947	275.59	298.96	0.9868	0.01603	272.87	295.31	0.9658	0.01340	269.89	291.33	0.9457
80	0.02051	285.62	310.24	1.0192	0.01701	283.29	307.10	0.9997	0.01435	280.78	303.74	0.9813
90	0.02150	295.59	321.39	1.0503	0.01792	293.55	318.63	1.0319	0.01521	291.39	315.72	1.0148
100	0.02244	305.54	332.47	1.0804	0.01878	303.73	330.02	1.0628	0.01601	301.84	327.46	1.0467
110	0.02335	315.50	343.52	1.1096	0.01960	313.88	341.32	1.0927	0.01677	312.20	339.04	1.0773
120	0.02423	325.51	354.58	1.1381	0.02039	324.05	352.59	1.1218	0.01750	322.53	350.53	1.1069
130	0.02508	335.58	365.68	1.1660	0.02115	334.25	363.86	1.1501	0.01820	332.87	361.99	1.1357
140	0.02592	345.73	376.83	1.1933	0.02189	344.50	375.15	1.1777	0.01887	343.24	373.44	1.1638
150	0.02674	355.95	388.04	1.2201	0.02262	354.82	386.49	1.2048	0.01953	353.66	384.91	1.1912
160	0.02754	366.27	399.33	1.2465	0.02333	365.22	397.89	1.2315	0.02017	364.15	396.43	1.2181
170	0.02834	376.69	410.70	1.2724	0.02403	375.71	409.36	1.2576	0.02080	374.71	407.99	1.2445
180	0.02912	387.21	422.16	1.2980	0.02472	386.29	420.90	1.2834	0.02142	385.35	419.62	1.2704
190					0.02541	396.96	432.53	1.3088	0.02203	396.08	431.33	1.2960
200					0.02608	407.73	444.24	1.3338	0.02263	406.90	443.11	1.3212

R-134a